In Vitro to In Vivo Extrapolation of Transporter-Mediated Clearance of Drugs Using Quantitative Proteomics

Vineet Kumar

A dissertation

submitted in partial fulfillment of the

requirements for the degree of

Doctor of Philosophy

University of Washington

2019

Reading Committee:

Jashvant D. Unadkat, Chair

Joanne Wang

Bhagwat Prasad

Program Authorized to Offer Degree:

Pharmaceutics

University of Washington

Abstract

In Vitro to In Vivo Extrapolation of Transporter-Mediated Clearance of Drugs Using Quantitative Proteomics

Vineet Kumar

Chair of the Supervisory Committee:

Professor Jashvant D. Unadkat

Pharmaceutics

Prediction of in vivo drug clearance (CL) is an important aspect of drug discovery and development. Our ability to predict *in vivo* hepatic metabolic clearance and metabolic drug-drug interactions from in vitro studies using liver microsomes, cytosols, and hepatocytes has been relatively successful. However, prediction of transporter-mediated clearance remains a challenge. Even where primary cells like hepatocytes (suspended, plated and sandwich-cultured hepatocytes) are available, they do not predict well the *in vivo* transporter-mediated clearance of drugs for the following reasons. First, transporters are transmembrane proteins and functional only when present on the plasma membrane. Because purified protein standards for transporters are not available, methods need to be developed to not only quantify the total abundance of these proteins, but also the plasma membrane abundance (PMA) of these transporters. Second, it is not clear if transporter abundance (total or PMA) in primary cells (e.g. human hepatocytes) faithfully

replicates that in human tissues. Third, primary cells (e.g. hepatocytes) are not readily available for all organs of interest (intestine, kidney, brain). Fourth, transporter-mediated clearance of drugs is a complex interplay between multiple transporters and metabolism. For example, hepatic or renal clearance of drugs can occur by multiple transporters located on different faces of the hepatocytes and kidney epithelial cells. Thus, the rate-determining steps in their clearance could be their uptake into the tissue (sinusoidal or kidney epithelial basal transporters), or metabolism, or efflux (canalicular or kidney epithelial apical transporters) from the tissue. Based on the above information, there is an urgent need to develop methods to predict in vivo transporter-mediated CL of drugs that are high-throughput, inexpensive and utilize in vitro tools. Therefore, we have hypothesized "*In vivo renal/hepatic CL of drugs can be predicted by measurement of transporter protein abundance and activity in transporter-expressing cells as well as transporter protein abundance in kidney/hepatic tissues*".

The focus of this dissertation was to address the above hypothesis with studies to predict the hepatic uptake and renal secretory CL of rosuvastatin (RSV) and metformin, respectively. To do so, we first developed a LC-MS/MS-based quantitative cell-surface biotinylation methodology to measure the plasma membrane abundance in various cells including hepatocytes. Second, the total and PMA of transporters were used to generate REF to scale in vitro CL of these drugs in transporter-expressing cells to that in vivo. The predicted metformin renal secretory CL ($CL_{r,sec}$) using transporter-expressing cells was within the range of clinically observed $CL_{r,sec}$ of metformin. In contrast, the transporter-expressing cells underpredicted the in vivo hepatic uptake CL of RSV but well-predicted the uptake CL of RSV into hepatocytes. Though the reason for this underprediction is not known, it could be due to lower intrinsic uptake CL of RSV in transporter-expressing cells in the absence of plasma proteins. Nevertheless, the

predicted hepatic CL of RSV by transporter-expressing cells was better than that predicted by any of the hepatocyte models. Additional studies are warranted to investigate the effect of plasma proteins on the transporter-mediated CL of a drug to bridge the gap between observed and predicted CL of RSV. Collectively, our data suggest that transporter-expressing cells better predict transporter-mediated CL of RSV than human hepatocytes.

ACKNOWLEDGEMENTS

I never thought one of the most difficult parts of dissertation writing would be to say thank you to one and all for all kinds of help, support, understanding, encouragement, patience and motivation given by numerous people throughout the period of my time that took me to write this dissertation. To put in simple words, this thesis work could not have been possible all on my own. I am very grateful to all of you.

Special mention goes to my supervisor, Dr. Jashvant D. Unadkat. My Ph.D. has been an incredible experience and I thank Dr. Unadkat wholeheartedly, not only for his tremendous support, patience and consistent encouragement, but also for giving me so many wonderful opportunities. I appreciate all his contributions of time, ideas, and constructive criticism to make my Ph.D. experience productive and stimulating. The elation and passion he have for his research was contagious and motivational for me, even during tough times in the Ph.D. pursuit. I could not have imagined having a better advisor and mentor for my Ph.D study.

Besides my advisor, I would like to thank my thesis reading and doctoral supervisory committee members, Dr. Thummel, Dr. Wang, Dr. Prasad, and Dr. Nath for their insightful comments and encouragement, but also for their scientific guidance, support, patience and valuable time from their busy schedules, and of course the critical questions which made me to analyze my research from various perspectives. Each one of you encouraged and guided me every time I had a conversation with you. This feat was not possible without the unconditional support provided by Dr. Prasad with an amicable and positive disposition.

My sincere thanks also go to the faculty of Pharmaceutics and Medicinal Chemistry departments for nurturing a collaborative, inspiring and intense scientific environment to learn as a scientist.

I am also very grateful to all staffs of the Pharmaceutics and Medicinal Chemistry departments for helping me with all administrative issues that I had no clues about.

My deep appreciation goes out to all the present and past members of the Unadkat Lab. They all have been my endless source of friendship and moral boost in both my professional and personal life. In particular, I am grateful to Tot and Dr. Ishida for their unreserved support. Thanks to all my batch mates and friends, Mike, David, Eli, Jing and Alenka for all the fun and interesting academic discussions.

I am indebted to all my friends in Seattle who opened their homes to me during my time at the University of Washington and who were always so helpful in numerous ways. Special thanks to Pooja, Tanmay, and Areha.

I would like to express my gratitude to my parents-in-law Sadhana Kotasthane and Pramod Kotasthane for their unfailing emotional support. I also thank my brother-in-law Deodutt for his heartwarming compassion. No words can express the love, support and affection that I received from Aajoba and my late Aaji.

Finally, I would like to say a heartfelt thanks and the deepest gratitude to my grandparents, my parents, Urmila Singh and Vijay Bahadur Singh, my brother Amit and his wife Sushma, my niece Soumya and nephew Vikash for their unconditional love and support. My father is always the first person who believed in me to achieve anything that I ever dreamt in my life.

I owe thanks to a very special person, my wife, Anuja for her continued eternal love, support and understanding during my pursuit of Ph.D. that made the completion of thesis possible. You were always around at times I thought that it is impossible to continue, you helped me to keep things in perspective. I greatly value her contribution and deeply appreciate her belief in me. I appreciate my little boy Devashish for abiding my ignorance and the patience he showed during

my thesis writing. Words would never say how grateful I am to both of you. I consider myself the luckiest in the world to have such a lovely and caring family, standing beside me with their love and unconditional support.

DEDICATION

I would like to dedicate this doctoral thesis to my beloved family especially:

To my dear parents, Urmila Singh and Vijay Bahadur Singh, whose love, blessings, sacrifices and trust in me have helped me reach where I am today.

To my dear son, Devashish, and my wife, Anuja, for all their support, love and patience all through my journey of doctoral study.

TABLE OF CONTENTS

LIST OF FIGURES

LIST OF TABLES

Chapter 1. Introduction

1.1 PREDICTION OF TRANSPORTER-MEDIATED CLEARANCE: AN OVERVIEW

In the drug development process, the ability to predict the clearance (CL) and intracellular concentration of drugs is important to predict the first in human dose, the efficacy and/or toxicity of drugs, drug metabolizing enzyme (DME)/transporter-mediated drug-drug interactions (DDI), and the influence of pharmacogenetics on the disposition of drugs (DeGorter and Kim, 2009). Increasing literature data suggest that transporters can have a significant role in the absorption, distribution, metabolism and excretion (ADME) of drugs and their metabolites (Endres et al., 2006; Shugarts and Benet, 2009; Giacomini et al., 2010). In recent decades, many transporters important in drug disposition have been characterized due to advancement in human genome sequencing and proteomics. Transporters are transmembrane proteins that are present in many cells and organelles, controlling the flux of vital endogenous substrates like glucose transporters. The specificity of many of these transporters is not limited to physiological substrates, but also includes xenobiotics. Transporters expressed on the membranes of liver and kidney play an important role in renal/hepatobiliary CL of drugs and therefore control the intracellular concentration and disposition of many drugs such as statins, antihypertensives and antivirals (Giacomini et al., 2010; Hua et al., 2012; Kock and Brouwer, 2012).

While in vitro and in silico methods (e.g. physiologically based pharmacokinetic (PBPK) models) have been successfully developed to predict disposition of drugs cleared by metabolic enzymes (Fan et al., 2010), such methods are less well developed to predict transporter-mediated disposition of drugs (Giacomini et al., 2010). There are few examples of PBPK model to predict transporter-mediated CL (Watanabe et al., 2009; Varma et al., 2012; Mao et al., 2018), however most of the methods do an inadequate job of predicting transporter-mediated CL and some use

an empirical scaling factor for predicting in vivo CL from in vitro experiments and therefore cannot be generalizable to other drugs (Li et al., 2010; Jones et al., 2012).

To predict renal CL of drugs, there are generally three different approaches used namely, quantitative structure pharmacokinetic relationships (QSPKR) (Dave and Morris, 2015), allometric scaling (Paine et al., 2011) and relative activity factor (RAF) (Mathialagan et al., 2017). Unfortunately, these methods have several limitations, e.g., the RAF approach assumes that the reference drug and the drug(s) for which the prediction is made, is transported by the same single transporter and the rate-determining step in the clearance of the two drugs is identical. The limitations of QSPKR and allometry model are the dependence on the physicochemical transporters alone and interspecies difference in the transporter affinity and abundance respectively.

Likewise, the same in vitro or in silico approaches have been used to predict in vivo hepatic clearance, but without much success. One of the most commonly used in vitro method is to predict hepatic CL of drugs is the use of hepatocytes, either suspended (SH), plated (PH), or sandwich-cultured human hepatocytes (SCHH) (Ghibellini et al., 2007). However, there are consistent reports in the literature about underprediction of the hepatic uptake CL of drugs using SCHH (Chiba et al., 2009; Jones et al., 2012), probably due to the difference in the transporter abundance in the in vitro systems and in vivo. Also, this method has a number of other shortcomings, primarily high cost, and low throughput. In addition, tissue derived primary cell-based approach (like SCHH) cannot be extended to disposition of drugs by other tissues, such as the intestine or kidneys, because primary cells of these tissues are currently not routinely available nor validated. Thus, alternative in vitro methods to predict in vivo transporter-mediated CL of drugs are needed. These methods ideally should be independent of the need to have access

to primary cells from the organ of interest and should not need to make assumptions about the transporters involved or the rate-determining step in the CL of the drug. In fact, this method should provide information on the rate-determining step since this information is absolutely necessary to predict the in vivo CL of the drug as well as the potential for DDI or genetic polymorphism to affect the in vivo CL of the drug. Moreover, identifying the rate-determining step can also help predict the unbound tissue concentration of the drug as it will differ from the unbound plasma concentration of the drug due to the presence of transporters. Therefore, the central hypothesis of this thesis is:

In-vivo renal/hepatic CL of drugs can be predicted by measurement of transporter protein abundance and activity in transporter-expressing cells as well as transporter protein abundance in kidney/hepatic tissues.

This hypothesis is developed on the following assumptions: 1) the identity of the transporters involved in the CL of the drug is known or can be identified using transporter-expressing cells; 2) since it is the transporters present on the cell surface that are active, the plasma membrane abundance (PMA) of the transporters in transporter-expressing cells and in the tissue of interest can be quantified using methods such as quantitative proteomics; 3) the transporter activity (K_m) or the catalytic activity (k_{cat}) of the transporter-drug interaction does not change from transporter-expressing cells to in vivo. That is the mechanism of transport in vivo is conserved/replicated in transporter-expressing cells. Since the liver and the kidney are the two most important organs for drug CL, the focus of this thesis will be to predict transporter-mediated clearance of drugs via these organs. To test our hypothesis, we have chosen to study two model drugs, rosuvastatin (RSV) and metformin. RSV is primarily cleared by excretion of the unchanged drug into the bile by multiple transporters. First, it is taken up by the sinusoidal

OATPs (OATP1B1, 1B3 and OATP2B1) and NTCP and then effluxed into the bile via BCRP and perhaps P-gp/MRP2. In contrast, metformin is primarily excreted unchanged in the urine by filtration and secretion, the latter via OCT2 and MATE1/MATE1-K located on the basal and apical membrane of the kidney epithelial cells.

1.2 SPECIFIC AIMS

We tested the above hypothesis with the following specific aims:

Aim 1 – **Chapter 2:** To develop and optimize a quantitative LC-MS/MS-based proteomics supported cell-surface biotinylation methodology to quantify the plasma membrane abundance (PMA) of transporter proteins in transporter-expressing cells and human hepatocytes.

Aim 2 – Chapter 3: To predict the renal secretory clearance ($CL_{r,sec}$) of metformin using OCT2-expressing HEK293 cells by using cell-surface biotinylation (obtained in aim 1) and REF.

Aim 3 – Chapter 4: To measure the total or plasma membrane hepatic transporter abundance in human liver, suspended (SH), plated (PH), and sandwich-cultured human hepatocytes (SCHH) and quantify the culture-dependent changes in such abundance.

Aim 4 – Chapter 5: To predict the in vivo hepatic uptake CL ($CL_{in\ vivo,\ blood}$) of RSV using the REF approach and transporter-expressing cells (IVIVE) and compare the prediction with that obtained by using the human hepatocyte models (SH, PH and SCHH) and the traditional IVIVE scaling approach. In addition, we will predict the intrinsic uptake CL of RSV by the hepatocyte models from transporter-expressing cells (i.e. in vitro cells to in vitro hepatocyte extrapolation, IVCIVH).

1.3 BACKGROUND

The majority of drugs or their metabolites are primarily eliminated from the body either by liver or by the kidneys. Drug elimination from the liver consists of multiple sequential steps such as hepatic uptake, metabolism, and/or biliary excretion, which can be counteracted by sinusoidal efflux. Similarly, drugs or metabolites, which are polar in nature with a high aqueous solubility, are eliminated by the kidneys by glomerular filtration, tubular secretion and reabsorption. For those drugs, which are targeted to the liver (statins, anti-HCV) or kidneys, the magnitude of hepatic/renal uptake and biliary excretion/net secretion will determine the drug concentrations in the hepatocytes/kidney epithelial cells respectively and thus any efficacy or toxicity of drugs to these cells. The CL of a drug through a particular pathway (e.g. hepatic or renal secretion) can be determined by the rate-determining step, i.e. uptake CL of the drug into the tissue, the metabolic and /or biliary/renal apical secretion of the drug or all of the above (Patilea-Vrana and Unadkat, 2016; Patilea-Vrana and Unadkat, 2018). For example, if the rate-determining step is the hepatic uptake of the drug, then the systemic hepatic CL of the drug will equal the uptake CL of the drug. Indeed, this appears to be the case for RSV and metformin. That is the hepatic and renal secretory CL of RSV and metformin can be predicted from their respective uptake CL into the liver and kidney epithelial cells, respectively. Thus, the aims of this thesis are designed to predict, using transporter-expressing cells and REF, the hepatocyte and kidney epithelial cell uptake CL of RSV and metformin respectively. Our *a priori* criteria for success was to predict these CL within 2-fold of the observed values.

To date, many in vitro and in silico tools have been tested to predict in vivo transporter-mediated CL of drugs, without much success. Gandhi and Morris have used the physicochemical characteristics of drugs to build a QSPKR model to predict biliary efflux clearance of drugs in

rats (Gandhi and Morris, 2012). However, the biliary efflux clearance prediction was poor due to the diverse physicochemical nature (anions, cations, and neutrals) of selected drugs, including many which are substrates of hepatic uptake and/or efflux transporter. The QSPKR methodology was also tested for the prediction of in vivo renal CL of drugs (Dave and Morris, 2015). There are multiple QSPKR-based models created based on net absorption, net secretion, and on the basis of specific transported substrates. These models do not predict the mechanism of transport thus are unable to delineate the contribution of individual transporter if more than one transporter is involved in the active transport of a drug. Due to the above mentioned reasons, this QSPKR methodology will not be able to predict DDI or effect of polymorphic transporter on the renal CL of drugs (Dave and Morris, 2015). Another methodology used to predict transporter-mediated CL in human is allometric scaling by using data obtained in preclinical species. In one such attempt, when biliary clearance values of drugs determined in rats were scaled to humans based on body weight, the predicted biliary clearance was about 9 to 2500-fold higher than the observed biliary clearance (Grime and Paine, 2013). When allometry scaling was used to predict renal CL in humans using rats and dogs, the predicted renal CL from rats was more discrepant with the human data than that predicted from dogs (Paine et al., 2011). However, these findings are not surprising and it is well known that there are significant differences in transporter abundance (Wang et al., 2015) and activity between preclinical species and humans (Chu et al., 2013; Liao et al., 2018). The use of RAF approach for the prediction of hepatic/renal clearance is an attractive and simple method, but it works when the drug of interest is a substrate of only one transporter and in vivo data on hepatic/renal CL of a reference drug are available in humans. Often the latter are not available. Even where available, this approach often cannot be used since multiple transporters (e.g. OATPs, OATs) are involved in the hepatic/renal CL of many drugs.

Thus, this limitation poses a significant obstacle to using this method, especially because each drug will have different fraction transported (ft) by the transporters and this may differ from that for the reference drug (Mathialagan et al., 2017).

The most common in vitro approach to predict in vivo transporter-mediated hepatic clearance is the use of hepatocytes. Similar in vitro system for kidneys (i.e. kidney epithelial cells) are currently not routinely available nor validated. Among hepatocyte models, the sandwich-cultured hepatocyte (SCH) model is frequently used to predict in vivo biliary clearance of drugs, while suspended (SH) and plated (PH) are routinely used to predict in vivo hepatic uptake clearance. Unfortunately, none of the hepatocyte models have been shown to provide a reasonable prediction (within 2-fold of the observed CL) of in vivo transporter-mediated hepatic uptake or biliary efflux clearance without using an empirical scaling factor (Li et al., 2010; Jones et al., 2012; Zou et al., 2013). Jones et al used SCHH model to predict in vivo hepatic uptake CL of 7 drugs. The in vivo hepatic uptake CL was about 58-fold (range: 12 to 161-fold) underpredicted (Jones et al., 2012). Similarly, Zou et al., 2013 have used an empirical scaling factor of 10.2 to predict biliary clearance of drugs in sandwich-cultured rat hepatocytes (SCRH).

Due to the above-mentioned challenges, alternative methods need to be explored to predict in vivo transporter-mediated clearance of drugs. Western blot has been used to generate transporter abundance-based scaling factor from transporter-expressing cells to hepatocytes (Hirano et al., 2004), but in absence of purified transporter protein standard, this technique is semi-quantitative in nature. Recently, due to advancement in LC-MS/MS-based proteomics, our ability to measure the transporter protein abundance in in vitro systems and ex vivo tissues is now feasible (Prasad et al., 2013; Prasad et al., 2014; Prasad and Unadkat, 2014b; Prasad et al., 2016; Wang et al., 2016). The application of this technique was instrumental in identifying one

possible reason for the underprediction of transporter-mediated CL of drugs in rats. The hepatic transporter abundance in sandwich-cultured rat hepatocytes (SCRH) was considerably lower than in rat liver tissues (Kotani et al., 2011; Ishida et al., 2018). When the change in hepatic transporter abundance in rats was taken into consideration, the REF-based IVIVE of RSV hepatic uptake clearance from transporter-expressing cells successfully predicted the in vivo hepatic uptake CL of the drug in rats. Likewise, using LC-MS/MS-based proteomics, transporter-expressing cells successfully predicted pitavastatin (PTV) intracellular accumulation in SCHH (Vildhede et al., 2016).

Whether the difference in hepatic transporter abundance in SCHH and human liver is the reason for the underprediction of transporter-mediated hepatic CL of drugs in humans is not known. Transporters are transmembrane proteins, synthesized in endoplasmic reticulum, undergone post-translational modifications, and later translocated to the plasma membrane of the cells. In this process, transporters are susceptible to internalization on external or internal stimuli (Murray and Zhou, 2017). In addition, almost all of the IVIVE studies mentioned above where REF approach was used, total transporter abundance, and not the PMA was used. Therefore, before proceeding to use the REF approach for IVIVE of hepatic and renal uptake CL of metformin, in the next chapter (Chapter 2), we describe the refinement of the cell-surface biotinylation method to quantify the PMA of transporters in transporter-expressing cells and human hepatocyte models.

1.4 MODEL DRUGS SELECTED FOR IVIVE OF RENAL AND HEPATIC CL USING THE REF APPROACH

Metformin was selected as a model drug for the prediction of $CL_{r,sec}$. Metformin has a biguanide structure and is used for the treatment of type 2 diabetes. Though the site of action of metformin

is in the liver, it is almost exclusively eliminated by kidneys. The reasons for the selection of metformin as a model drug were as follows:

a. It is exclusively eliminated unchanged by the kidneys i.e. it does not undergo metabolism
b. Clinical studies in humans indicate that metformin's net renal secretory clearance is greater than its glomerular filtration CL. This renal secretory CL is mediated by OCT2-mediated uptake at the basolateral membrane of the kidney epithelial cells (please see chapter 3 for details).
c. Literature evidence suggests that the rate determining in the renal secretory CL of metformin is its OCT-mediated uptake into the kidney epithelial cells (Kusuhara et al., 2011; Song et al., 2016) (for more details see Ch 3).

RSV was selected as our 2nd model drug for IVIVE and IVCIVH. RSV is a cholesterol lowering drug and is eliminated from the body mostly as the unchanged drug (Martin et al., 2003b). Renal CL (13.6 L/hr) of RSV is about 28% of its IV plasma CL (48.9 L/hr) (Martin et al., 2003a). Thus, the hepatic CL of RSV is 35.3 L/hr. RSV hepatic uptake is by OATPs and NTCP transporters with minimal contribution from passive diffusion. Therefore, it is not surprising that in DDI studies with metabolic enzyme inhibitors (itraconazole, clarithromycin) , the increase in plasma RSV AUC is minimum (< 2-fold) (Prueksaritanont et al., 2017), but is considerably higher (2-13 fold) in the presence of hepatic transport inhibitors (rifampin, cyclosporine, faldaprevir) (Simonson et al., 2004; Huang et al., 2017; Prueksaritanont et al., 2017). These data suggest that RSV hepatic CL is the rate-determining step in its in vivo hepatic CL (see Chapter 5 for details).

1.5 METHODOLOGY TO ISOLATE PLASMA MEMBRANE AND QUANTIFY PMA OF TRANSPORTERS

We and others have shown that transporters can be located in membranes other than PMA (Bow et al., 2008; Kock and Brouwer, 2012; Kumar et al., 2015). Although cell-surface biotinylation is an established method, to date it has been used mostly for qualitative estimation of PMA of proteins using Western blotting (Cole et al., 1987). Therefore, we optimized this method to isolate pure plasma membrane fraction and then quantify the PMA of transporters using quantitative proteomics. The method was optimized for the membrane impermeable biotinylation reagent (sulfosuccinimidyl-2-[biotinamido]ethyl-1,3-dithiopropionate (EZ-Link Sulfo-NHS-SS-Biotin)) concentration, incubation time and temperature and the use of neutravidin columns. The optimized plasma membrane biotinylation study was used to quantify the PMA of OCT2 in HEK293 and MDCKII cells (specific aim 2: chapter – 3), OATP1B1 in plated OATP1B1-expressing CHO, MDCKII and HEK293 cells, OATP1B3 in plated OATP1B3-expressing HEK293 cells, OATP2B1 in plated OATP2B1-expressing MDCKII cells and NTCP in plated NTCP-expressing CHO cells (specific aim 3: chapter – 4) (Kumar et al., 2017). In addition it was used to quantify the PMA of hepatic transporters in hepatocyte models (SH, PH and SCHH) (Specific aim 3: Chapter – 4) (Kumar et al., 2019a). Then, these PMA data were used for IVIVE of metformin renal secretory CL in humans (specific aim 2: chapter – 3) (Kumar et al., 2018) and RSV hepatic uptake CL in humans using the REF approach (specific aim 4: chapter – 5).

1.6 PREDICTION OF RENAL SECRETORY CL OF METFORMIN

The goals of our study were to determine 1) if transporter-mediated in-vivo renal secretory CL ($CL_{r,sec}$) of metformin can be predicted using the abundance and activity of OCT2 in OCT2-expressing cell lines (HEK293 and MDCKII) as well as OCT2 abundance in the human

kidney cortex; and 2) whether this prediction could be improved by quantifying OCT2 abundance in the plasma membrane of OCT2-expressing cells. The difference in the transport mechanism (plasma membrane potential) of OCT2 transporter between in vivo and in vitro system was also utilized for IVIVE (see Chapter 3 for details).

1.7 DETERMINATION OF TOTAL OR PMA OF TRANSPORTERS IN THE HEPATOCYTES MODELS

The importance of using the plasma membrane transporter abundance in the IVIVE of metformin $CL_{r,sec}$ in chapter 2 instigated the determination of the plasma membrane transporter abundance in the hepatocyte models. Transporters are membrane proteins and contribute to the uptake or efflux activity only when present in the plasma membrane of cells. As mentioned above, the underprediction of hepatic uptake CL of drugs in humans could be due to the low total abundance (or PMA) of hepatic uptake transporters in hepatocyte models vs. liver tissue (Kotani et al., 2011; Ishida et al., 2018). Therefore, the total or plasma membrane hepatic transporter abundance was measured in human liver, SH, PH and SCHH (Specific Aim 3- chapter 4). Since these hepatocyte models are routinely used to determine transporter-mediated CL of drugs, it is important to quantify whether the abundance of drug transporters (total or PMA) differs between the three models and how it compares with the tissue from which the hepatocytes are derived. Data from these experiments will inform the user as to which hepatocyte models to use for their research.

1.8 IN VITRO TO IN VIVO EXTRAPOLATION (IVIVE) AND IN VITRO CELLS TO IN VITRO HEPATOCYTES EXTRAPOLATION (IVCIVH) OF RSV HEPATIC CL

The primary goal of this aim was to predict the in vivo hepatic CL of RSV ($CL_{in\ vivo,blood}$) from transporter-expressing cells using the REF approach (i.e. IVIVE) and compare it with the

observed $CL_{in\ vivo,blood}$ obtained after intravenous administration of RSV (Martin et al., 2003a). A secondary goal was to compared the REF approach with the traditional approach of predicting the $CL_{in\ vivo,blood}$ from the hepatocyte models. In addition, the REF approach based on transporter-expressing cells was used to predict the RSV intrinsic uptake CL ($CL_{int,uptake,hep}$) in hepatocyte models (IVCIVH). This comparison was done in case both the transporter-expressing cells and hepatocyte models underpredicted $CL_{in\ vivo,blood}$. In that event, if the IVCIVH was found to be successful, such a result would indicate the observed underprediction by IVIVE was due to some in vivo factors not present in vivo (see Chapter 5 for details). The comparison of $CL_{in\ vivo,blood}$ by the various hepatocyte models would also help to guide the best hepatocyte model (i.e. SH, PH or SCHH) for IVIVE. The IVIVE approaches described above are based on following assumptions. First, that the $CL_{in\ vivo,blood}$ is the rate-determining step in the hepatic CL of RSV. Second, the affinity (K_m) or k_{cat} (catalytic turnover) of RSV by the transporters is not different between in vitro and in vivo.

1.9 INTRODUCTION SUMMARY

In vivo transporter-mediated CL of drugs from in vitro systems has historically been underpredicted (Li et al., 2010; Jones et al., 2012). Therefore, the principle goal of this thesis (and the chapters to follow) was to generate data to begin to test the hypothesis that transporter-expressing cells and the REF approach can successfully predict transporter-mediated CL of drugs. If successful, our approach could be extended to predict the disposition/absorption of any drug where transporters are involved (e.g. intestine, kidney, brain) or when transport and metabolism are simultaneously involved. Of course, before doing so, the success of the REF approach would need to be tested with other drugs. Also, our approach could be used to predict tissue concentrations of drugs (without imaging), provided the various CL of the drug associated

with the influx and efflux into and out of the tissue was successfully predicted using transporter-expressing cells and REF. Thus, our proposed approach has the potential to help predict the rate-determining step of CL of drugs, the tissue drug concentrations and therefore their efficacy and/or toxicity including in the presence of drug interactions or genetic polymorphism. Collectively, our approach has the potential to significantly improve the pace of drug development.

Chapter 2. Optimization and Application of a Biotinylation Method for Quantification of Plasma Membrane Expression of Transporters in Cells

2.1 ABSTRACT

Quantitative proteomics, using LC-MS/MS, is increasingly used to quantify drug transporters present in tissues and cells. Most of these investigations quantify total transporter expression in the cells by utilizing a total membrane fraction, not only the plasma membrane. Here, we report development and optimization of a biotinylation method to quantify protein expression of transporters in the plasma membrane of cells.

The Pierce (Thermo Scientific, Rockford, IL) cell surface isolation protocol was optimized for plasma membrane isolation. Incubation of OATP1B1 expressing CHO cells with 0.78 mg/mL of membrane impermeable biotinylation reagent (sulfo-NHS-SS-biotin) at 37 °C for one hour resulted in optimum isolation of plasma membrane. Subsequently, the expression of transporters in the plasma membrane as a percent of the total was determined by quantitative proteomics using LC-MS/MS.

Mean (±SD) plasma membrane expression of OATP1B1 in plated OATP1B1-expressing CHO, MDCKII and HEK293 cells was found to be 79.7 (±4.7)%, 67.7 (±12.2)% and 65.3 (±6.8)% of total cell OATP1B1 expression. Mean (±SD) plasma membrane expression of OATP1B3 in plated OATP1B3-expressing HEK293 cells, OATP2B1 in plated OATP2B1-expressing MDCKII cells and NTCP in plated NTCP-expressing CHO cells was 63.2 (±1.6)%, 37.1 (±15.7)% and 71.7 (±1.2)% respectively. This method of quantifying transporter protein expression in plasma membrane will be useful to predict transporter-mediated drug disposition.

2.2 INTRODUCTION

Quantitative proteomics, using LC-MS/MS, is increasingly used to quantify drug transporters present in tissues and cells. Most of these investigations quantify total transporter expression in the cells by utilizing a total membrane fraction, not only the plasma membrane. Here, we report development and optimization of a biotinylation method to quantify protein expression of transporters in the plasma membrane of cells.

The Pierce (Thermo Scientific, Rockford, IL) cell surface isolation protocol was optimized for plasma membrane isolation. Incubation of OATP1B1 expressing CHO cells with 0.78 mg/mL of membrane impermeable biotinylation reagent (sulfo-NHS-SS-biotin) at 37 °C for one hour resulted in optimum isolation of plasma membrane. Subsequently, the expression of transporters in the plasma membrane as a percent of the total was determined by quantitative proteomics using LC-MS/MS.

Mean (±SD) plasma membrane expression of OATP1B1 in plated OATP1B1-expressing CHO, MDCKII and HEK293 cells was found to be 79.7 (±4.7)%, 67.7 (±12.2)% and 65.3 (±6.8)% of total cell OATP1B1 expression. Mean (±SD) plasma membrane expression of OATP1B3 in plated OATP1B3-expressing HEK293 cells, OATP2B1 in plated OATP2B1-expressing MDCKII cells and NTCP in plated NTCP-expressing CHO cells was 63.2 (±1.6)%, 37.1 (±15.7)% and 71.7 (±1.2)% respectively.

This method of quantifying transporter protein expression in plasma membrane will be useful to predict transporter-mediated drug disposition.

2.3 MATERIALS AND METHODS

2.3.1 *Chemicals and Reagents*

Synthetic signature peptides for OATP1B1, OATP2B1, OATP1B3, NTCP and Na^+- K^+ ATPase were obtained from New England Peptides (Boston, MA). The corresponding stable isotope labeled (SIL) peptides for OATP1B1, OATP2B1, OATP1B3, NTCP and Na^+- K^+ ATPase, protein quantification BCA assay kit, dithiothreitol (DTT), iodoacetamide (IAA), MS grade trypsin, DMEM (Dulbecco's Modified Eagle Medium) high glucose medium (Gibco, Life Technologies), DMEM low glucose medium (Gibco, Life Technologies), DPBS (Dulbecco's Phosphate-Buffered Saline), Hank's Balanced Salt Solution (HBSS), and Pierce cell surface protein isolation kit were obtained from Thermo Scientific (Rockford, IL). Human albumin was procured from Calbiochem (Temecula, CA). Pierce cell surface protein isolation kit contains sulfo-NHS-SS-biotin, quenching solution (100 mM glycine), lysis buffer, neutravidin agarose gel, wash buffer, column accessory pack, DTT, phosphate buffer and Tris buffer. Composition of lysis buffer and wash buffer was not disclosed in the Pierce cell surface protein isolation kit. All reagents were analytical grade.

2.3.2 *Transporter-expressing cell lines*

OATP1B1-expressing CHO and MDCKII cells were generously provided by Dr. Bruno Stieger, University Hospital Zurich, Switzerland and Dr. Markus Keiser, University of Greifswald, Germany, respectively. OATP1B1-expressing HEK293, OATP1B3-expressing HEK293, OATP2B1-expressing MDCKII and NTCP-expressing CHO cells were generously provided by SOLVO Biotechnology, Hungary.

2.3.3 *Cell culture*

Transporter-expressing cells: To isolate plasma membrane using biotinylation, transporter expressing cells were grown in T-75 cm2 flasks at a density of 1.4x106 cells per flask with 20 mL of low glucose (CHO cells) or high glucose (MDCKII, HEK293 cells) DMEM medium supplemented with 10% fetal bovine serum, 2 mM L-glutamine, 100 IU/mL penicillin, 100 mg/mL streptomycin. Medium was changed every 24 hours. Cells were incubated at 37 °C with 5% carbon dioxide in a humidified incubator for 2 days. Subsequently, for OATP1B1-expressing CHO and MDCKII cells, the medium was removed and replaced with DMEM medium containing 10 mM sodium butyrate for 24 hours (Kumar et al., 2015). The protocol for OTAP1B1-expressing HEK293, OATP2B1-expressing MDCKII, OATP1B3-expressing HEK293 and NTCP-expressing CHO cells did not recommend use of sodium butyrate.

2.3.4 *Biotinylation protocol for plasma membrane isolation*

The Pierce™ cell surface isolation protocol (to isolate plasma membrane) was optimized as described below (Fig. 2.1, 2.2). Recovery of Na^+- K^+ ATPase was used as a marker of plasma membrane. Briefly, at day 3 of cell culture, when confluency had been reached, the medium was removed, and cells were washed twice with 10 mL of DPBS buffer (pH 7.4) at 37 °C. The DPBS buffer was quickly replaced with 10 mL of varying concentrations of biotinylation reagent (sulfosuccinimidyl-2-(biotinamido) ethyl-1, 3-dithiopropionate; sulfo-NHS-SS-biotin). The cells were incubated with sulfo-NHS-SS-biotin for the duration and temperature listed below, to non-specifically biotinylate primary amines (e.g. lysine or arginine) or N-terminal primary amines of extracellular peptide residues in the plasma membrane. After the indicated time, the sulfo-NHS-SS-biotin solution was removed and the biotinylation reaction was quenched with 10 mL of DPBS buffer containing 500 µL of quenching solution (100 mM glycine). Then, cells were

scraped from the flask and centrifuged at 500 xg for 3 minutes at 4 °C. The supernatant was discarded, and the cell pellet was washed with 5 mL Tris saline buffer before further centrifugation at 500 xg for 3 minutes at 4 °C. After centrifugation, the supernatant was discarded and the cells were lysed in 500 µL lysis buffer (containing 2.5 µL protease inhibitor) by incubating them for 30 minutes on ice with intermittent vortexing and sonication (3 times, 5-10 seconds each, during 30 minutes incubation in ice). Sonication was done for a very short duration to ensure minimal or no inside-out membrane vesicle formation (Steck et al., 1970). The cell lysate was centrifuged at 10,000 xg at 4 °C to pellet intact nuclei and mitochondria. The supernatant of cell lysate [containing total cell membrane; sample no. 1] was collected and 375 µL of it was incubated (about 125 µL was stored at -80 °C for further proteomics analysis) at room temperature with end-over-end mixing in a column containing neutravidin resin for 1 hour. This column was then centrifuged (1,000 xg for 1 min) and the first centrifugate containing non-biotinylated membrane was collected [sample no. 2]. The column was washed three times with 400 µL, 250 µL, and 200 µL of wash buffer containing protease inhibitor (5 µL/ mL) [sample no. 3, 4 and 5] and centrifuged (1,000 xg for 1 min) after each washing. Each time, the centrifugate (also containing the non-biotinylated membrane) was collected and volume was measured accurately and stored at -80 °C for further proteomics analysis. Then, the biotinylated plasma membrane was eluted from the neutravidin resin column by incubating the column with 400 µL of elution buffer [sample no. 6], containing 50 mM DTT. DTT reduces the disulfide bonds, between the extracellular lysine or arginine residues and biotin, thus allowing the plasma membrane to elute. Then, the neutravidin resin column was washed twice with 250 µL and 200 µL of wash buffer [sample no. 7 and 8; also containing the plasma membrane] containing protease inhibitor (5 µL/ mL) followed by centrifugation (1,000 xg for 1 min). The centrifugate,

containing the plasma membrane, was collected and volume was measured accurately and stored at -80 °C for further proteomics analysis.

To ensure that biotinylated plasma membrane was not lost in sample 2, 250 µL of this centrifugate was incubated with another neutravidin resin column for 1 hour at room temperature. The column was centrifuged at 1,000 xg for 1 min [sample no. 9] then washed with 400 µL of wash buffer [sample no. 10] containing protease inhibitor (5 µL/ mL) and centrifuged (1,000 xg for 1 min). The centrifugate (containing non-biotinylated membrane) was collected and volume was measured accurately and stored at -80 °C for further proteomics analysis. The biotinylated plasma membrane was eluted from 2nd neutravidin resin column [sample no. 11] by centrifugation (1,000 xg for 1 min) and washed with 250 µL of wash buffer [sample no. 12]. Sample no. 1 contained the total cell membrane. The biotinylated plasma membrane was assumed to be contained in sample no. 6, 7, 8, 11 and 12 and the non-biotinylated membrane were assumed to be contained in sample no. 2, 3, 4 and 5.

Tot Bui Nguyen (Dept. of Pharmaceutics, University of Washington) helped me in conducting cell-surface biotinylation studies.

2.3.5 *Optimization of biotinylation experimental conditions*

a) Optimization of biotin reagent (sulfo-NHS-SS-biotin) concentration for plasma membrane isolation from OATP1B1-expressing plated CHO cells at 4 °C

OATP1B1-expressing CHO cells were plated at a cell density of 1.4x106 cells/ T-75 cm2 flask. Two flasks were used for each concentration of sulfo-NHS-SS-biotin reagent. Once the cells were confluent in three days, they were incubated with various concentrations (0.24 mg/mL, 0.78 mg/mL, 1.02 mg/mL, 1.26 mg/mL, 1.5 mg/mL, 1.98 mg/mL or 2.46 mg/mL) of the membrane impermeable biotinylation reagent (sulfo-NHS-SS-biotin) for one hr at 4 °C.

Then, the percent of OATP1B1, Na+- K+ ATPase and calreticulin (an endoplasmic reticulum (ER) marker) (Eggleton and Michalak, 2003) in the biotinylated plasma membrane fractions, at each sulfo-NHS-SS-biotin concentration, was compared.

b) **Optimization of incubation temperature**

To study the effect of incubation temperature on isolation of plasma membrane, biotinylation of cells was conducted at two different temperatures (4 °C and 37 °C) with plated OATP1B1-expressing cells. At day 3 of cell culture, OATP1B1-expressing CHO cells were incubated with 1.50 mg/mL of sulfo-NHS-SS-biotin for 1 hour at 4 °C and 37 °C. Then, the percent of OATP1B1, Na^+- K^+ ATPase and calreticulin in the biotinylated plasma membrane fraction was compared between 4 °C and 37 °C.

c) Optimization of biotin reagent concentration at 37 °C

This was conducted as described above for 4 °C, except that based on the data obtained at 4 °C only 0.24 mg/mL, 0.78 mg/mL and 1.5 mg/mL of sulfo-NHS-SS-biotin were used.

The above optimized biotinylation method was used to determine plasma membrane protein expression of OATP1B1 in OATP1B1-expressing CHO, MDCKII or HEK293 cells, OATP2B1 in OATP2B1-expressing MDCKII cells, OATP1B3 in OATP1B3-expressing HEK293 cells, and NTCP in NTCP-expressing CHO cells.

2.3.6 *Sample preparation for LC-MS/MS proteomics:*

The sample preparation method was as described previously (Wang et al., 2015). Twenty microliters of 2.0 mg/mL (or lower protein concentration) of the transporter expressing cell line or samples obtained through biotinylation experiments were mixed with 18 µL of 3% sodium deoxycholate (w/v), 6 µL DTT (100 mM), 15 µL of ammonium bicarbonate buffer (50 mM, pH

7.8) and 10 µL of human albumin (10 mg/mL). After incubation at 95 °C for 5 minutes, followed by cooling at room temperature, 6 µL of iodoacetamide (200 mM; an alkylating agent) were added to the mixture, followed by incubation at room temperature for 20 minutes in the dark. To concentrate the sample, ice-cold methanol (0.5 mL), chloroform (0.2 mL), and water (0.45 mL) were added to each sample. After centrifugation at 4 °C for 8 minutes at 13,000 xg, the pellet was washed once with ice-cold methanol (1.0 mL) and was dissolved in 55 µL of reconstituted solution (a mixture of 15 µL sodium deoxycholate 3% (w/v) and 40 µL ammonium bicarbonate buffer). Finally, the protein sample was digested with 20 µL of trypsin. Protein to trypsin ratio was 25:1 (w/w). After the 24-hour incubation at 37 °C, the digestion reaction was quenched by 30 µL of labeled peptide internal standard (SIL) cocktail (prepared in 80% acetonitrile in water containing 0.1% formic acid; final concentration of SIL: 0.1–0.25 nM). The samples were centrifuged at 5000 xg for 5 minutes at 4 °C, and 5 µL of the supernatant were introduced into the LC-MS/MS system.

2.3.7 *LC-MS/MS quantification of transporters and marker proteins*

The protein expression of OATP1B1, OATP2B1, OATP1B3, NTCP, plasma membrane marker (Na^+- K^+ ATPase) or ER marker (calreticulin) in cell lines were quantified using LC-MS/MS and surrogate peptides as described before (Prasad et al., 2013; Kumar et al., 2015) (Table 2.1). The chosen surrogate peptides were peptide sequences in the intracellular domain of the transporters and therefore should not be modified by the membrane impermeable sulfo-NHS-SS-biotin provided the transporters are predominantly present in the plasma membrane. The corresponding heavy labeled peptide was used as an internal standard. The MRM parameters for quantification of the subcellular marker proteins are shown in Table 2.1. Total protein concentration in individual samples was determined using the BCA protein assay kit (Thermo Fisher Scientific).

2.3.8 *Analytical method parameters*

Sciex 6500 triple-quadrupole mass spectrometer (Sciex, Framingham, MA, U.S.A.) coupled to the Water Acquity UPLC system (Waters Corporation, Milford, MA) operated in electrospray positive ionization mode was used for liquid chromatography-tandem mass spectroscopy (LC-MS/ MS) analysis of the signature peptides. The doubly charged parent to singly charged product transitions for the analyte peptides and their respective SIL peptides were monitored using optimized LC-MS/MS parameters (Table 2.1). The signature peptides and SIL peptide internal standards were separated on an Acquity UPLC HSS T3 Column, (1.8 µm, 2.1 mm X 100 mm) with a 0.2 µm Inlet frits (Waters, Milford, MA, USA). Mobile phases (0.3 mL/min) consisted of 0.1% formic acid in water (A) and 0.1% formic acid in acetonitrile (B). The gradient program for UPLC method for determination of OATP1B1, Na^+- K^+ ATPase and calreticulin in OATP1B1-expressing CHO/MDCKII/HEK293 cells in biotinylation study was: 0–2 minutes: 3% B; 2–9 minutes: 3–50% B; 9–9.5 minutes: 50–90% B; 9.5–10.5 minutes: 90% B; 10.5–11 minutes: 90–3%B; 11–14 minutes: 3–3%B including washing and re-equilibration for 3 minutes. The gradient program for UPLC method for determination of OATP1B3, OATP2B1, NTCP, Na^+- K^+ ATPase and calreticulin in OATP1B3 or OATP2B1 or NTCP expressing cells was: 0–2 minutes: 3% B; 2–20 minutes: 3–45% B; 20–23 minutes: 45–90% B; 23–24 minutes: 90% B; 24–24.5 minutes: 90–3%B; 24.5–28 minutes: 3–3%B including washing and re-equilibration for 3.5 minutes.

2.3.9 *Data analysis*

Determination of percent of transporters expressed in the plasma membrane

The aim of this study was to estimate the fraction of transporter expressed in the plasma membrane compared to the total cell expression. So, determination of the absolute transporter expression was not necessary. Therefore, for each sample from the biotinylation experiment, the

area ratio (analyte/internal standard area ratio) was multiplied by the volume of the sample and the obtained value was used for calculation of percent transporter expression in the plasma membrane (equation 1) and total protein recovery (equation 2). A single biotinylation experiment yielded 12 samples including the lysate, biotinylated, non-biotinylated and wash fractions (Fig. 2.2). The volume of every sample was measured accurately. The expression of OATP1B1, OATP1B3, OATP2B1, NTCP, Na^+- K^+ ATPase and calreticulin was quantified by measuring surrogate peptide response using LC-MS/MS in the tryptic digests of cell lysate, non-biotinylated membrane, biotinylated membrane and various associated wash fractions. Corresponding stable labeled peptides were used as internal standards to determine the area ratio of OATP1B1, OATP2B1, OATP1B3, NTCP and Na^+- K^+ ATPase in the samples obtained through biotinylation experiment (Table 2.1). For calreticulin, stable labeled internal standard was not available so, the area ratio was determined using the stable labeled internal standard of Na^+- K^+-ATPase. Samples containing biotinylated fraction had DTT (reducing agent), which interfered with protein estimation by BCA assay, so activity/expression could not be normalized to total protein. The recovery of each protein was calculated as total recovered in biotinylated plus non-biotinylated fractions expressed as a percent of that in the lysate.

Equation 1.

$$\text{Biotinylation (\%)} = \left(\frac{\sum(\text{area ratio} \times \text{volume (µL)}) \; of \; sample \; 6,7 \; and \; 8}{\text{Area ratio of sample no. } 1 \times 375 \text{ µL}} \times 100\right) + \left(\frac{\sum(\text{area ratio} \times \text{volume (µL)}) \; of \; sample \; 11 \; and \; 12}{\text{Area ratio of sample no. } 2 \times 250 \text{ µL}} \times 100\right)$$

Equation 2.

$$\text{Recovery (\%)} = \frac{\sum(\text{area ratio } \times \text{volume (µL)}) \; of \; sample \; 2,3,4,5,6,7 \; and \; 8}{\text{Area ratio of sample no. } 1 \times 375 \text{ µL}} \times 100$$

Statistical Analysis

Mann–Whitney U test was performed to test the statistical difference between plasma membrane expression of OATP1B1 in OATP1B1-expressing CHO, MDCKII cells and HEK293 cells.

2.4 RESULTS

2.4.1 *Optimization of biotinylation conditions to isolate plasma membrane from OATP1B1-expressing CHO cells*

The effect of sulfo-NHS-SS-biotin concentration, at 4 °C, on the yield of plasma membrane from OATP1B1 expressing cells: The recovery of OATP1B1 and Na^+- K^+ ATPase in the biotinylated plasma membrane fraction was markedly increased with increasing sulfo-NHS-SS-biotin concentration and appeared to plateau at 1.5 mg/mL of sulfo-NHS-SS-biotin (Fig. 2.3). Negligible presence of the intracellular protein, calreticulin, was observed in the plasma membrane fraction at all concentrations of sulfo-NHS-SS-biotin. Mass balance showed that the recovery of all three proteins was 87.5-115.5% irrespective of the sulfo-NHS-SS-biotin concentration.

Effect of incubation temperature (37 °C vs. 4 °C) on the yield of plasma membrane isolated from OATP1B1-expressing CHO cells at sulfo-NHS-SS-biotin concentration of 1.5 mg/mL: There was a substantial increase in biotinylation of plasma membrane at 37 °C vs. 4 °C, which was reflected in increased yield of OATP1B1 (90.4 % versus 58.0%) and Na^+- K^+ ATPase (80.2 % versus 53.5%) in the biotinylated fraction (data not shown). The corresponding yield of calreticulin remained low (<10%). Mass balance showed that the recovery of all three proteins

was 92.1-102.3%. Therefore, the incubation temperature of 37 °C was used in all subsequent biotinylation studies.

Optimization of sulfo-NHS-SS-biotin concentration, at 37 °C: The yield of plasma membrane, as measured by recovery of OATP1B1 (94.1%) and Na^+- K^+ ATPase (84.0%) in the biotinylated fraction, was maximal at 0.78 mg/mL of sulfo-NHS-SS-biotin (Fig. 2.4). The corresponding yield of the intracellular protein calreticulin remained negligible (<10%). Mass balance studies showed that the recovery of all three proteins was 101.8-117.2%. Consequently, 0.78 mg/mL of sulfo-NHS-SS-biotin and 37 °C was used in all subsequent biotinylation studies described below to determine the percent of a transporter expressed in the plasma membrane of cells expressing the transporter of interest.

2.4.2 *Quantification of percent of transporter expressed in plasma membrane of transporter-expressing cells, using the optimized biotinylation protocol*

Mean (± SD) Percent of OATP1B1 expressed in the plasma membrane of CHO, MDCKII and HEK293 cells was 79.7% (±4.7%), 67.7% (±12.2%) and 65.3 (±6.8%) respectively (Fig. 2.5). The percent of plasma membrane expression of OATP1B1 in MDCK or HEK293 was significantly lower than that in CHO cells. The percent of plasma membrane expression of OATP1B3 in HEK293 cells, OATP2B1 in MDCKII cells and NTCP in CHO cells was 63.2% (±1.6 %), 37.1% (±15.7%) and 71.7% (±1.2%) respectively (Fig. 2.6). Recovery of all proteins was found to be 79.4-115.7%.

2.5 DISCUSSION

For successful IVIVE of transporter-based clearance, it is important to quantify the protein expression of the transporter in the plasma membrane of cells (transfected or primary cells) vs.

the expression of the transporter in total cell membrane. If the latter does not equal the former, IVIVE of pharmacokinetics of a drug based on the total membrane transporter expression will lead to incorrect prediction of the plasma clearance and in vivo plasma and tissue concentrations of the drug. For IVIVE of the transporter-mediated clearance of a new chemical entity, prediction of clearance of the new chemical entity within ~2-fold of its ultimately determined clearance in a Phase 1 clinical trial during dug development would be acceptable, Therefore, we examined in whether plasma membrane expression of the investigated hepatic uptake transporters deviated substantially from 100% , a situation where there would be a need to add a correction factor (i.e. percent expressed in the plasma membrane) for IVIVE of transporter-mediated clearance.

Here, we report optimization of a biotinylation method for quantitative determination of the percent of a transporter protein expressed in the plasma membrane compared to its total cell expression. To conduct this optimization, we began with the biotinylation method recommended by the manufacturer (Prasad et al., 2013). Cell surface biotinylation method (or similar methods) has been previously used by others (Loder and Melikian, 2003; Powell et al., 2014; Sun et al., 2016) for relative quantification of plasma membrane expression of membrane proteins in cells, especially in studies where the protein has been genetically modified (Ho et al., 2004; Lee et al., 2005; Urquhart et al., 2008). To our knowledge, the manufacturer's protocol has been adopted by researchers without examining the optimal conditions for its application. Therefore, we optimized the method and coupled it to LC-MS/MS proteomics for absolute quantification of plasma membrane protein of interest as well as Na^+/K^+-ATPase (a plasma membrane marker protein) and calreticulin (an ER marker protein). The latter allowed us to confirm that the biotinylation reagent was indeed "plasma membrane impermeable". In addition, through mass

balance, we ensured that our method resulted in complete recovery of all the proteins quantified. Where this recovery was not within 100±25% of the total protein expression in the cell homogenate, the data were discarded.

We found that the optimized biotinylation protocol (0.78 mg/mL of sulfo-NHS-SS-biotin incubated for 1 hr with OATP1B1 expressing CHO cells at 37 °C) resulted in maximum yield of plasma membrane as measured by percent of OATP1B1 (94.1%) and Na^+- K^+ ATPase (84.0%) in biotinylated plasma membrane and negligible presence (<12%) of the intracellular protein, calreticulin, in the biotinylated fraction (Fig. 2.4). Loder et al. also found that plasma membrane expression of the dopamine transporter, in stably transfected PC12 cells, was greater at 37 °C (physiologically relevant temperature) than 4 °C in a biotinylation study (Loder and Melikian, 2003). They concluded that at 4 °C, the dopamine transporter was internalized. While that may also be true for OATP1B1, it is also possible that the biotinylation reaction was incomplete at 4 °C. But the latter hypothesis can be discounted as longer incubation times (> 2 hr) at 4 °C did not result in increased yield of the plasma membrane (data not shown). In all these experiments, the presence of calreticulin in the biotinylated plasma membrane fraction was minimal, indicating little intracellular penetration of the biotinylation reagent. Moreover, the percent of Na^+- K^+ ATPase in the plasma membrane closely tracked the percent of transporter expressed in the membrane. The optimal biotinylation conditions described here were confirmed in another cell line (HEK293 cells; data not shown). Although Na^+- K^+ ATPase is considered to be a plasma membrane marker, it is not surprising that its expression in the plasma membrane was not 100% as it is synthesized and trafficked to the plasma membrane.

Next, we determined if the percent of OATP1B1 in the plasma membrane was dependent on the host cell-line. A survey of the literature indicated that researchers typically use CHO, HEK293 or

MDCKII cells expressing OATP1B1. Our data show that OATP1B1 is predominantly expressed in the plasma membrane of all these cell lines (Fig. 2.5). The presence of calreticulin in the plasma membrane vs. total membrane fraction was less than 10.5%, indicated high purity of the plasma membrane preparation. Although the percent of OATP1B1 expressed in the plasma membrane of CHO cells was significantly higher than that in MDCKII and HEK293 cells, we do not consider this difference to be biologically significant. Though the biotinylation studies with OATP1B1-expressing CHO and MDCKII cells were conducted over a one-year period, the fraction of OATP1B1 expressed in plasma membrane to the total expression remained consistent over time.

Next, we determined the percent of OATP1B3, OATP2B1 and NTCP expressed in the plasma membrane when these transporters were expressed in HEK293, MDCKII or CHO cells respectively. These host cell lines (CHO, HEK293 and MDCKII) were used as they were the cells that were readily available to us and are frequently used by various pharmaceutical companies. The majority of OATP1B3 and NTCP were found to be expressed in the plasma membrane of these cells (Fig. 2.6). However, only 37% of OATP2B1 was expressed in the plasma membrane of MDCKII cells. Whether this is due to host cell-line or otherwise is not clear. OATP1B1 expression in MDCKII cells (65.3±6.8%) was comparable to that in HEK293 cells (67.7±12.2%) suggesting that the lower expression of OATP2B1 in MDCKII cells may not be a generalized host cell-dependent phenomenon. It has been shown through immunofluorescence microscopy study in human liver that OATP1B1, OATP2B1, and OATP1B3 are predominantly localized at the basolateral membrane and MRP2 is predominately located at the canalicular membrane (Kopplow et al., 2005). Therefore, IVIVE of transporter-

mediated clearance based on their expressions in cell lines will need a scaling factor based on the percent of the transporter expressed in the plasma membrane of these cells.

For drugs predominantly eliminated unchanged in the feces by the liver, the gold standard in vitro model to predict hepatobiliary clearance is sandwich culture human hepatocytes (SCHH). Yet, this in vitro model is reported to underpredict transporter mediated hepatic uptake clearance of drugs (Menochet et al., 2012). One proposed reason for this observation is that plasma or total transporter expression in SCHH differs from in vivo liver tissue (Kotani et al., 2011). However, determination of plasma membrane expression of transporters in liver tissues, using biotinylation, is not possible without isolating hepatocytes. This is because homogenization of tissue to determine transporter expression will result in rupture of the cells. Therefore, a solution for this problem is to assume that the percent of transporters expressed in the plasma membrane immediately after isolation of the cells (i.e. primary cells) represents the percent of transporters expressed in the plasma membrane in the corresponding tissue. This plasma membrane isolation technique through cell surface biotinylation is applicable to all mentioned cell lines (CHO, HEK293 and MDCKII) irrespective of the transporter expression level. The limiting step could be LC-MS/MS sensitivity in the case of very low expression of the transporter. It will be important to see if transporter-expression-based IVIVE of drug disposition based on such primary cells (e.g. cryopreserved human hepatocytes) is successful after determination of percent of transporter expressed in the plasma membrane.

In summary, we have described an optimized biotinylation method to quantify the plasma membrane expression of transporters (or for that matter any protein) in cell lines. This protocol should also be applicable to quantify plasma membrane expression of transporters in primary cells (e.g. human hepatocytes). In the future, it will be important to apply this technique to

determine if plasma membrane expression of drug transporters, other than OATP1B1, is independent of the host cell line. In addition, before others use the data presented above for the various transporters and cell lines, it will be important to demonstrate that these values are invariant across laboratories. Moreover, the optimized biotinylation technique presented here has utility beyond IVIVE of transporter-based clearance. This optimized biotinylation protocol could be used in the future to understand the impact of post-translational modifications, polymorphism, disease and drugs on trafficking of proteins to the plasma membrane.

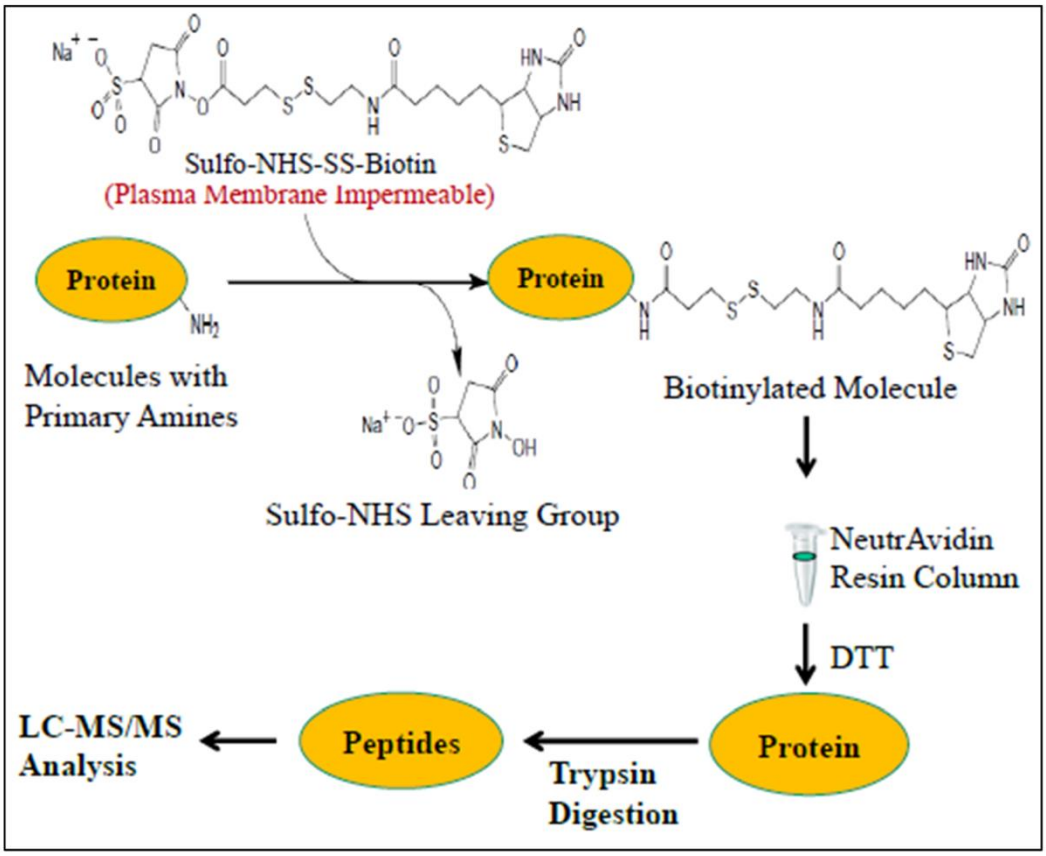

Fig. 2.1. Cell-surface Biotinylation Concept: Sulfo-NHS-SS-biotin is a thiol-cleavable amine-reactive plasma membrane impermeable biotinylation reagent. This reagent reacts non-specifically with all proteins, with free primary amines. Biotinylated membrane binds avidly to the neutravidin resin and the membrane can be subsequently eluted with DTT and the proteins contained in the membrane can be quantified by LC-MS/MS.

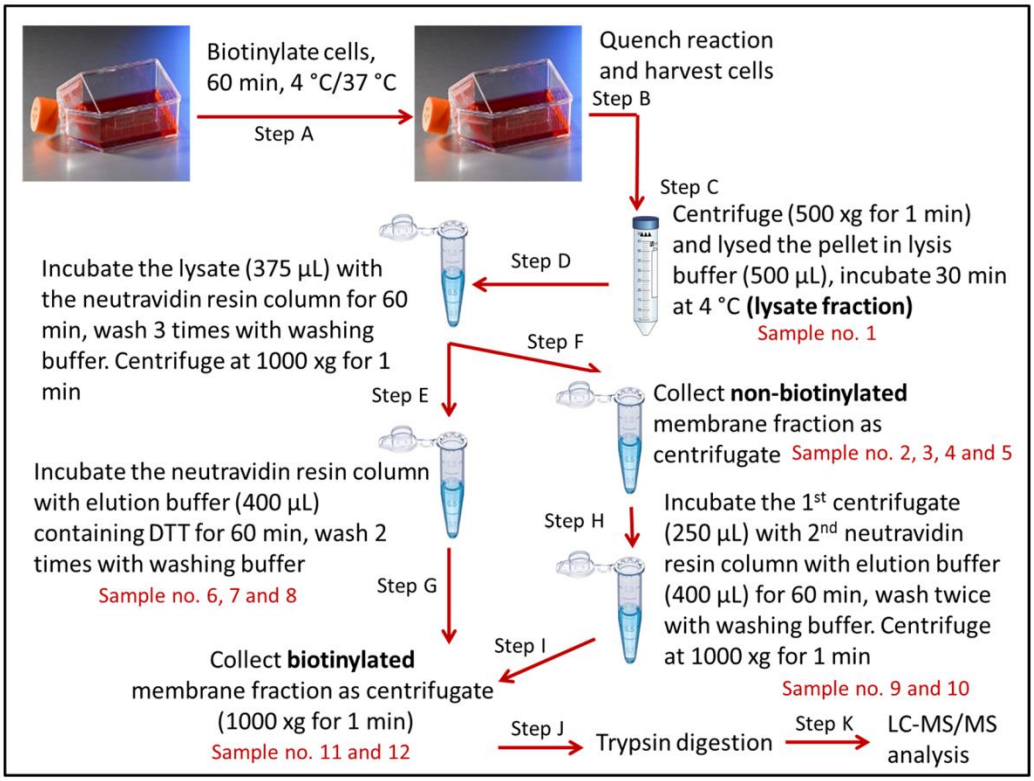

Fig. 2.2. Workflow of cell-surface biotinylation protocol: Transporter-expressing cells were incubated with the sulfo-NHS-SS-biotin reagent. Two neutravidin resin columns were used to maximize the yield of biotinylated membrane. Major steps (encircled in red) and all 12 samples generated from steps A-K are shown.

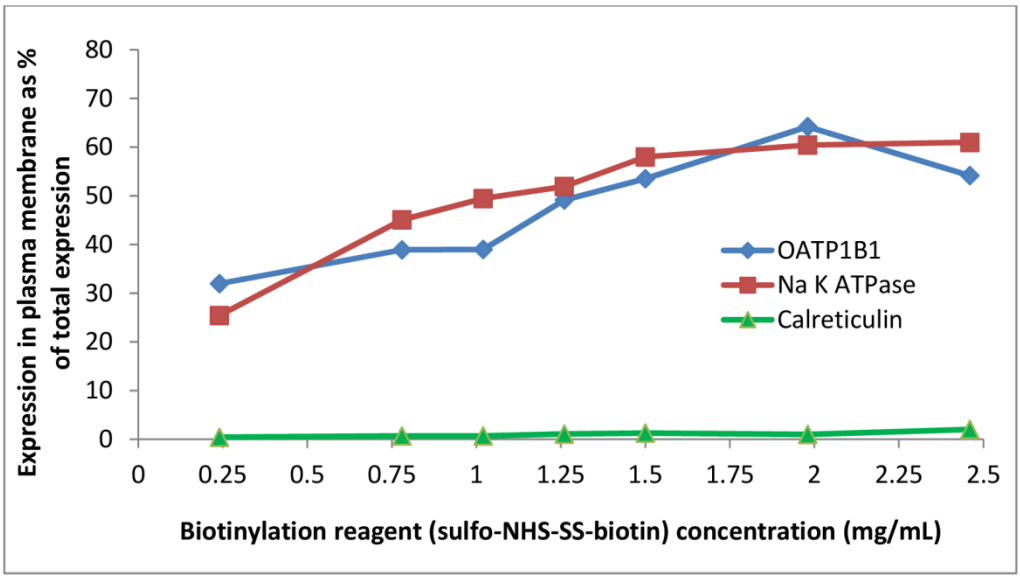

Fig. 2.3. Sulfo-NHS-SS-Biotin concentration-dependent biotinylation of plasma membrane of OATP1B1-CHO cells at 4 °C. Maximum biotinylation of plasma membrane was achieved with 1.5 - 1.98 mg/mL sulfo-NHS-SS-biotin concentration as evaluated by the presence of OAT1B1 and Na^+- K^+ ATPase in the biotinylated membrane. There was negligible presence of the intracellular protein, calreticulin, in the biotinylated plasma membrane. Data are average of two independent experiments. Recovery values for all proteins were between 87.5 and 115.5%.

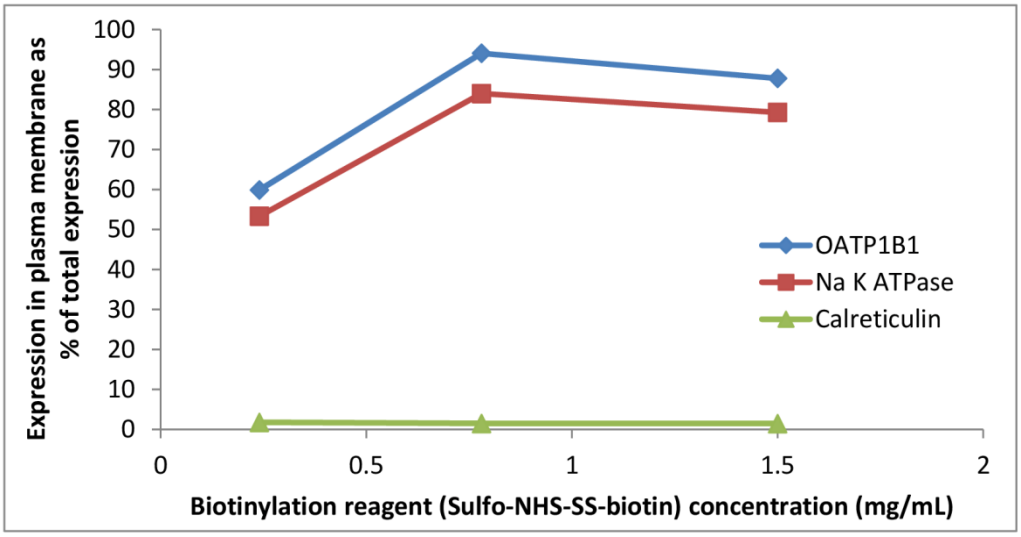

Fig. 2.4. Sulfo-NHS-SS-Biotin concentration-dependent biotinylation of plasma membrane of OATP1B1-CHO cells at 37 °C. Maximum biotinylation of plasma membrane was achieved with 0.78 mg/mL sulfo-NHS-SS-biotin as evaluated by the presence of OAT1B1 and Na^+- K^+ ATPase in the biotinylated membrane. There was negligible presence (<2%) of the intracellular protein, calreticulin, in the biotinylated plasma membrane. Recovery values for all proteins were 101.8-117.2%. Data are from one experiment at each sulfo-NHS-SS-biotin concentration conducted in singlicate.

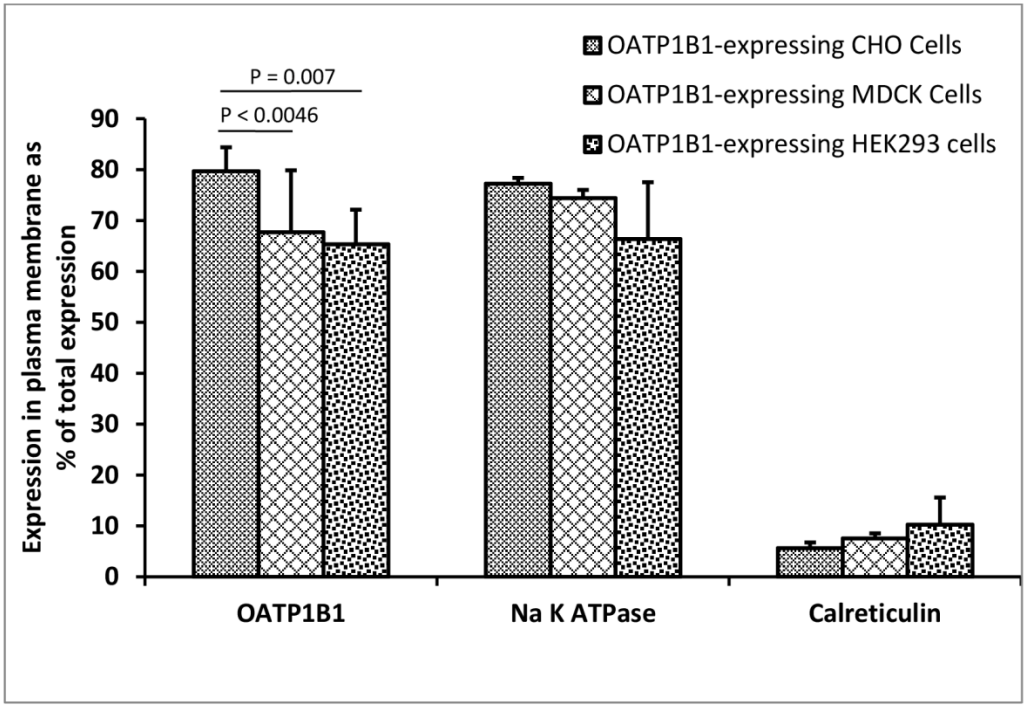

Fig. 2.5. Plasma membrane expression of OATP1B1 in OATP1B1-expressing CHO, MDCKII and HEK293 cells. Using optimal temperature and sulfo-NHS-SS-biotin reagent concentration, 79.7 (±4.7)%, 67.7 (±12.2)% and 65.3 (±6.8)% of total OATP1B1 was expressed in the plasma membrane of OATP1B1-expressing CHO, MDCKII and HEK293 cells respectively. Data are reported as mean ± S.D of 10 independent experiments for OATP1B1-expressing CHO and MDCKII cells and 3 independent experiments for OATP1B1-expressing HEK293 cells. Recovery values for all proteins were 85.8-114.6%. Data were analyzed using the Mann–Whitney U test.

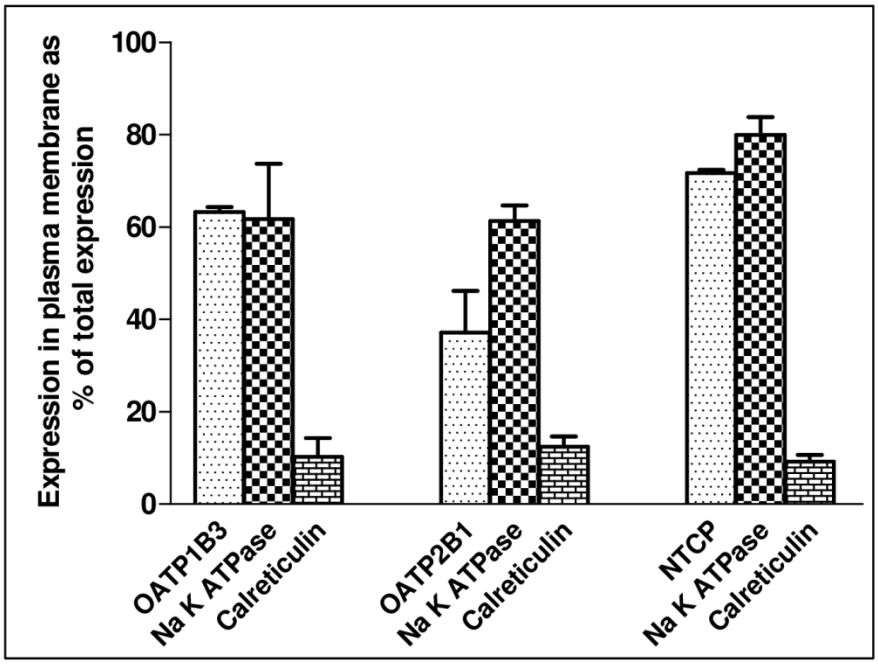

Fig. 2.6. Plasma membrane expression of OATP1B3 in OATP1B3-expressing HEK293, OATP2B1 in OATP2B1-expressing MDCKII and NTCP in NTCP-expressing CHO cells. Using optimal temperature and biotin reagent concentration, 63.2 (±1.6)%, 37.1 (±15.6)% and 71.7% (±1.2%) of total cell OATP1B3, OATP2B1 and NTCP was expressed in the plasma membrane of HEK293, MDCKII and CHO cell lines respectively. Data are reported as mean ± S.D of 3 independent experiments. Recovery values for all proteins were 79.4-115.7%.

Table 2.1. MRM Parameters Used for Quantification of Transporter and Marker Proteins

Protein	Surrogate Peptide	Parent ion (m/z)	Product ion (m/z)	Declustering potential (V)	Collision energy (V)
OATP1B1	NVTGFFQSFK	587.9	961.4	50	24
	NVTGFFQSF***K***	591.9	969.5		
OATP2B1	VLAVTDSPAR	514.8	816.4	60	26
	VLAVTDSPA***R***	519.8	826.4		
OATP1B3	NVTGFFQSLK	570.8	927.5	60	23
	NVTGFFQSL***K***	574.8	935.5		
NTCP	GIYDGDLK	440.7	710.3	58	24
	GIYDGDL***K***	444.7	718.3		
Na^+- K^+ ATPase	AAVPDAVGK	414.2	586.3	50	18
	AAVPDAVG***K***	418.2	594.3		
Calreticulin (CHO, MDCKII)	FYALSAR	414.2	517.3	50	19
Calreticulin (HEK293)	EQFLDGDGWTSR	705.8	893.4, 778.4	50	33

Bold letters indicate stable labeled amino acid residues. FYALSAR (CHO and MDCKII) and EQFLDGDGWTSR (HEK293) were two different surrogate peptides used in the study because of their species-dependent specificity.

Chapter 3. The Importance of Incorporating OCT2 Plasma Membrane Expression and Membrane Potential in IVIVE of Metformin Renal Secretory Clearance

3.1 ABSTRACT

Transporter expression, determined by quantitative proteomics, together with PBPK models is a promising approach for *in vitro* to *in vivo* extrapolation (IVIVE) of transporter-mediated drug clearance. OCT2-expressing HEK293 and MDCKII cells were used to predict *in vivo* renal secretory clearance ($CL_{r,sec}$) of metformin. [^{14}C]-Metformin uptake clearance in OCT2-expressing cells was determined and scaled to *in vivo* $CL_{r,sec}$ by using OCT2-expression in the cells vs. the human kidney cortex. Using quantitative targeted proteomics, the total expression of OCT2 in HEK293, MDCKII cells and human kidney cortex was 369.4±26.8, 19±1.1 and 7.6±3.8 pmol/mg cellular protein, respectively. The expression of OCT2 in the plasma membrane of HEK293 and MDCKII cells, measured using an optimized biotinylation method followed by quantitative proteomics, was 30.2% and 51.6%, respectively. After correcting for percent of OCT2 expressed in the plasma membrane and the resting membrane potential (mV) difference between the OCT2-expressing cells and the renal epithelial cells, the predicted $CL_{r,sec}$ of metformin was 250.7 mL/min, a value within the range of the observed $CL_{r,sec}$ of metformin. These data demonstrate the promise of using quantitative proteomics for IVIVE of transporter-mediated drug clearance and highlight the importance of quantifying plasma membrane expression of transporters and utilizing cells that mimic the *in vivo* mechanism(s) of transport of drugs.

3.2 INTRODUCTION

Transporters play an important role in drug absorption, distribution and elimination. When a drug under development or its active/toxic metabolite(s) has significant renal clearance,

prediction of its *in vivo* renal clearance from *in vitro* studies (IVIVE) is important to predict the first in human dose, systemic clearance of the drug, renal drug-drug interaction, and kidney epithelial cell drug concentrations. While the filtration clearance of a drug can readily be predicted from the average glomerular filtration rate and the fraction of drug unbound in the plasma, IVIVE of the renal secretory clearance of a drug is challenging. While allometry (Paine et al., 2011) or quantitative structure-activity relationship (Dave and Morris, 2015) have been used to predict the renal clearance of drugs, these methods do not account for involvement of transporters and therefore lack the ability to predict *in vivo* transporter-mediated renal secretory clearance ($CL_{r,sec}$) or renal transporter-mediated drug-drug interactions. Although, tools (e.g. primary kidney epithelial cells) to predict $CL_{r,sec}$ of a drug are becoming available, their predictive abilities have yet to be tested. Thus, alternate methods are needed to predict $CL_{r,sec}$ of a drug. We (Ishida et al., 2018), and others (Bosgra et al., 2014; Vildhede et al., 2016) have shown that transport activity of a drug in cell lines overexpressing the transporter(s) of interest can be used to predict transporter-mediated drug clearance if a scaling factor to account for differences in transporter expression in the cell line and in the tissue (e.g. kidneys) is considered. Theoretically, since it is the transporters at the plasma membrane that are responsible for the cellular uptake and/or efflux of drugs, quantifying such expression may improve IVIVE of drug clearance (Kumar et al., 2017). Therefore, as a proof of concept, the goals of our study were to determine 1) if transporter-mediated *in vivo* $CL_{r,sec}$ of metformin can be predicted within the range of the observed values using protein expression and transport activity of organic cation transporter 2 (OCT2) in OCT2-expressing cell lines (HEK293 and MDCKII) as well as OCT2 protein expression in the human kidney cortex; and 2) whether this prediction could be improved by incorporating plasma membrane expression of OCT2-expressing cells and the membrane

potential of these cells vs. human renal epithelial cells. We chose metformin as our model drug as literature evidence suggests (see discussion) that its $CL_{r,sec}$ is determined primarily by OCT2.

3.3 MATERIALS AND METHODS

3.3.1 *Chemicals and Reagents*

Synthetic signature peptides for OCT2 were obtained from New England Peptides (Boston, MA). The corresponding stable isotope labeled (SIL) peptides for OCT2 and Na^+-K^+ ATPase, total protein quantification bicinchoninic acid assay (BCA) kit, dithiothreitol (DTT), iodoacetamide (IAA), mass spectrometry grade trypsin, Dulbecco's Modified Eagle Medium (DMEM) with high glucose (Gibco, Life Technologies), Dulbecco's Phosphate-Buffered Saline (DPBS), Krebs-Ringer-HEPES (KRH) buffer, and Pierce cell surface protein isolation kit were obtained from Thermo Scientific (Rockford, IL). Pierce cell surface protein isolation kit contains sulfosuccinimidyl-2-(biotinamido) ethyl-1, 3-dithiopropionate (sulfo-NHS-SS-biotin), quenching solution (100 mM glycine), lysis buffer, neutravidin agarose gel, wash buffer, column accessory pack, DTT, phosphate buffer and Tris buffer. Metformin [biguanido-^{14}C] hydrochloride (98 mCi/mmol) was purchased from Moravek Biochemicals, Inc. (Brea, CA). ScintiVerse BD Cocktail liquid scintillant and HPLC-grade acetonitrile were purchased from Fischer Scientific (Fair Lawn, NJ). Cimetidine, metformin (hydrochloride salt) and formic acid were purchased from Sigma-Aldrich (St. Louis, MO). All reagents were analytical grade.

3.3.2 *Human kidney cortex and transporter-expressing cell lines*

Transplant quality human kidney cortices (for demographics see Supplementary Table 2S in Prasad et al., 2016) were obtained from Newcastle University, England (n = 5, randomly

selected). OCT2-expressing HEK293 and MDCKII cells were created as described previously (Yin et al., 2015; Yin et al., 2016).

3.3.3 *Measurement of OCT2 transporter uptake activity in HEK293 and MDCKII cells*

Transport studies were conducted in OCT2-expressing MDCKII and HEK293 cells with [^{14}C]-metformin with or without 1mM cimetidine (OCT2 inhibitor). For transport assays, OCT2-expressing MDCKII and HEK293 cells were grown in 24-well poly-D-lysine coated plates, at a density of 75,000 cells per well with 1 mL of high glucose DMEM medium (changed daily). At day 3, cells were washed with 1mL/well DPBS buffer and incubated at 37 °C with KRH buffer (5.6 mM glucose, 125 mM NaCl, 4.8 mM KCl, 1.2 mM KH_2PO_4, 1.2 mM $CaCl_2$, 1.2 mM $MgSO_4$, and 25 mM HEPES) containing 5.5 µM [^{14}C]-metformin with or without 1mM cimetidine (OCT2 inhibitor). After 2 minutes (when uptake is linear), the uptake (in triplicate) was terminated by washing the cells three times with ice-cold KRH buffer (1 mL each). Then, the cells were lysed with 0.5 mL 1 M NaOH at 37 °C for 2 hours and neutralized with 0.5 mL 1 M HCl. 30 µL of this lysate solution were used for total protein estimation using the BCA method and 200 µL were used to analyze total radioactivity by Tri-Carb Liquid Scintillation Counters (PerkinElmer). OCT2-mediated uptake was determined by the difference in the metformin uptake in the presence/absence of 1 mM cimetidine. The *in vitro* OCT2-mediated clearance of metformin was calculated as the ratio of OCT2-mediated uptake and metformin concentration in the media.

Metformin uptake study in OCT2-expressing HEK293 and MDCKII cells was conducted by Jia Yin from Dr. Joanne Wang lab, Pharmaceutics, University of Washington.

3.3.4 *LC-MS/MS quantification of total OCT2 expression in human kidney cortex as well as total and plasma membrane OCT2 expression in HEK293 and MDCKII cells*

Plasma membrane isolation from OCT2-expressing HEK293 and MDCKII cells: Plasma membranes from OCT2-expressing HEK293 and MDCKII cells were isolated in 3 and 2 independent experiments respectively, using a biotinylation methodology optimized in our laboratory (Kumar et al., 2017). Briefly, HEK293 and MDCKII cells were grown in 75 cm^2 flasks till 80-100% confluency and incubated with 10 mL of 0.78 mg/mL of sulfo-NHS-SS-biotin at 37 °C for one hour to biotinylate extracellular free primary amines (lysine or arginine) or N-terminal primary amines of extracellular peptide residues in the plasma membrane. After cell lysis, biotinylated plasma membranes were isolated using neutravidin resin columns.

Determination of percent plasma membrane expression of OCT2 in OCT2-expressing cells: The expression of OCT2, Na^+-K^+ ATPase, and calreticulin in the lysate, the non-biotinylated and the biotinylated fractions was quantified using LC-MS/MS (see below). Stable labeled internal standards of OCT2 and Na^+-K^+ ATPase unique peptides were used to determine the area ratio (analyte:SIL ratio) of the respective peaks in the samples obtained from the biotinylation experiment. For calreticulin, the stable labeled internal standard was not available and therefore the stable labeled internal standard of Na^+-K^+ ATPase was used to estimate the calreticulin peak area ratio (Kumar et al., 2017).

OCT2 total protein quantification in kidney cortex: Sample preparation and quantitative proteomics were performed as described previously (Prasad et al., 2016). Total protein content (wt/wt) in kidney cortex homogenate was quantified by BCA assay. OCT2 expression was determined in triplicate for each kidney cortex homogenate. Briefly, 20 µL of 2.0 mg/mL (or lower concentration) of the human kidney cortex or transporter-expressing cell line or samples obtained through biotinylation experiments was treated with 15 µL of ammonium bicarbonate

buffer (50 mM, pH 7.8), 18 µL of 3% sodium deoxycholate (w/v), 6 µL DTT (100 mM), and 10 µL of human albumin (10 mg/mL). Proteins present in the sample was denatured and disulfide bond between cysteine residues was reduced by incubation at 95 °C for 5 minutes, followed by the addition of 6 µL of IAA (200 mM; an alkylating agent) and treatment with ice-cold methanol (0.5 mL), chloroform (0.2 mL), and water (0.45 mL) and centrifugation. Lastly, the protein sample was digested with 20 µL of trypsin followed by centrifugation at 5000 g for 5 minutes at 4 °C, and 5 µL of the supernatant was introduced into the LC-MS/MS system. The calibration standards were prepared by spiking peptide standards into the extraction buffer II of the membrane protein extraction kit. Samples were analyzed as described before by Kumar et al., 2017. Briefly, AB Sciex 6500 triple-quadrupole mass spectrometer (Sciex, Framingham, MA, U.S.A.) coupled to the Water Acquity UPLC system (Waters Corporation, Milford, MA) was operated in electrospray positive ionization mode for liquid chromatography-tandem mass spectroscopy (LC-MS/ MS) analysis of the signature peptides (Table 3.2). The transitions from doubly charged parent ion to singly charged product ions for the analyte peptides and their respective SIL peptides were monitored (Table 3.2). The chromatographic separation and resolution were obtained on an Acquity UPLC HSS T3 Column, (1.8 µm, 2.1 mm X 100 mm) with a 0.2 µm inlet frits (Waters, Milford, MA, USA). Mobile phases (0.3 mL/min) consisted of 0.1% formic acid in water (A) and 0.1% formic acid in acetonitrile (B). The gradient program for UPLC method for determination of OCT2 in human kidney cortex and OCT2-expressing HEK293 and MDCKII cells was: 0–2 minutes: 3% B; 2–20 minutes: 3–45% B; 20–23 minutes: 45–90% B; 23–24 minutes: 90% B; 24–24.5 minutes: 90–3%B; 24.5–28 minutes: 3–3%B including washing and re-equilibration for 3.5 minutes. Seven calibration standards ranging from 0.14 to 70.4 fmol (on the column) were used to quantify OCT2.

3.3.5 *Prediction of metformin in vivo $CL_{r,sec}$*

Metformin *in vivo* $CL_{r,sec}$ was scaled from experimentally determined metformin *in vitro* clearance by using the expression of OCT2 in expressed cells and human kidney cortex (Eq. 1, Table 3.1) and the plasma membrane potential difference between HEK293/MDCKII cells and human renal epithelial cells. To do so, we made the following assumptions: a) OCT2-mediated metformin uptake into the human kidney is the rate determining step in metformin's $CL_{r,sec,}$; b) *In vivo*, OCT2 is expressed entirely in the plasma membrane of human kidney renal epithelial cells (Fisel et al., 2016); c) The human kidney cortex is 70% of total kidney by weight (Bouchet et al., 2003). In addition, we experimentally determined the total protein content in the human kidney cortex homogenate (wt/wt). Therefore:

$$CL_{r,sec} = 2\ (\text{due to 2 kidneys}) \times CL_{in\ vitro} \times \frac{[E]in\ vivo}{[E]in\ vitro} \times \text{cortex weight} \times \text{Total tissue protein per unit cortex weight} \quad (1)$$

Where [*E*] = Total OCT2 expression in human kidneys (*in vivo*) and in OCT2-expressing cells (*in vitro*), respectively. Total tissue protein per unit cortex weight was estimated by the BCA assay

The OCT2 total cell expression-based predicted metformin $CL_{r,sec}$ was corrected as follows: 1) the percent of OCT2 expressed in the plasma membrane in OCT2-expressing cells; 2) the difference in plasma membrane potential between HEK293/MDCKII cells and human renal epithelial cells. The latter was based on the observations by Burt et al. (2016), Koepsell and Keller (2016). The rate of OCT2-mediated metformin transport was directly proportional to the difference in electrochemical driving force across the plasma membrane of OCT2-expressing cells and kidney epithelial cells (Burt et al., 2016; Koepsell and Keller, 2016). We assumed that both HEK293 and MDCKII cells had a similar resting membrane potential difference of -35mV

(see discussion for details). Correcting for the 2-fold difference between the plasma membrane potential of the OCT2-expressing cells (-35 mV) and kidney epithelial cells (-70 mV), resulted in a 2-fold correction of our predicted metformin $CL_{r,sec}$.

3.4 RESULTS

3.4.1 *OCT2-mediated [^{14}C] metformin uptake clearance in OCT2-expressing HEK293 and MDCKII cells*

[^{14}C] Metformin uptake clearance (mean±SD) was 36.7±2.8 and 2.0±0.1 µL/mg cellular protein/min (n=3 replicates from a single experiment) in HEK293 and MDCKII cells, respectively.

3.4.2 *Total expression of OCT2 in the human kidney cortex and OCT2-expressing HEK293 and MDCKII cells*

Total OCT2 expression (mean±SD) in the human kidney cortex, HEK293 and MDCKII cells was 7.6±3.8 pmol/mg protein, 369.4±26.8 pmol/mg and 19±1.1 pmol/mg protein respectively (Fig. 3.1A, Table 3.1). Total protein content in human kidney cortex homogenate was 30% wt/wt.

3.4.3 *Plasma membrane expression of OCT2 in OCT2-expressing HEK293 and MDCKII cells*

The percent of OCT2 expressed in the plasma membrane of OCT2-expressing HEK293 and MDCKII cells was only 30.2±1.9 and 51.6, respectively (Fig. 3.1B) while that of Na^+-K^+ ATPase (plasma membrane marker) was 58.8±3.6 and 83.7, respectively (Fig. 3.1B). The corresponding percent of calreticulin (endoplasmic reticulum (ER) marker) biotinylated was only

6.7±2.3 and 11.1, confirming minimal intracellular penetration of the sulfosuccinimidyl-2-(biotinamido) ethyl-1, 3-dithiopropionate (sulfo-NHS-SS-biotin) reagent. (Fig. 3.1B).

3.4.4 *IVIVE of in vivo $CL_{r,sec}$ of metformin based on OCT2 expression as well as resting membrane potential*

A literature review of human *in vivo* metformin renal clearance data from multiple studies resulted in a mean (geometric mean) $CL_{r,sec}$ (assuming $CL_{filtration}$ is 120 mL/min) of 415 mL/min (range 215 to 643 mL/min; Table 3.3). Assuming 100% of OCT2 transporters are expressed in the plasma membrane of OCT2-expressing HEK293 and MDCKII cells, metformin's $CL_{r,sec}$ was predicted (Equation 1) to be 46.2 mL/min and 50.4 mL/min, respectively. When corrected for OCT2 plasma membrane expression in HEK293 and MDCKII cells, the predicted metformin $CL_{r,sec}$ improved to 153.0mL/min and 97.7 mL/min respectively (Table 3.1). When this predicted metformin $CL_{r,sec}$ (mL/min) was further corrected for the membrane potential difference between OCT2-expressing cells and the renal epithelial cells, the predicted metformin $CL_{r,sec}$ improved to an average value of 250.7 mL/min (Table 3.1) a value lower than the observed geometric mean of $CL_{r,sec}$ but within the observed range (215 to 643 mL/min).

3.5 DISCUSSION

To predict the clearance of a drug when transporters are involved, it is important that the plasma membrane expression of the transporter(s) be used to scale *in vitro* transport clearance to *in vivo*. Therefore, we have optimized a cell-surface biotinylation method to determine the percent of expression of a transporter on the plasma membrane (Kumar et al., 2017). The use of this optimized biotinylation method (Kumar et al., 2017) showed that ≤ 52% of OCT2 is expressed in the plasma membrane of OCT2-expressing HEK293 and MDCKII cells (Fig. 3.1B). We

confirmed that this result was not due to sulfo-NHS-SS-biotin concentration being limiting (data not shown).

Metformin is primarily cleared (~70%) by active renal secretion ($CL_{r,sec}$) mediated exclusively by OCT2 located in the basolateral membrane of the proximal tubule epithelial cells (Burt et al., 2016). Then, it is effluxed into the renal tubule by the apical MATE1 and MATE2-K. Moreover, OCT2-mediated uptake of metformin (from the plasma) appears to be the rate-determining step in metformin's $CL_{r,sec}$. Human studies have shown that inhibition of OCT2 by dolutegravir (50 mg, bid for 7 days) increases metformin plasma AUC to a larger extent (145%) than inhibition of both MATE1 and MATE2-K, by a 50 mg oral dose of pyrimethamine (35%, (Song et al., 2016) and (Kusuhara et al., 2011)). Dolutegravir does not inhibit MATE1 and MATE2-K at doses used (Song et al., 2016) and pyrimethamine is a more potent inhibitor of MATE1 and MATE2-K (IC_{50}: 0.1 µM) than OCT2 (IC_{50}: 4.8 µM).

Although the involvement of other transporters in metformin $CL_{r,sec}$ cannot be discounted, based on the above data, it is reasonable to assume that OCT2 is the rate-determining step in $CL_{r,sec}$ of metformin. If this is the case, as described by us (Patilea-Vrana and Unadkat, 2016), the renal secretory clearance of metformin will be determined only by its OCT2-mediated clearance. Thus, the renal secretory clearance of metformin should be well-predicted by the uptake clearance of metformin by OCT2-expressing cells provided this uptake clearance is scaled to that *in vivo* by the difference in OCT2 expression in the cells vs. kidney cortex. When we assumed that 100% of OCT2 was located in the plasma membrane of non-polarized HEK293 and polarized MDCKII cells, the *in vivo* $CL_{r,sec}$ of metformin was under predicted (~50 mL/min *vs.* 415 [range 215 to 643] mL/min) by about 8-fold. When this IVIVE was corrected for the plasma membrane expression of OCT2, the prediction of $CL_{r,sec}$ of metformin improved markedly, but was still

lower (153.0 mL/min and 97.7 mL/min in OCT2-HEK293 and MDCKII cells, respectively, Table 3.1) than its *in vivo* secretory $CL_{r,sec}$.

For accurate IVIVE of the clearance of a drug, the cell line must replicate the mechanism of transport *in vivo*. Based on literature data, this is not the case here. OCT2 transport activity is driven by the negative resting membrane potential of the cell. The resting membrane potential of the human renal epithelial cells is -70 mV (Wright and Dantzler, 2004) while for HEK293 and MDCKII cells it is -20 mV to -35 mV (Condreay et al., 2006; Hsu et al., 2010) and -20 mV to -50 mV respectively (Westphale et al., 1992; Lang and Paulmichl, 1995). Correcting for this difference in membrane potential between OCT2-expressing cells and renal epithelial cells improved our prediction of metformin $CL_{r,sec}$ (250.7 mL/min) and resulted in a value within the range observed *in vivo* (215 to 643 mL/min; mean 415 mL/min).

An interesting question that arises from our data is: what is the percent of plasma membrane expression of OCT2 in kidney epithelial cells? Immunolocalization data suggests that OCT2 is predominately located on the plasma membrane of the kidney epithelial cells (Fisel et al., 2016). Unfortunately, this question cannot be addressed by biotinylation without first culturing the cells. Therefore, it will be interesting in the future to determine the plasma membrane expression of OCT2 in primary kidney epithelial cells. Nevertheless, if less than 100% of OCT2 were expressed in the plasma membrane of these cells, the above IVIVE would be even more discrepant. Therefore, assuming that OCT2 in kidney epithelial cells is 100% expressed in the plasma membrane is not a reason for the underprediction of the *in vivo* metformin $CL_{r,sec}$.

Many groups have used primary cells (e.g. human/rat hepatocytes) and empirical scaling factors (Jones et al., 2012; Zou et al., 2013; Izumi et al., 2017) to predict hepatobiliary clearance of drugs. Such methods lack mechanistic insight and therefore may not necessarily apply to a new

molecular entity. By incorporating mechanisms of transport and quantitative proteomics to account for the difference in expression of transporters between hepatocytes and liver tissue, such IVIVE has been shown to be successful without using an empirical scaling factor (Bosgra et al., 2014; Ishida et al., 2018). However, this approach has never been applied to the renal secretory clearance of a drug. Here we report the first such successful IVIVE where our prediction falls within the observed metformin $CL_{r,sec}$ values (albeit lower than the mean). Moreover, our data highlights the importance of utilizing cells that mimic the mechanism(s) of transport of drugs *in vivo* as well as proteomics to quantify plasma membrane expression of transporters to conduct IVIVE of transporter-mediated clearance of a drug.

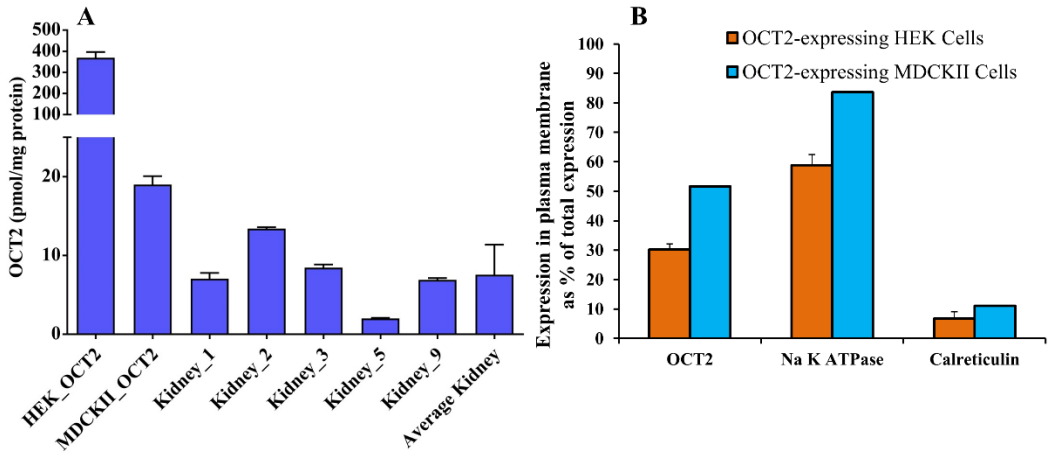

Fig. 3.1. Total cellular expression of OCT2 in human kidney cortex and OCT2-expressing HEK293 and MDCKII cells and plasma membrane expression of OCT2 in OCT2-expressing HEK293 and MDCKII cells. (A) OCT2 expression in the human kidney cortex (n = 5), HEK293 and MDCKII cells was 7.6±3.9, 369.4±26.8 pmol/mg and 19±1.1 pmol/mg protein (mean ± S.D. of triplicates of a single experiment). (B) The percent of total OCT2, Na^+-K^+ ATPase and calreticulin expressed in the plasma membrane of OCT2-expressing HEK293 (mean ± S.D, n=3 independent experiments) was 30.2±1.9, 58.8±3.6, and 6.7±2.3 respectively while that in MDCKII (average of n=2 independent experiments) was 51.6, 83.7, and 11.1 respectively. Mass balance showed that the recovery of all proteins was 94.5-114.4%. Data are average of two and three independent experiments for OCT2-expressing MDCKII and HEK293 cells respectively.

Table 3.1 Values used for IVIVE of metformin $CL_{r,sec}$

Human *in vivo* $CL_{r,sec}$ of metformin: geometric mean (range) 415 (215 to 643) mL/min		
	HEK293	**MDCKII**
Human kidney weight (g)	150	150
Cortex weight/kidney (70% of total kidney weight) (g)[a]	105	105
OCT2 expression in cells (pmol/mg protein)	369.4	19
OCT2 expression in kidney cortex (pmol/mg protein)	7.6	7.6
In vitro metformin clearance (µL/mg protein/min)	36.7±2.8	2.0±0.1
Scaling factor (SF)*: $[E]in\ vivo/[E]in\ vitro$	0.02	0.40
mg of protein per mg human kidney cortex weight[b]	0.3	0.3
[^{14}C] Metformin Uptake (pmol/min/mg protein)[b]	202.1±15.6	10.9±0.7
Predicted metformin $CL_{r,sec}$ (mL/min) (assuming 100% of OCT2 is expressed in the plasma membrane)	46.2	50.4
Predicted metformin $CLr_{,sec}$ (mL/min) (based on % OCT2 expression in the plasma membrane)	152.98	97.7
Predicted metformin $CL_{r,sec}$ (mL/min) based on plasma membrane expression and an average of 2-fold extrapolation of membrane resting potential based on data by Burt et al. (Burt et al., 2016) and Koepsell and Keller (Koepsell and Keller, 2016)	305.96	195.4
Predicted average $CL_{r,sec}$ (average of 305.96 and 195.4 mL/min) (based on plasma membrane expression and membrane resting potential)	250.7	

a: [(Bouchet et al., 2003)], b: Experimentally determined; *SF is the ratio of expression of OCT2 in the kidney cortex vs. the cells.

Table 3.2 MRM parameters used for quantification of OCT2 and marker proteins

Protein	Surrogate Peptide	Parent ion (m/z)	Product ion (m/z)	Declustering potential (V)	Collision energy (V)
OCT2	LNPSFLDLVR	587.3	946.5, 228.1	50	28
	LNPSFLDLV***R***	592.3	956.5, 228.1		
Na^+-K^+ ATPase	AAVPDAVGK	414.2	586.3	50	18
	AAVPDAVG***K***	418.2	594.3		
Calreticulin (MDCKII)	FYALSAR	414.2	517.3	50	19
Calreticulin (HEK293)	EQFLDGDGWTSR	705.8	893.4, 778.4	50	33

Italicized and bolded letters indicate stable labeled amino acid residues. Two different surrogate peptides of calreticulin (FYALSAR in CHO and MDCKII cells and EQFLDGDGWTSR in HEK293 cells) were used because of their species-dependent specificity.

Table 3.3 Renal clearance (CL_r) of metformin in healthy human subjects

Metformin Dose	(CL_r) ($L*hr^{-1}$)	$CL_{r,sec}$ (mL/min)	Number of healthy subjects	Reference
1850 mg, PO	46.0±4.2	643±71	12	(Hibma et al., 2016)
850 mg, PO	42.3±12.9	585±215	12	(Li et al., 2016)
2000 mg, PO	32.3±6.7	418.3±112.2	18	(Devineni et al., 2015)
500 mg, PO	36.4±6.5	486.0±108	24	(Klamerus et al., 2014)
1000 mg, PO	38.2±8.5	516.7±141.7	27	(Shin et al., 2014)
1000 mg, PO	36.1±8.4	481.7±140.2	14	(Johansson et al., 2014)
500 mg, PO	33.0±8.5	430.0±141.7	43	(Oefelein et al., 2013)
250 mg, PO	23.7±1.9	275.0±31	8	(Kusuhara et al., 2011)
850 mg, PO	26.5±6.5	340±97	14	(Chen et al., 2009)
850 mg, PO	31.5±3.4	405.0±57.2	9	(Sambol et al., 1996)
1700 mg, PO	27.3±2.3	335.0±38.9	9	
2550 mg, PO	27.7±2.3	341.7±37.8	9	
927±12 mg, IV	20.1±2.8	215.0±46	5	(Sirtori et al., 1978)
250 mg, PO	31.6±9.9	407±165	7	(Somogyi et al., 1987)
250 mg, IV	32.6±3.7	408.5±68.3	4	(Tucker et al., 1981)
500 mg, PO	31.5±7.5	389.5±104.8	4	
1500 mg, PO	31.1±16.7	383.5±247.9	4	
500 mg, IV	27.2±4.9	333.7±81.5	3	(Pentikainen et al., 1979)
500 mg, PO	26.6±3.0	323.6±50.7	5	
CL_r values listed above are mean ± SD, PO, Oral; IV, intravenous. $CL_{filtration}$ (if not stated in the cited manuscript) was assumed to be 120 mL/min, the geometric mean $CL_{r,sec}$ of metformin was calculated as 415 mL/min.				

Chapter 4. A Comparison of Total and Plasma Membrane Abundance of Transporters in Suspended, Plated, Sandwich-Cultured Human Hepatocytes vs. Human Liver Tissue Using Quantitative Targeted Proteomics and Cell-Surface Biotinylation

4.1 ABSTRACT

Suspended (SH), plated (PH) and sandwich-cultured hepatocytes (SCH) are commonly used models to predict in vivo transporter-mediated hepatic uptake (SH or PH) or biliary (SCH) clearance of drugs. When doing so, the total and the plasma membrane abundance (PMA) of transporter is assumed not to differ between hepatocytes and liver tissue (LT). This assumption has never been tested. Here, we tested this assumption by measuring the total and PMA of the transporters in human hepatocyte models vs. LT (total only) from which they were isolated. Total abundance of OATP1B1/2B1/1B3, OCT1 and OAT2 was not significantly different between the hepatocytes and LT. The same was true for the PMA of these transporters across the hepatocyte models. In contrast, total abundance of the sinusoidal efflux transporter, MRP3, and the canalicular efflux transporters, MRP2 and P-gp, was significantly greater ($P<0.05$) in SCH vs. LT. Of the transporters tested, only the percent PMA of OATP1B1, P-gp and MRP3, in SCH (82.8±7.3%, 57.5±10.9%, 69.3±5.7%) was significantly greater ($P<0.05$) than in SH (73.3 ±6.4%, 27.4±6.4%, 53.6±4.1%). If the transporters measured in the plasma membrane are functional and the PMA in SH is representative of that in LT, these data suggest that SH, PH, and SCH will result in equal prediction of hepatic uptake clearance of drugs mediated by the transporters tested above. However, SCH will predict higher sinusoidal efflux and biliary clearance of drugs if the change in PMA of these transporters is not taken into consideration.

4.2 INTRODUCTION

The liver, by either hepatic uptake/efflux transport or metabolism or both predominately clears the majority of small molecule drugs on the market or in development. Predicting in vivo hepatobiliary clearances of new molecular entities is important to predict their first in human dose, potential drug-drug interactions (DDI) and the impact of genetic polymorphism of transporters/enzymes on their disposition. If the liver is the target organ for drug therapy, such predictions could also help estimate the hepatic exposure of a drug at a given dosage regimen.

Several hepatocyte models are commonly used to predict in vivo hepatobiliary clearance of drugs. Suspended (SH) or plated hepatocytes (PH) are used to predict in vivo hepatic uptake clearance of drugs while sandwich-cultured hepatocytes (SCH) are used to predict both in vivo uptake and biliary clearance (CL_b) of drugs. While these hepatocyte models have been successfully used to predict in vivo metabolic clearance (CL) of drugs (Naritomi et al., 2003; Soars et al., 2007), they have been shown to severely under-predict the in vivo transporter-mediated CL of drugs (Abe et al., 2008; Jones et al., 2012; Zou et al., 2013). One possible reason for this under-prediction could be a difference in hepatic transporter abundance (total and/or plasma membrane) between hepatocyte models and liver tissue (LT). Indeed, we have previously shown this to be the case in the rat SCH vs. LT (Ishida et al., 2018). Taking into consideration such difference in the total transporter abundance (SCH vs. LT) enabled us to successfully predict rosuvastatin hepatic uptake CL in rats determined by PET imaging (Ishida et al., 2018). Therefore, to investigate if the same was true for human hepatocytes, we determined the total and the plasma membrane transporter abundance in the hepatocyte models vs. human LT (total only) using targeted quantitative proteomics. To do so, we included the following unique design features not hitherto implemented by others: a) the abundance of hepatic transporters in the

hepatocyte models was compared with the LT from which the hepatocytes were isolated; b) the percent plasma membrane abundance (PMA) of hepatic transporters was quantified in the hepatocyte models using a cell-surface biotinylation method optimized in our laboratory; c) to avoid interindividual variability in the total membrane isolation (a method routinely used by us and others), the total abundance of transporters was quantified in the homogenate (not total membrane) of human liver tissues and hepatocytes. Here, we present data from these studies, which can guide selection of the appropriate hepatocyte model to predict in vivo hepatic uptake and biliary efflux CL of drugs.

4.3 MATERIALS AND METHODS

4.3.1 *Chemicals and Reagents*

Synthetic signature peptides for OATP1B1, OATP2B1, OATP1B3, NTCP, OCT1, OAT2, MRP3, MRP2, P-gp, and BSEP were obtained from New England Peptides (Boston, MA). The corresponding stable isotope labeled (SIL) peptides for above transporters and Na^+-K^+ ATPase, dithiothreitol (DTT), iodoacetamide (IAA), mass spectrometry grade trypsin, William's E Medium (no glutamine), cryopreserved hepatocyte recovery medium, total protein quantification bicinchoninic acid assay (BCA) kit, Hank's balanced salt solution with calcium and magnesium (HBSS) and Pierce cell surface protein isolation kit were obtained from Thermo Scientific (Rockford, IL). Pierce cell surface protein isolation kit contains sulfosuccinimidyl-2-(biotinamido) ethyl-1, 3-dithiopropionate (sulfo-NHS-SS-biotin), quenching solution (100 mm glycine), lysis buffer, neutravidin agarose gel, wash buffer, column accessory pack, DTT, phosphate buffer and Tris buffer. HPLC-grade acetonitrile and sodium dodecyl sulfate (SDS) were purchased from Fischer Scientific (Fair Lawn, NJ). Formic acid was purchased from Sigma-Aldrich (St. Louis, MO). All reagents were analytical grade. 24-well collagen-coated

plates and matrigel were purchased from Corning (Kennebunk, ME). Human hepatocyte thaw medium, INVITROGRO CP medium, INVITROGRO HI medium, and TORPEDO antibiotic mix were obtained from BioIVT (Westbury, NY).

4.3.2 *Procurement of Human Liver Tissues and Hepatocytes*

Human liver frozen tissues (about 150-250 mg, n = 4) and cryopreserved human hepatocytes isolated from the respective human liver tissues were obtained from BioIVT (Westbury, NY). The demographics of the human liver donors are shown in Table 4.1.

4.3.3 *Homogenate Preparation of Human Liver Tissue and Hepatocytes (SH, PH and SCH) to Quantify Total Transporter Abundance*

LT: About 50-100 mg of the human liver tissue from each donor was homogenized in extraction buffer II (Pierce cell surface protein isolation kit) in Omni Bead Ruptor at 4 °C. The homogenized liver tissue was dissolved in extraction buffer II and 2% SDS (1:1) for protein quantification by LC-MS/MS analyses.

SH: Cryopreserved human hepatocytes were partially thawed at 37 °C and then quickly transferred to a 15 ml tube containing 5 ml of cryopreserved hepatocyte recovery medium (4 °C). After centrifugation at 1000 g for 5 mins at 4 °C, the cryopreserved hepatocyte recovery medium was aspirated and 5 ml of William's E medium (37 °C) were added to the hepatocytes. The live hepatocytes were counted using the trypan blue exclusion method. About 8.4×10^6 viable hepatocytes were transferred to 15 ml tube containing HBSS buffer and incubated at 37 °C for 30 minutes. Then, the hepatocytes were pelleted by centrifuging the tube at 1000 g for 5 mins at 4 °C. The pellet was dissolved in extraction buffer II and 2% SDS (1:1) for protein quantification by LC-MS/MS analyses.

PH: About 0.35×10^6 hepatocytes were plated per well in a 24-well collagen-coated plate for 5 hours with 0.5 ml/well TORPEDO containing INVITROGRO CP medium (1:9 (v/v). Then, the cells were scraped and centrifuged at 1000 g for 5 mins at 4 °C to collect the hepatocytes pellet. The pellet was dissolved in extraction buffer II and 2% SDS (1:1) for protein quantification by LC-MS/MS analyses.

SCH: About 0.35×10^6 hepatocytes/well were plated in a 24-well collagen-coated plate for 24 hours with 0.5 ml/well TORPEDO containing INVITROGRO CP medium (1:9 (v/v). Then, the medium was replaced with TORPEDO containing INVITROGRO HI medium with 0.25 mg/ml matrigel. Medium was replaced daily with 0.5 ml/well fresh TORPEDO containing INVITROGRO HI. On day 4 of the sandwich culture, the cells were scraped and centrifuged at 1000 g for 5 mins at 4 °C to collect the hepatocytes pellet. The pellet was dissolved in 2 ml of extraction buffer II and 2% SDS (1:1) for protein quantification by LC-MS/MS analyses.

4.3.4 *Plasma Membrane Isolation from SH, PH and SCHH by Cell-Surface Biotinylation*

Plasma membrane from SH, PH and SCH were isolated, using a cell-surface biotinylation methodology optimized in our laboratory (Kumar et al., 2017; Kumar et al., 2018). The cell-surface biotinylation method non-specifically biotinylates plasma membrane proteins, including many proteins other than the transporters of interest. This non-specific biotinylation allows one to isolate pure plasma membrane fractions from cells and hepatocytes. Briefly, SH (~ 8.4×10^6 hepatocytes) or PH/SCH (0.35×10^6 hepatocytes/well, 24 well plate) were incubated with 10 ml or 0.5 ml/well of sulfo-NHS-SS-biotin (0.78 mg/ml), respectively, at 37 °C for 30 minutes. Then, hepatocytes were washed twice with 10 ml of PBS buffer, scraped and centrifuged at 500 g for 3 minutes at 4 °C to collect the hepatocytes pellet and lysed in 750 µl lysis buffer. After cell lysis, the biotinylated plasma membrane was isolated using neutravidin resin columns. Fractions

representing biotinylated (plasma membrane fraction) and non-biotinylated (intracellular fraction) were collected for protein quantification by LC-MS/MS analyses. As a quality control check, only samples that fell within the range of 100±30% recovery of cellular proteins (relative to the homogenate) were deemed acceptable.

Applying the cell-surface biotinylation method (Kumar et al., 2017) to SCH posed an interesting question. Should this method be applied to SCH in the presence or absence of calcium (Ca^{++})? In the presence of Ca^{++}, the hepatocytes form tight junctions (Pfeifer et al., 2013). These tight junctions, which may hinder accessibility of the biotinylation reagent to the canalicular membrane, are disrupted in the absence of Ca^{++}. Therefore, to investigate if there was any difference in the efficiency of cell-surface biotinylation, we conducted a pilot study of cell-surface biotinylation of SCH in the presence and absence of Ca^{++}. The abundance of plasma membrane hepatic transporters as a percent of total (homogenate), in presence or absence of Ca^{++}, was statistically not different (Wilcoxon signed rank test; Fig. 4.5). Therefore, all subsequent cell-surface biotinylation experiments in hepatocytes were conducted in the presence of Ca^{++}.

4.3.5 *LC-MS/MS Quantification of Total and Plasma Membrane Transporter Abundance*

Total protein content in human liver and hepatocytes homogenate was quantified by the BCA assay. Transporter abundance was quantified using validated proteomics protocols implemented in our laboratory (Prasad and Unadkat, 2014b; Prasad and Unadkat, 2014a; Wang et al., 2015). Briefly, liver tissue/hepatocyte homogenates (equivalent to 0.2 mg total protein) were treated with 45 µl of ammonium bicarbonate buffer (100 mM, pH 7.8), 25 µl of 3% sodium deoxycholate (w/v), 12.5 µl DTT (250 mM), and 5 µl of human albumin (10 mg/ml). Proteins

present in the sample was denatured and disulfide bond between cysteine residues was reduced by incubation at 95 °C for 5 minutes, followed by the addition of 25 µl of IAA (200 mM; an alkylating agent) and treatment with ice-cold methanol (0.5 ml), chloroform (0.2 ml), and water (0.45 ml) and centrifugation (12,000 g). Lastly, the protein sample was digested with 20 µl of trypsin (equivalent to 3.2 µg of trypsin), mixed with 20 µl labeled internal standards, and followed by centrifugation at 5000 g for 5 minutes at 4 °C, and 5 µl of the supernatant was introduced into the LC-MS/MS system. The calibration standards were prepared by spiking peptide standards into the extraction buffer II of the membrane protein extraction kit. As an internal biological control, total membrane isolated from 39 human livers was pooled (PHL) (Wang et al., 2016), aliquoted and stored at -80 °C. This PHL sample was processed and analyzed in each LC-MS/MS run to ensure that the data from PHL were consistent (within 100±20 %) with the liver transporter abundance data published by us (Wang et al., 2016). We note here that the surrogate peptide of interest for each transporter protein was localized intracellularly (except NTCP, Table 4.3). Thus, it will not be modified by the biotinylation reagent (because this reagent does not permeate the cell membrane) (Fig. 4.7).

Samples were analyzed as described before (Kumar et al., 2018). Briefly, AB Sciex 6500 triple-quadrupole mass spectrometer (Sciex, Framingham, MA, U.S.A.) coupled to the Water Acquity UPLC system (Waters Corporation, Milford, MA) was operated in electrospray positive ionization mode for liquid chromatography-tandem mass spectroscopy (LC-MS/ MS) analysis of the signature peptides (Table 4.2). The NTCP peptide was quantified on a Waters Xevo TQS tandem mass spectrometer (Table 4.2) due to the greater sensitivity of detection of this peptide afforded by this instrument. The transitions from doubly charged parent ion to singly charged product ions for the analyte peptides and their respective SIL peptides were monitored (Table

4.2). The chromatographic separation and resolution were obtained on an Acquity UPLC HSS T3 Column, (1.8 µm, 2.1 mm X 100 mm) with a 0.2 µm inlet frits (Waters, Milford, MA, USA). Mobile phases (0.3 ml/min) consisted of 0.1% formic acid in water (A) and 0.1% formic acid in acetonitrile (B). The gradient program for UPLC method for determination of transporters in hepatocytes and LT was: 0–3 minutes: 3% B; 3–10 minutes: 3–13% B; 10–20 minutes: 13–25% B; 20–22 minutes: 25–33.3% B; 22–24 minutes: 33.3–80% B; 24–25 minutes: 80% B; 25–26 minutes: 80–3% B; 26–30 minutes: 3% B including washing and re-equilibration for 4 minutes.

In all the above analyses, Na^+-K^+ ATPase and calreticulin were used as positive controls of plasma membrane and intracellular (endoplasmic reticulum) marker proteins respectively. For calreticulin, the stable labeled internal standard was not procured, therefore the stable labeled internal standard of Na^+-K^+-ATPase was used to estimate the calreticulin peak area ratio, as reported previously (Kumar et al., 2017; Kumar et al., 2018). The unlabeled peptide of Na^+-K^+ ATPase was not procured. Thus, Na^+-K^+ ATPase area ratio was used to determine the correlation with hepatic transporter abundance in LT and hepatocyte models (Fig. 4.6).

4.3.6 *Data and Statistical Analyses*

Determination of total transporter abundance in LT and hepatocyte models: For each donor, the total transporter abundance in the homogenates of LT and hepatocyte models was determined as a mean ± SD of 3-5 independent experiments (only single experiment for NTCP).

Determination of percent PMA of transporters in hepatocyte models: The percent PMA of hepatic transporters, calreticulin, and Na^+-K^+ ATPase in hepatocyte models (using cell-surface biotinylation) was calculated as reported previously (Kumar et al., 2017). The PMA of transporters in hepatocyte models was obtained by multiplying the percent PMA with the total

transporter abundance in homogenate and the data are reported as mean ± SD of 4 lots of hepatocytes from 3 independent experiments (only single experiment for NTCP).

Statistical analysis: Friedman test with Dunn's multiple comparison nonparametric statistical method (using Prism 7, version 7.03) was used to compare (pairwise comparison for each donor) the percent PMA, PMA or total abundance of the hepatic transporters in hepatocyte models and LT. Wilcoxon signed rank test was used to compare the percent PMA of hepatic transporters in SCH in the presence or absence of calcium.

4.4 RESULTS

4.4.1 *A Comparison of Total Transporter Abundance in Suspended, Plated, Sandwich-Cultured Human Hepatocytes and Human Liver Tissue*

In general, the total transporter abundance was most variable between the donors and between SCH and other hepatocyte models or LT. For each donor, the total abundance of sinusoidal uptake transporter proteins (OATP1B1/2B1/1B3, OCT1 and OAT2) was relatively consistent between different hepatocyte models and LT (Fig. 4.1). However, the total protein abundance of the sinusoidal efflux transporter, MRP3, and the canalicular efflux transporters, MRP2 and P-gp, was significantly increased in SCH compared to their respective LT (Fig. 4.1). NTCP and BSEP abundance in PH was significantly, but modestly, higher than LT but similar to SH and SCH.

4.4.2 *A Comparison of Plasma Membrane Abundance of Transporters in Suspended, Plated and Sandwich-Cultured Human Hepatocytes*

As expected, the localization of the intracellular (ER) marker, calreticulin, and the plasma membrane marker, Na^+-K^+ ATPase, was predominantly intracellular and in the plasma membrane, respectively (Fig. 4.2). For each donor, the percent PMA of hepatic transporters in

the hepatocyte models was highly reproducible with % CV of <30%. The majority (i.e. >50%) of the sinusoidal uptake transporters were localized in the plasma membrane of the SH, PH and SCH (Fig. 4.2). There was no significant difference in the percent PMA of sinusoidal uptake transporters in SH, PH and SCH (except OATP1B1) (Fig. 4.2). Comparison of the PMA of NTCP in SCH vs. other models could not be performed for YTW because NTCP could not be quantified in SCH for this donor (Fig. 4.3). The majority of the efflux transporters, P-gp (except in SCH) and BSEP, were intracellular while the majority of MRP2 and MRP3 transporters were in the plasma membrane. The percent PMA of the efflux transporters, MRP2 and BSEP, was found to be similar in SH, PH and SCH (Fig. 4.2). In contrast, the percent PMA of MRP3 and P-gp was significantly higher in SCH (69.3 and 57.5%) compared with SH (57.6 and 27.4%) (Fig. 4.2). The cell-surface biotinylation method can be applied only to intact cells and not to tissues. Therefore, PMA of transporters was compared amongst only the hepatocyte models. The abundance of sinusoidal uptake transporters in the plasma membrane in the different hepatocyte models was not significantly different (Fig. 4.3). In contrast, amongst the efflux transporters, only the PMA of MRP3, MRP2 and P-gp in SCH was found to be significantly greater than that in SH (Fig. 4.3). This difference was variable amongst the donors studied. For donor ADR, the change in PMA of MRP3, P-gp and MRP2 between SCH vs. SH was large, about 600 to 2000%, while for JEL there was minimal or no change between SCH vs. SH (Fig. 4.3).

4.4.3 *Correlation of Total Transporter Abundance in Suspended, Plated, Sandwich-Cultured Human Hepatocytes and Human Liver Tissue*

The total abundance of the sinusoidal efflux, MRP3, and the canalicular efflux transporters, MRP2 and P-gp (but not BSEP), was highly correlated ($R^2 \geq 0.88$) with each other (Fig. 4.4A, B and C). The total abundance of OATP1B1 and OATP2B1 showed good correlation with that of

OAT2 and OCT1 (Fig. 4.4D and E, $R^2 \geq 0.67$) respectively. The abundance of other transporters showed poor correlation ($R^2 \leq 0.5$) with each other (Fig 4F, see Table 4.3).

4.4.4 *Correlation of Abundance of Total and Plasma Membrane Transporter with the Abundance of Na+-K+ ATPase in Suspended, Plated and Sandwich-Cultured Human Hepatocytes*

Total transporter abundance of sinusoidal and canalicular transporters showed poor correlation ($R^2 \leq 0.28$) with total abundance of Na^+-K^+ ATPase in the hepatocyte models (Fig. 4.6A). Except for MRP2, MRP3, and P-gp, the same was true for PMA of these transporters. The PMA of MRP2, MRP3, and P-gp was highly correlated ($R^2 \geq 0.7$) with that of Na^+-K^+ ATPase (Fig. 4.6B).

4.5 DISCUSSION

To address the aims of our study, we deliberately incorporated, in our experiments, three distinct and unique design features, not hitherto implemented by others (Li et al., 2010; Jones et al., 2012; Schaefer et al., 2012; Vildhede et al., 2018). First, we systematically compared the changes in transporter abundance in SH, PH and SCH relative to that in the liver tissue from which they were isolated. This design increased our power to discern the change in abundance of transporters in the hepatocyte models vs. that in the corresponding liver tissue. Second, to avoid inter-batch variability in total membrane yield, we determined the transporter abundance in the homogenate rather than in the total membrane isolated from the various samples (Billington et al., 2018; Vildhede et al., 2018). However, the disadvantage of this design (Wegler et al., 2017) was that it did not allow us to quantify the low abundance transporters MATE1, MRP4, and BCRP. Third, since it is the transporter abundance in the plasma membrane that is functionally important for the uptake or efflux of drugs, we determined this abundance in the hepatocyte

models used. The plasma membrane transporter abundance data also answered the question whether the change (if any) in plasma membrane transporter abundance in the hepatocyte models was due to the change in total abundance or the change in the percent PMA or both.

There was significant inter-individual variability in total transporter abundance between hepatocyte donors. This inter-individual variability in OATP1B1 abundance was not due to genetic polymorphisms (Table 4.1) which are known to affect the transporter abundance/activity (Prasad et al., 2014; Li and Barton, 2018). We have shown that the hepatic abundance of OATP1B1 is haplotype-dependent and follows the order *1b (e.g. FEA and JEL) > *1a (e.g. YTW) >*5 (e.g. ADR) (Prasad et al., 2014). Despite having the same OATP1B1 haplotype as FEA, one donor, JEL (African American), demonstrated higher total abundance of OATP1B1 and behaved differently from the other donors with respect to total and PMA in SCH *vs*. other hepatocyte models (Fig. 4.1 & 4.3).

The lack of difference in the total abundance of the sinusoidal uptake transporters (except NTCP, Fig. 4.1) in the various hepatocyte models vs. LT is contrary to our observation and those of others with rat hepatocytes. In the rat, a significant decrease in the total abundance of the sinusoidal Oatp transporters was observed in SCH vs. LT (De Bruyn et al., 2013; Ishida et al., 2018). As was the case here for the suspended hepatocytes, we and others have previously shown that the total membrane abundance of MRP2, MRP3, P-gp, and BSEP (in total membrane) is similar between freshly isolated or cryopreserved hepatocytes vs. human LT (Li et al., 2009b; Lundquist et al., 2014). The significantly higher total abundance of MRP2, MRP3, and P-gp in SCH vs. LT (Fig. 4.1) is consistent with previously published data (though sparse) (Hoffmaster et al., 2004; Li et al., 2009a) obtained with Western blotting after cell lysis or quantitative proteomic analysis of total membrane (not homogenate) isolated from hepatocytes and LT.

Similarly, rat Mrp2 abundance in cell lysate is stable in SCH over 4-days in culture (Zhang et al., 2005) but the abundance of rat P-gp, human P-gp and MRP2 in cell lysate or total membrane isolated from SCH increases over 6-days in culture (Hoffmaster et al., 2004; Li et al., 2009a). Kimoto et al., (2012) have reported that OATP transporter abundance in human liver tissue is about twice that in cryopreserved human hepatocytes or SCH (Kimoto et al., 2012), but similar between cryopreserved human hepatocytes and SCH. Others have reported that all measured transporter abundance in total membrane was lower (except OCT1 and OAT2) in freshly isolated human hepatocytes compared to human liver tissue (Vildhede et al., 2015). However, the difference in transporter abundance between liver tissue and hepatocytes observed by others (Kimoto et al., 2012; Vildhede et al., 2015) could be due to differential loss in membrane as none of these studies was conducted with the homogenate of liver tissue or hepatocytes.

Since it is the PMA of the transporter that is important for in vitro to in vivo extrapolation (IVIVE) of transporter-mediated clearances, we determined the percent PMA in hepatocyte models. As indicated earlier, the cell-surface biotinylation methodology used here to isolate plasma membrane cannot be applied to tissues, therefore the percent PMA of transporters in LT could not be determined. While most (>50%) of the uptake transporters were localized in the plasma membrane of the hepatocytes, so were some of the efflux transporters, namely MRP2 and MRP3. However, most of P-gp (except in SCH) and BSEP were localized in the intracellular compartment. When the hepatocytes were sandwich-cultured, the percent of PMA of both MRP3 and P-gp increased significantly ($P<0.05$) compared to that in the SH. This change was most remarkable for P-gp, where the percent PMA of P-gp was ~2-fold higher in SCH (~58%) than in SH or PH (~30%).

When the above data were combined, a clear picture emerged of the PMA of the transporters in the hepatocyte models. While there was significant inter-individual variability in the PMA of the transporters in SCH vs. SH, the PMA in the other hepatocyte models (SH and PH) remained consistent with each other. Remarkably, PMA of MRP3, MRP2 and P-gp significantly increased in SCH vs. SH with the greatest change occurring for P-gp (e.g. ~2000% in ADR). The increase in PMA of P-gp and MRP3 in SCH vs. SH was due to an increase in total abundance (Fig. 4.1) as well as an increase in the percent PMA (Fig. 4.2). In contrast, the increased PMA of MRP2 in SCH vs. SH was due to an increase in the total transporter abundance (Fig. 4.1) but not in the percent PMA (Fig. 4.2). This could be an alternate explanation for the widely reported "internalization" of MRP2 in SCH (see below).

There are contradictory reports about internalization or intracellular localization of canalicular efflux transporters resulting in decreased abundance in the plasma membrane of hepatocyte models (SH and PH). In freshly isolated hepatocytes, rat Mrp2 and Mdr1a/b are predominately localized intracellularly (Bow et al., 2008). However**,** when sandwich-cultured (day 5 and 6), Mdr1a/b and MDR1 are predominantly expressed in the plasma membrane of rat and human hepatocytes respectively (Hoffmaster et al., 2004). In contrast, immunolocalization studies of Lundquist et al. (2014) have shown that the majority of the ABC transporters (P-gp, MRP2, and BCRP) are localized in the plasma membrane of the cryopreserved human hepatocytes and human livers. They also demonstrated transport activity of BCRP and P-gp in plated human and rat hepatocytes suggesting that some (or perhaps all) of these transporters are localized to the plasma membrane (Lundquist et al., 2014). Unfortunately, all of the localization studies cited above are immunolocalization studies. Thus, the percent of transporters in the plasma membrane vs. that in the intracellular compartments was not quantified. To our knowledge, ours is the first

study to quantify PMA of hepatic transporters in SH, PH and SCH. Nevertheless, our data, along with others (Hoffmaster et al., 2004; Lam and Benet, 2004; Lam et al., 2006; Bow et al., 2008; Lundquist et al., 2014) indicate that canalicular transporters in human suspended and plated hepatocytes are not all internalized, but are also present in the plasma membrane.

If the percent PMA of sinusoidal uptake transporters in SH is representative of the LT and all transporters expressed in the plasma membrane are functional, our data (Fig. 4.1- 4.3) suggest that a) any of human hepatocyte models (SH or PH or SCH) can be used to predict the *in vivo* hepatic uptake clearance of drugs mediated by OATP1B1, OATP1B3, OAT2, and OCT1 (Kumar et al., 2015) without the need to measure the plasma membrane or total abundance of the transporters. Likewise, SH or PH could be used to predict sinusoidal (or perhaps even biliary efflux) clearance of drugs without quantifying the total or PMA of these transporters. Whether SH or PH can be used to predict efflux clearance of drugs remains to be explored. In contrast, SCH, the most commonly used hepatocyte model to estimate *in vivo* CL_b, will over-predict CL_b and $CL_{s,eff}$ mediated by the transporters, MRP2/P-gp and MRP3, respectively unless changes in the PMA of these transporters are quantified. It is worth noting that there are a few limitations to this conclusion. First, the PMA of the transporters in LT and the hepatocyte model is assumed to be proportional to their activity. Second, since there is considerable inter-individual variability in the abundance of transporters, this conclusion is made based on a limited data set of four lots of hepatocytes. If the percent PMA of the transporter in LT is higher than in SH, PH or SCH, then these hepatocyte models will under-predict the hepatic uptake clearances of drugs but, SCH will likely over-predict efflux clearance (MRP2 or MRP3 or P-gp-mediated). Take for example MRP3, which shows the lowest increase (3-fold) in total abundance in SCH vs. LT. Thus, even if the percent PMA of MRP3 in LT is 100%, the SCH will over-predict the biliary clearance of

drugs. If the percent percent PMA of MRP3 in LT is much less than in SH, this over-prediction will be even greater.

The high correlation ($R^2 > 0.67$) of total transporter abundance of MRP2 vs. MRP3, MRP2 vs. P-gp, MRP3 vs. P-gp, OAT2 vs. OATP1B1 and OCT1 vs. OATP2B1 (Fig. 4.4) suggests a common regulatory mechanism of these transporters (Chen et al., 2012). The good correlation of plasma membrane canalicular efflux transporter (MRP2, MRP3 and P-gp) abundance with Na^+-K^+ ATPase (Fig. 4.6B) could be the result of simultaneous targeting of these proteins to the newly formed canalicular membrane in SCH.

In summary, we have conducted a systematic study to quantify the total and PMA of hepatic transporters in commonly used human hepatocyte models and compared it with total abundance of the transporters in LT from which they were derived. Based on the total abundance data, all three hepatocyte models, suspended, plated, and sandwich-cultured human hepatocytes can be used for IVIVE sinusoidal uptake clearance of drugs in humans. However, for IVIVE of efflux clearance, although all three models could potentially be used, the increase in PMA of MRP3, MPR2, and P-gp in SCH need to be considered. Of course, for both approaches, the complimentary in vitro clearance of the drug by the respective transporter needs to be obtained. As to whether such data can be reliably obtained for the efflux transporters (in SH and PH) needs to be explored. Importantly, these data do not support the hypothesis that lower abundance of transporters (total or plasma membrane) in the hepatocyte models vs. LT is the reason for lack of success in IVIVE of transporter-mediated hepatobiliary clearance of drugs in humans. Thus, other factors to explain this failure (if any) need to be sought. Such factors include correct identification of the rate-determining step in the clearance of the drug, considering the difference between in vitro and in vivo in the mechanism of transport of the drug (Kumar et al., 2018), and

refining in vitro methods to accurately determine both the active and passive clearance of the drug. We have recently shown that when these factors are carefully considered, the in vivo hepatic and renal uptake clearance of rosuvastatin and metformin can be accurately predicted by proteomics-informed scaling of the in vitro uptake clearance of these drugs in transporter-expressing cells (Ishida et al., 2018; Kumar et al., 2018). Such studies with additional drugs, including prediction(s) and verification (e.g. by PET imaging) of in vivo efflux clearance using this proteomics-informed approach are needed.

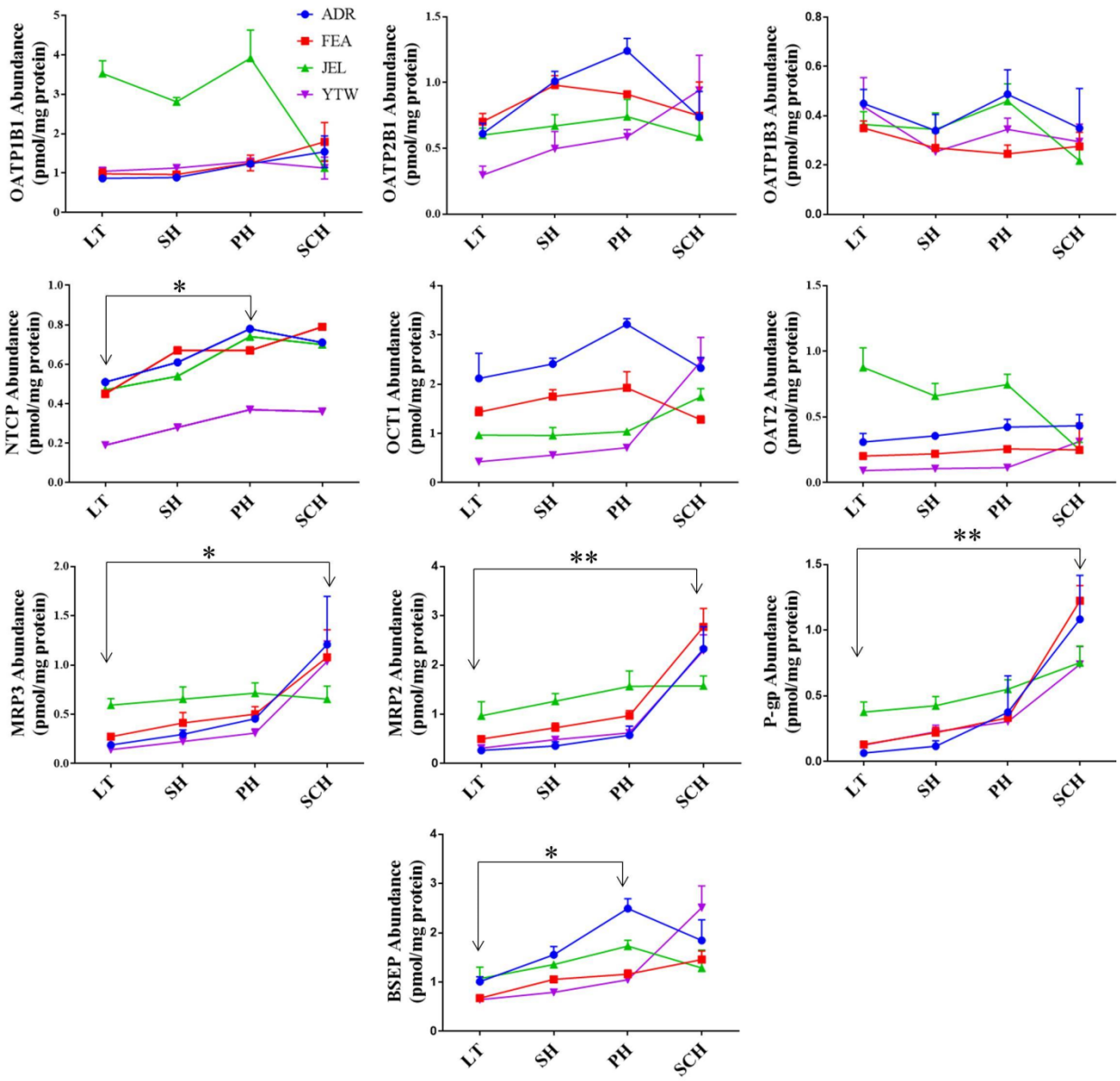

Fig. 4.1. Total hepatic transporter abundance in LT, SH, PH and SCH. There was no significant difference in the total abundance of uptake transporters OATP1B1/2B1/1B3, OCT1, and OAT2 between LT, SH, PH and SCH. In contrast, total abundance of the efflux transporters MRP2, MRP3, and P-gp was significantly greater in SCH vs. LT. NTCP and BSEP abundance was significantly higher in PH vs. LT. Data for each donor are mean ± S.D. of 3-5 independent experiments (only single experiment for NTCP). * $P < 0.05$, ** $P < 0.01$

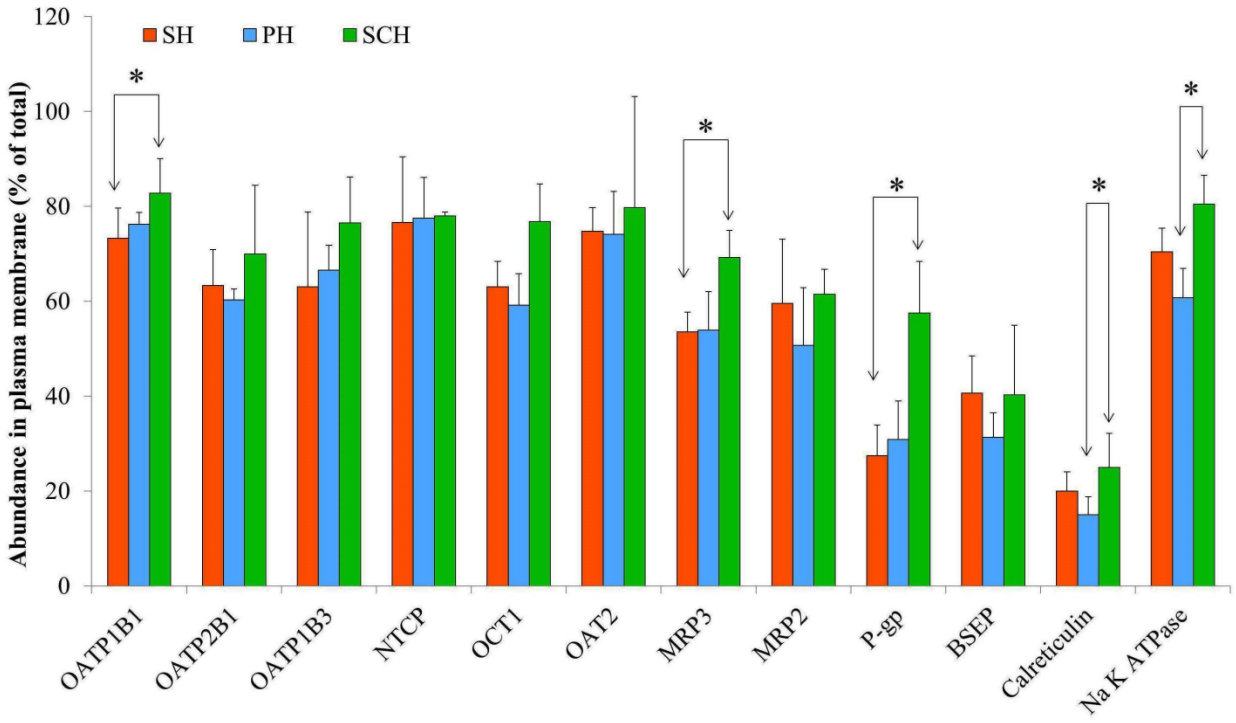

Fig. 4.2. Percent plasma membrane abundance of hepatic transporters in SH, PH, and SCH. Hepatic uptake transporters (OATP1B1/2B1/1B3, NTCP, OCT1, OAT2) were mostly (> 50%) localized in the plasma membrane of SH, PH or SCH. P-gp and BSEP were mostly localized intracellularly in SH and PH, but in SCH, the localization in the plasma membrane of P-gp, but not BSEP, increased significantly to >50%. Na^+-K^+ ATPase and calreticulin were used as a positive control for plasma membrane and intracellular (endoplasmic reticulum) marker respectively. Cell-surface biotinylation experiment was conducted in presence of calcium containing HBSS buffer. Data are reported as mean ± S.D. of 4 hepatocyte donors (except SCH-NTCP: 3 donors), with data for each donor as the mean of 3 independent experiments (only single experiment for NTCP). * $P < 0.05$

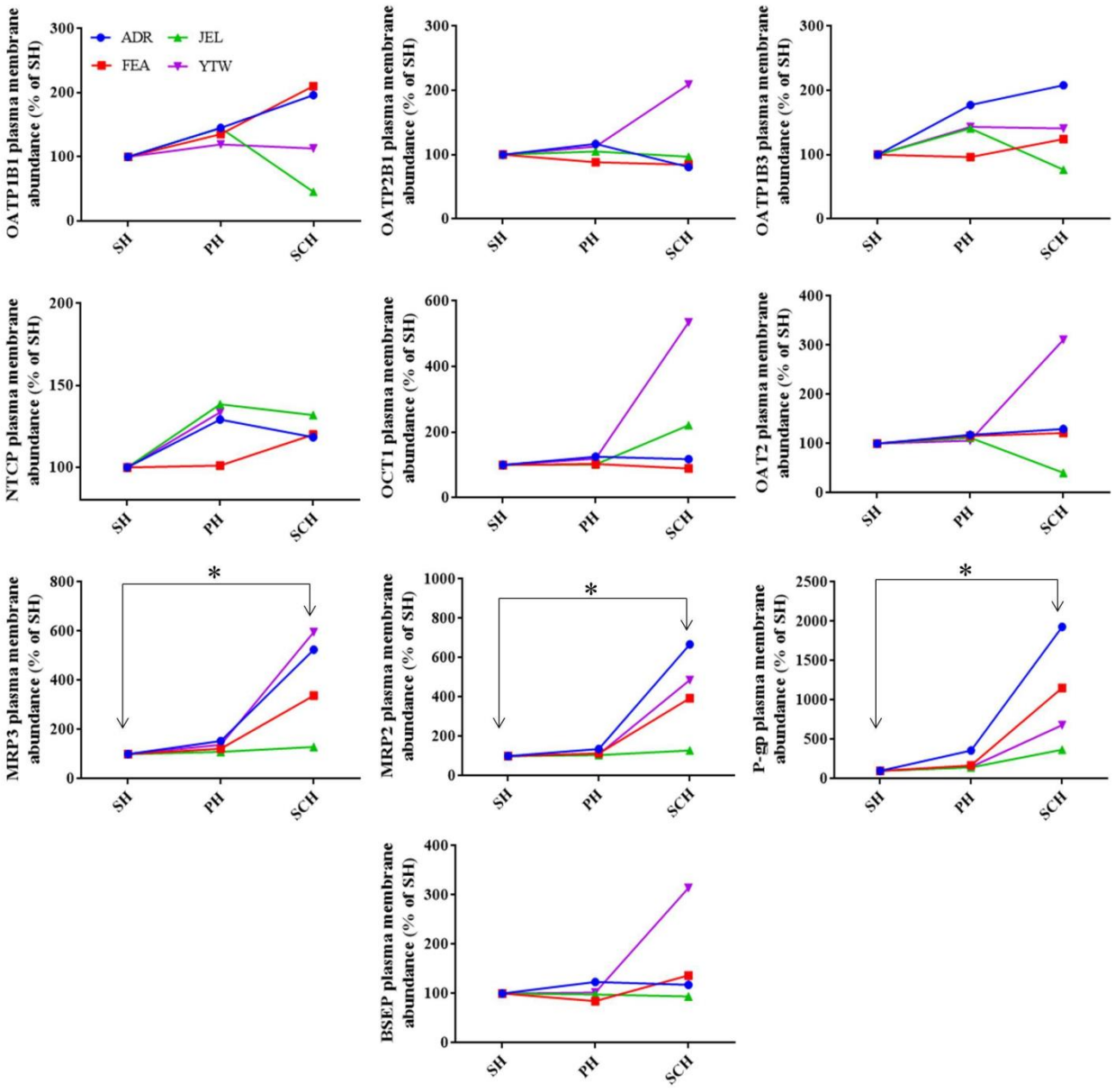

Fig. 4.3. Plasma membrane abundance of hepatic transporters in SH, PH and SCH. Values are expressed as percent abundance relative to the respective SH (derived from Fig. 1 and 2). Of the transporters studied, the PMA of MRP2, MRP3, and P-gp was significantly higher in SCH vs. SH. Data for each donor are reported as mean of 3-5 independent experiments (only single experiment for NTCP). * $P < 0.05$

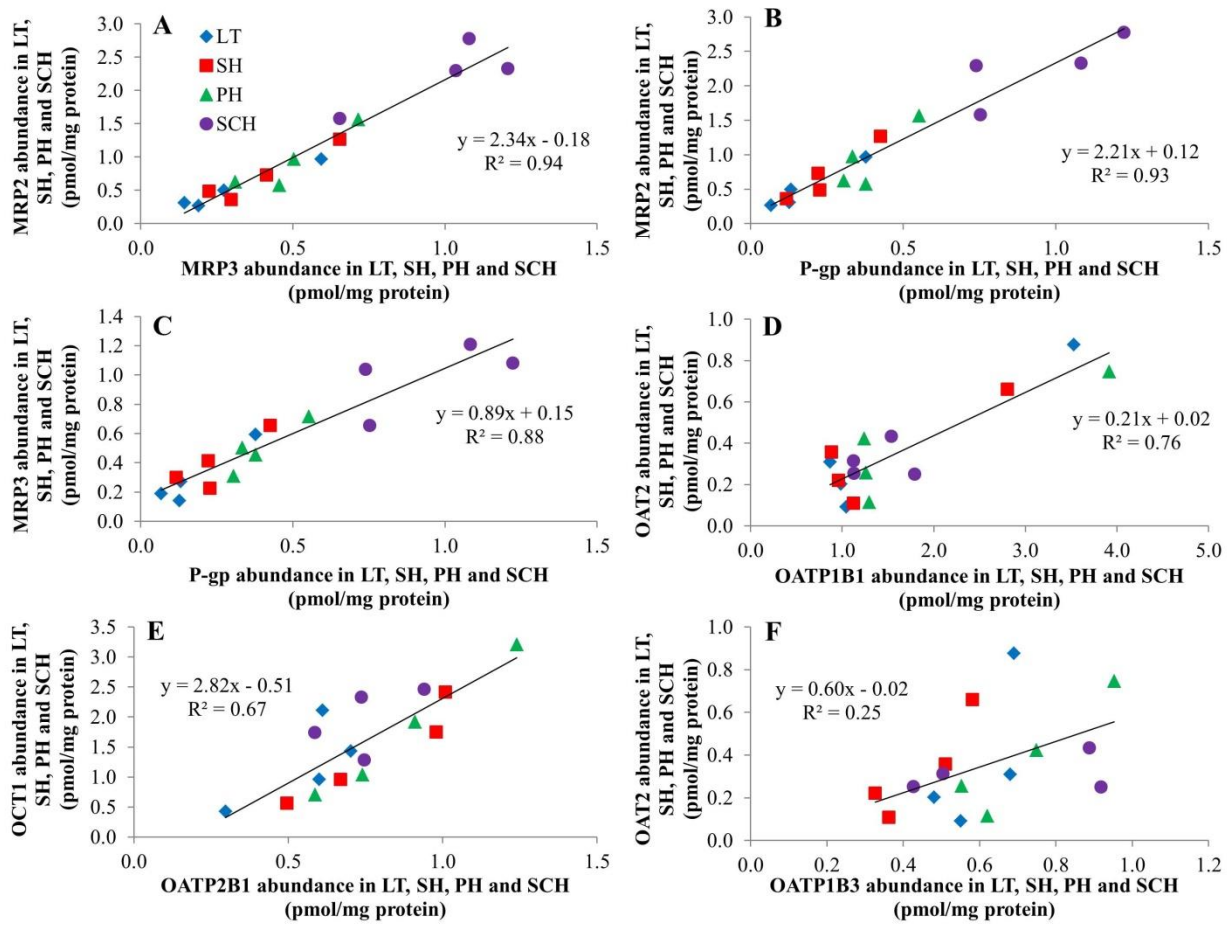

Fig. 4.4. Correlation of total transporter abundance across LT, SH, PH, and SCH. The total abundance of MRP2, MRP3 and P-gp was highly correlated with each other (A, B and C, $R^2 \geq 0.88$). OAT2 and OCT1 abundance showed good correlation with OATP1B1 and OATP2B1 (D and E, $R^2 \geq 0.67$) respectively, but the abundance of OAT2 was poorly correlated ($R^2 \leq 0.5$) with OATP1B3 (F; representative of those showing poor correlation – see Table 4.3). Each datum is mean of 3-5 independent experiments.

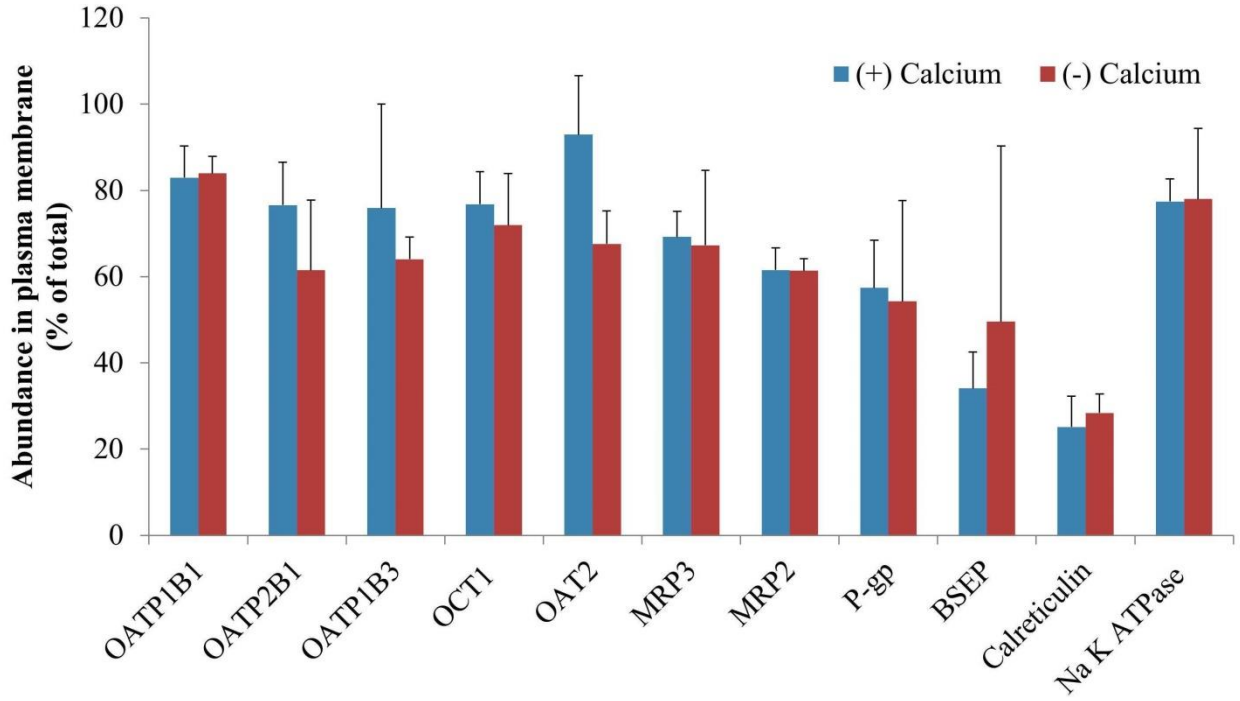

Fig. 4.5. Percent plasma membrane abundance of hepatic transporters, calreticulin and Na^+-K^+ ATPase in SCH in the presence and absence of calcium. The percent PMA of hepatic transporters in the presence and absence of calcium was not significantly different (Wilcoxon signed rank test). The percent PMA of the transporters was consistent with the data shown in Fig. 2. Na^+-K^+ ATPase and calreticulin were used as a positive control as plasma membrane and intracellular (endoplasmic reticulum) markers respectively. Data are mean±SD of 4 hepatocyte donors.

A

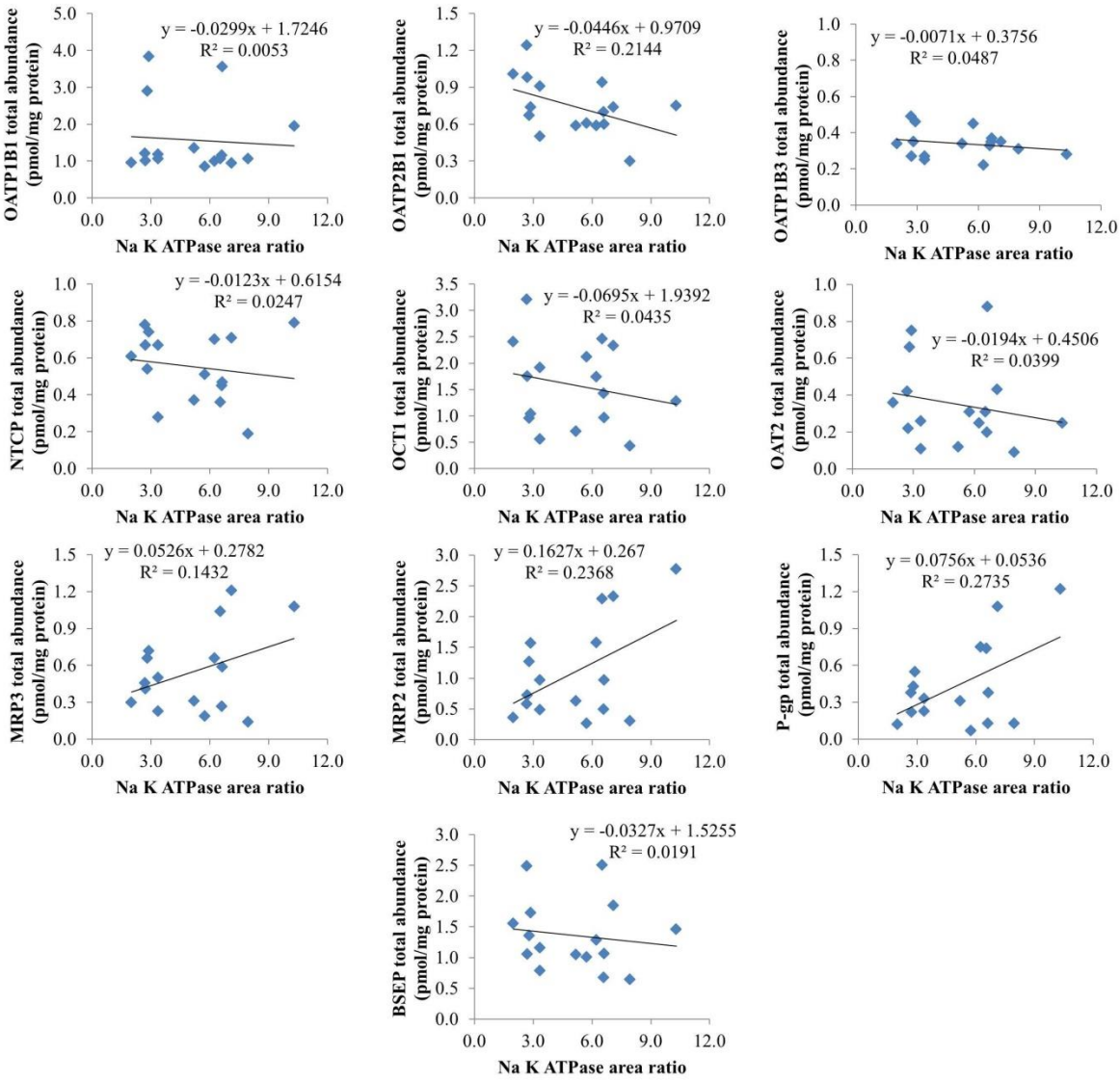
OATP1B1 total abundance (pmol/mg protein)
y = -0.0299x + 1.7246
R² = 0.0053
Na K ATPase area ratio
OATP2B1 total abundance (pmol/mg protein)
y = -0.0446x + 0.9709
R² = 0.2144
Na K ATPase area ratio
OATP1B3 total abundance (pmol/mg protein)
y = -0.0071x + 0.3756
R² = 0.0487
Na K ATPase area ratio
NTCP total abundance (pmol/mg protein)
y = -0.0123x + 0.6154
R² = 0.0247
Na K ATPase area ratio
OCT1 total abundance (pmol/mg protein)
y = -0.0695x + 1.9392
R² = 0.0435
Na K ATPase area ratio
OAT2 total abundance (pmol/mg protein)
y = -0.0194x + 0.4506
R² = 0.0399
Na K ATPase area ratio
MRP3 total abundance (pmol/mg protein)
y = 0.0526x + 0.2782
R² = 0.1432
Na K ATPase area ratio
MRP2 total abundance (pmol/mg protein)
y = 0.1627x + 0.267
R² = 0.2368
Na K ATPase area ratio
P-gp total abundance (pmol/mg protein)
y = 0.0756x + 0.0536
R² = 0.2735
Na K ATPase area ratio
BSEP total abundance (pmol/mg protein)
y = -0.0327x + 1.5255
R² = 0.0191
Na K ATPase area ratio

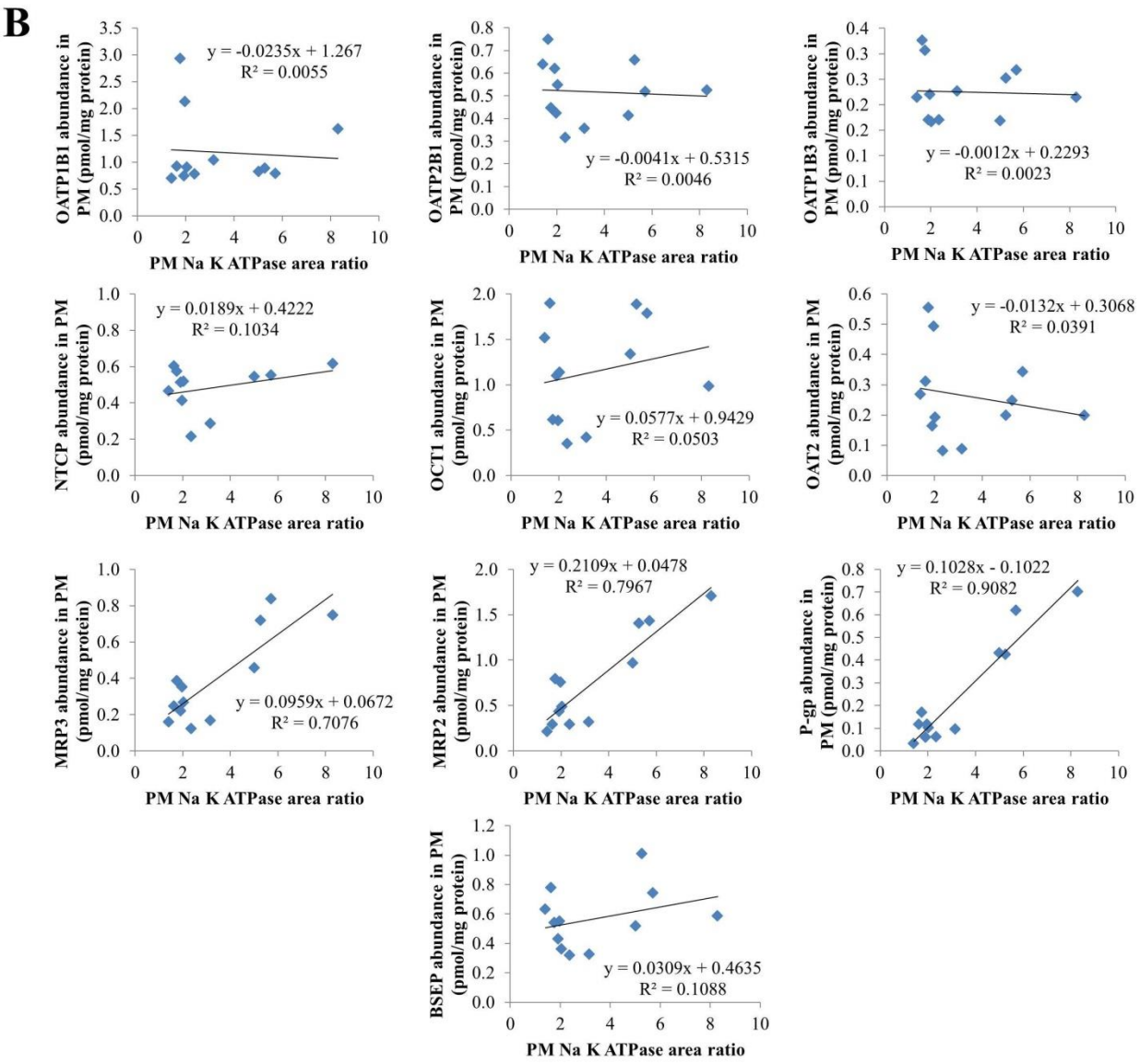

Fig. 4.6. Correlation of Total (A) and plasma membrane (B) transporter and Na^+-K^+ ATPase abundance in SH, PH and SCH. Of the transported studied, total abundance of the transporter was poorly correlated ($R^2 \leq 0.28$) with total abundance of Na^+-K^+ ATPase (A). Only PMA of MRP2, MRP3, and P-gp was highly correlated ($R^2 \geq 0.7$) with the PMA of Na^+-K^+ ATPase (B). The latter is shown as an area ratio (ratio of the Na^+-K^+ ATPase analyte peptide peak and Na^+-K^+ ATPase labeled internal standard peptide peak) because we did not have the standards of the analyte peptide (see methods). Each data are mean of 3-5 independent experiments.

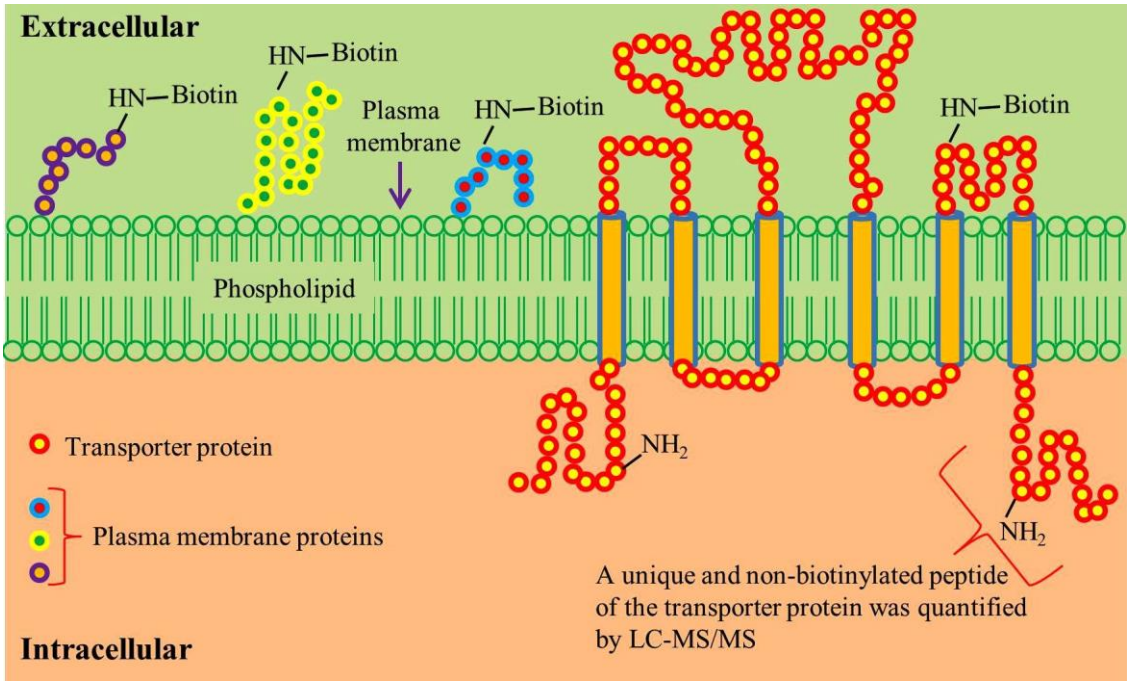

Fig. 4.7. A schematic diagram of the biotinylation of plasma membrane proteins in hepatocyte models and transporter-expressing cells. Cell surface biotinylation reagent (Sulfo-NHS-SS-Biotin) reacts non-specifically with free primary amines of plasma membrane proteins. The ability of this biotinylation reagent to permeate the plasma membrane and biotinylate the intracellular peptide of interest is limited due to its polarity.

Table 4.1. Demographic information and genotype of OATP1B1 of the hepatocyte donors

Lot #	Age	BMI	Gender	Race	Alcohol/ Tobacco/ Substance use	OATP1B1 Haplotype	OATP1B1 (SLCO1B1)		
							A388G	T521C	G1463C
ADR	38	28.7	Female	Caucasian	No	*5	A/A	T/C	G/C
FEA	57	32.4	Female	Caucasian	No	*1b	A/G	T/T	G/C
JEL	27	28.2	Female	African American	No	*1b	A/G	T/T	G/C
YTW	19	18.8	Male	Caucasian	No	*1a	G/G	T/T	G/C

Table 4.2. MRM parameters of peptides selected for targeted analysis of human hepatic transporter abundance. The labeled amino acid residue of the internal standard is shown in bold.

AB Sciex 6500 triple-quadrupole mass spectrometer parameters					
Protein	Surrogate Peptide	Parent ion (m/z)	Product ion (m/z)	Declustering potential (V)	Collision energy (V)
OATP1B1	NVTGFFQSFK	587.9	961.4	50	24
	NVTGFFQSF**K**	591.9	969.5		
OATP2B1	VLAVTDSPAR	514.8	816.4	60	26
	VLAVTDSPA**R**	519.8	826.4		
OATP1B3	NVTGFFQSLK	570.8	927.5	60	23
	NVTGFFQSL**K**	574.8	935.5		
OCT1	LSPSFADLFR	576.8	476.7	60	27
	LSPSFADLF**R**	581.8	481.8		
OAT2	NVALLALPR	483.8	753.5	56.4	19.3
	NVALLALP**R**	488.8	763.5		
MRP3	ADGALTQEEK	531.3	747.4	60	26
	ADGALTQEE**K**	535.3	755.4		
MRP2	LTIIPQDPILFSGSLR	885.4	665.5	60	39
	LTIIPQDPILFSGSL**R**	890.5	670.4		
P-gp	NTTGALTTR	467.8	719.4	70	26
	NTTGALTT**R**	472.8	729.4		
BSEP	STALQLIQR	515.3	657.4	68.7	22.4
	STALQLIQ**R**	520.3	667.4		
Na^+-K^+ ATPase	AAVPDAVGK	414.2	586.3	61.3	18.8
	AAVPDAVG**K**	418.2	594.3		
Calreticulin	EQFLDGDGWTSR	705.8	893.4	50	33
Waters Xevo TQS tandem mass spectrometer parameters					
Protein	Surrogate Peptide	Parent ion (m/z)	Product ion (m/z)	Cone voltage (V)	Collision energy (V)
NTCP	GIYDGDLK	440.7	710.1	30	10
	GIYDGDL**K**	444.7	718.3		
Na^+-K^+ ATPase	AAVPDAVGK	414.2	586.3	30	14
	AAVPDAVG**K**	418.2	594.3		
Calreticulin	EQFLDGDGWTSR	705.8	893.4	35	18

Table 4.3. Correlation (R^2) of total transporter abundance across LT, SH, PH, and SCH. Transporters showing good correlation ($R^2 \geq 0.67$) in their total abundance are in bold.

	OATP1B1	***OATP2B1***	***OATP1B3***	***NTCP***	***OCT1***	***OAT2***	***MRP3***	***MRP2***	***P-gp***	***BSEP***
OATP1B1	1									
OATP2B1	0.017	1								
OATP1B3	0.299	0.005	1							
NTCP	0.044	0.379	0.227	1						
OCT1	0.130	**0.671**	0.010	0.288	1					
OAT2	**0.762**	0.024	0.245	0.117	0.002	1				
MRP3	0.112	0.055	0.283	0.234	0.072	0.126	1			
MRP2	0.086	0.013	0.244	0.182	0.018	0.050	**0.938**	1		
P-gp	0.054	0.008	0.301	0.243	0.024	0.027	**0.878**	**0.927**	1	
BSEP	0.013	0.494	0.159	0.214	0.510	0.109	0.386	0.266	0.246	1

Table 4.4. Topology of selected unique peptides[#]. All selected peptides are localized in the intracellular domain (except OAT2 and NTCP) and are not exposed to the biotinylation reagent present in the extracellular space.

Protein	Peptide	Amino acid sequence in protein[#]	Localization[#]
OATP1B1	NVTGFFQSFK	321-330	Intracellular
OATP2B1	VLAVTDSPAR	314-323	Intracellular
OATP1B3	NVTGFFQSLK	321-330	Intracellular
NTCP	GIYDGDLK	144-151	Extracellular[$]
OCT1	LSPSFADLFR	330-330	Intracellular
OAT2	NVALLALPR	20-28	Intracellular and transmembrane[*]
MRP3	ADGALTQEEK	939-948	Intracellular
MRP2	LTIIPQDPILFSGSLR	1377-1392	Intracellular
P-gp	NTTGALTTR	809-817	Intracellular
BSEP	STALQLIQR	461-470	Intracellular
Na^+-K^+ ATPase	AAVPDAVGK	587-595	Intracellular
Calreticulin	EQFLDGDGWTSR	25-36	ER lumen

Reference: https://www.uniprot.org, $: http://topcons.cbr.su.se/pred/result/rst_1STpul/

*****Amino acid "N" (Asparagine, number 20) is localized intracellularly and the rest of the amino acids (VALLALPR, number 21-28) are localized in the transmembrane domain.

Chapter 5. Predicting Transporter-Mediated Hepatic Clearance of Rosuvastatin in Humans and Human Hepatocyte Models from Transporter-Expressing Cells

5.1 ABSTRACT

During drug development, suspended (SH), plated (PH) or sandwich-cultured human hepatocytes (SCHH) are routinely used to extrapolate in vitro transporter-mediated hepatic clearance (CL) of drugs to in vivo (IVIVE). However, these hepatocyte models have been reported to underpredict transporter-mediated in vivo hepatic uptake CL ($CL_{in\ vivo,blood}$) of drugs. Therefore, we determined if transporter-expressing cells can accurately predict in vivo $CL_{in\ vivo,blood}$ of drugs. To do so, we determined the uptake CL ($CL_{int,uptake,cells}$) of rosuvastatin (RSV) by transporter-expressing cells (OATPs/NTCP) and then scaled this $CL_{int,uptake,cells}$ by REF (the ratio of transporter abundance in human livers and transporter-expressing cells) determined by LC-MS/MS-based quantitative proteomics. Our success criteria was to predict the hepatic RSV $CL_{in\ vivo,blood}$ within 2-fold of the observed value (i.e. 850.5±175.5 ml/min). Assuming that the in vivo RSV hepatic uptake is the rate-determining step in hepatic CL of RSV, the predicted in vivo hepatic clearance ($CL_{in\ vivo,pred}$) by transporter-expressing cells, SH, PH and SCHH was 303.2±100.6, 138.9±53.8, 175.2.1±71.2, and 121.5±31.3 ml/min respectively. Both the transporter-expressing cells and hepatocyte models underpredicted the observed RSV $CL_{in\ vivo,blood}$. Interestingly, using REF, the transporter-expressing cells successfully predicted RSV $CL_{int,uptake,hep}$ in the hepatocyte models. Therefore, the underprediction of the in vivo RSV $CL_{in\ vivo,blood}$ by the transporter-expressing cells and hepatocytes is likely due to an endogenous factor(s) missing in transporter-expressing cells and hepatocyte models. If replicated with other drugs, the REF approach could be a better, economical, and high-throughput alternative to hepatocytes when predicting the in vivo transporter-mediated hepatic $CL_{in\ vivo,blood}$ of a drug.

5.2 INTRODUCTION

In drug development, predicting human pharmacokinetics (PK) of a drug is critical in the selection of new molecular entities with desired PK properties. With increased understanding of the absorption, distribution, metabolism, and excretion (ADME) processes, transporters are well recognized for their significant role in the ADME of drugs and their metabolites (Endres et al., 2006; Giacomini et al., 2010). For example, transporters play an important role in the hepatobiliary clearance (CL) and therefore hepatic concentrations of many drugs including drug used for hypercholesterolemia, diabetes and HCV infection (Endres et al., 2006; Giacomini et al., 2010; Kock and Brouwer, 2012).

While in vitro and in silico methods (e.g. physiologically based pharmacokinetic (PBPK) models) have been developed to successfully predict hepatic metabolic clearance (CL) of drugs (Sager et al., 2015), such methods have yet to be validated to successfully predict transporter-mediated CL of drugs. Currently, hepatocyte models, such as suspended (SH) or plated (PH) hepatocytes are used for in vitro to in vivo extrapolation (IVIVE) of transporter-mediated hepatic CL of drugs. However, these hepatocyte models are widely reported to underpredict the in vivo hepatic CL of drugs (Abe et al., 2008; Li et al., 2010; Jones et al., 2012; Zou et al., 2013). In addition, they are costly and show considerable inter-lot variability in transporter CL (Vildhede et al., 2014; Izumi et al., 2017). To overcome these shortcomings, we have hypothesized that the in vivo transporter-mediated CL of drugs can be predicted by first measuring the transporter-mediated CL of the drug in transporter-expressing cells; then, scaling this CL using the relative abundance of the transporter in cells vs. human tissue (REF), determined by LC-MS/MS-based quantitative targeted proteomics. We have recently shown the success of this proteomics-

informed approach by successfully predicting the hepatic uptake CL of rosuvastatin (RSV) in rats (Ishida et al., 2018) and the renal secretory CL of metformin in humans (Kumar et al., 2018).

To date, this REF approach has been based on the total transporter abundance in both the transporter-expressing cells and in human tissue. However, only transporters present in the plasma membrane actively transport drugs. Therefore, we optimized a quantitative biotinylation method to determine the plasma membrane abundance (PMA) of transporters in transporter-expressing cells and hepatocytes (Kumar et al., 2017; Kumar et al., 2019b). Utilizing data from these studies, here we present data where we determined 1) whether the proteomics-informed REF approach can successfully predict the in vivo human hepatic uptake CL of rosuvastatin (RSV), an OATP, NTCP and BCRP substrate; 2) if the use of PMA vs. total abundance of transporters improves the predictions of the REF approach; 3) if the proteomics-informed REF approach better predicts the in vivo human hepatic RSV CL than the traditional hepatocyte models, namely suspended (SH), plated (PH) or sandwich-cultured human hepatocytes (SCHH); and 4) if RSV uptake CL in SH, PH or SCHH can be predicted from transporter-expressing cells using the REF approach (i.e. in vitro cell to in vitro hepatocytes extrapolation (IVCIVH). This last aim was designed in case neither approach (i.e. in 3 above) successfully predicted the in vivo RSV hepatic uptake CL. As we have done previously, here we set our success criteria as being able to predict the hepatic uptake clearance of RSV within 2-fold of the observed value (Kumar et al., 2017; Ishida et al., 2018).

5.3 MATERIALS AND METHODS

5.3.1 *Chemicals and Reagents*

Synthetic signature peptides for OATP1B1, OATP2B1, OATP1B3, and NTCP were obtained from New England Peptides (Boston, MA). The corresponding stable isotope labeled (SIL) peptides for the above transporters, dithiothreitol (DTT), iodoacetamide (IAA), mass spectrometry grade trypsin, William's E Medium (no glutamine), cryopreserved hepatocyte recovery medium, total protein quantification bicinchoninic acid assay (BCA) kit, Hank's balanced salt solution with calcium and magnesium (HBSS), and Pierce cell surface protein isolation kit were obtained from Thermo Scientific (Rockford, IL). Pierce cell surface protein isolation kit contains sulfosuccinimidyl-2-(biotinamido) ethyl-1, 3-dithiopropionate (sulfo-NHS-SS-biotin), quenching solution (100 mm glycine), lysis buffer, neutravidin agarose gel, wash buffer, column accessory pack, DTT, phosphate buffer and Tris buffer. HPLC-grade acetonitrile and sodium dodecyl sulfate (SDS) were purchased from Fischer Scientific (Fair Lawn, NJ). Formic acid was purchased from Sigma-Aldrich (St. Louis, MO). All reagents were analytical grade. 24-well collagen-coated plates and matrigel were purchased from Corning (Kennebunk, ME). Human hepatocyte thaw medium, INVITROGRO CP medium, INVITROGRO HI medium, and TORPEDO antibiotic mix were obtained from BioIVT (Westbury, NY). Radiolabeled [^{3}H]RSV and cold RSV were purchased from American Radiolabeled Chemicals (Saint Louis, MO) and Toronto Research Chemicals (North York, ON, Canada) respectively.

5.3.2 *Procurement of Human Hepatocytes and Transporter-Expressing Cells*

Human liver frozen tissues and cryopreserved human hepatocytes were obtained from BioIVT (Westbury, NY). The demographics of the human liver donors (n = 4, ADR, FEA, JEL, and

YTW) were as described before (Kumar et al., 2019b). OATP1B1-expressing CHO cells were generously provided by Dr. Bruno Stieger, University Hospital Zurich, Switzerland. OATP1B3-expressing HEK293, OATP2B1-expressing MDCKII, and NTCP-expressing HEK293 cells were generously provided by SOLVO Biotechnology, Hungary.

5.3.3 *[^{3}H]RSV Uptake Study in OATP1B1/2B1/1B3 or NTCP Transporter-Expressing Cells*

[^{3}H]RSV transport studies were conducted in OATP1B1-expressing CHO cells, OATP2B1-expressing MDCKII cells, OATP1B3-expressing HE293 cells and NTCP-expressing HEK293 cells. Transporter-expressing cells were grown in 24-well poly-D-lysine coated plates, at a density of 0.5 million cells per well with 1 ml of DMEM (CHO cells: low glucose DMEM, HEK293 cells and MDCKII cells: high glucose DMEM) medium for 24 hr. After 24 hr, cells were washed twice with 1 ml/well DPBS buffer. Then, they were incubated at 37 °C with Ca^{2+} and Mg^{2+}- containing HBSS buffer (hereafter referred as Ca^{2+}-containing HBSS buffer) containing 30 nM [^{3}H]RSV and 70 nM unlabeled RSV with or without 200 µM bromsulphthalein (BSP) (OATP cells) or with (Ca^{2+}-containing HBSS) or sodium-free HBSS buffer (NTCP cells) (Bi et al., 2013). To determine transporter-mediated uptake CL of [^{3}H]RSV the uptake (in triplicate) of [^{3}H]RSV was terminated after 5 sec (within linear phase) by washing the cells three times with ice-cold HBSS buffer (1 ml each). [^{3}H]RSV uptake at 5 and 60 sec (within linear phase) in the presence of 200 µM BSP or in the absence of sodium was used to estimate [^{3}H]RSV passive diffusion clearance. Then, the cells were lysed at 37 °C for 2 hours with 1 ml 2% SDS. Forty microliters of this lysate were used for total protein determination using the BCA method, and 700 µl was used to quantify total radioactivity by Tri-Carb Liquid Scintillation Counters (PerkinElmer, Waltham, MA).

5.3.4 *[^{3}H]RSV Uptake Study in Human Hepatocyte Models (SH, PH and SCHH)*

SH: Cryopreserved human hepatocytes were thawed and processed as described before (Kumar et al., 2019b). Briefly, the hepatocytes were centrifuged at 1000 g for 5 mins at 4 °C to remove cryopreserved hepatocyte recovery medium. Then, the hepatocytes were reconstituted in Ca^{2+}-containing or Na^{+}-free HBSS medium and the medium containing 0.35×10^6 viable hepatocytes (50 µl) were transferred to a 1.5 ml centrifuge tube and placed in a 37 °C water bath. The transport study was started by the addition of 50 µl of Ca^{2+}-containing or Na^{+}-free HBSS medium containing 60 nM [^{3}H]RSV and 140 nM RSV with or without 400 µM BSP to achieve a final concentration of 30 nM [^{3}H]RSV, 70 nM RSV and 200 µM BSP. At 2 and 10 min (within linear phase), the transport was terminated, as follows, using the oil-stop method. First, 150 µl of ice-cold Na^{+}-free HBSS was added to the hepatocyte incubation. Then, 200 µl of the medium containing the hepatocytes were transferred slowly to the top of the oil layer (containing 200 µl of 3% cesium chloride with 200 µl of the mixture of silicone oil: mineral oil (5:1)) and centrifuged for 15 sec at 12000 g. The supernatant was immediately aspirated and the tube containing the pellet was cut, and the pellet was transferred and dissolved in 1 ml of 2% SDS. The total radioactivity in SH lysate (700 µl) was measured using a liquid scintillation counter (PerkinElmer, Waltham, MA). In addition, 40 µL of SH lysate was used to measure total protein using the BCA Protein Assay Kit (Thermo Fisher Scientific, Rockford, IL).

PH: Cryopreserved human hepatocytes were thawed and plated as described before (Kumar et al., 2019b). About 0.35×10^6 hepatocytes were plated per well in a 24-well collagen-coated plate for 5 hours with 0.5 ml/well TORPEDO containing INVITROGRO CP medium (1:9 (v/v). [^{3}H]RSV uptake (at 2 and 10 min; within linear phase) by the plated human hepatocytes incubated with Ca^{2+}-containing or Na^{+}-free HBSS medium containing 30 nM labeled [^{3}H]RSV

and 70 nM unlabeled RSV was measured, as described above, in the presence or absence of Na^+ or 200 µM BSP. Immediately afterwards, 1 ml of 2% SDS was added to each well to lyse the cells (uptake phase) and processed as described above.

SCHH: Cryopreserved human hepatocytes were thawed and sandwich-cultured as described before (Kumar et al., 2019b). SCHH protocol was adopted from Liu et al., 1999 and Pfeifer et al.,2013 (Liu et al., 1999; Pfeifer et al., 2013). Briefly, on day 4 after sandwich-culturing the SCHH (0.35×10^6 hepatocytes /well) were washed twice with 1 ml of Ca^{2+}-containing HBSS buffer and then pre-incubated for 10 minutes at 37 °C with 500 µl of Ca^{2+}-containing HBSS. Then, the SCHH were incubated at 37 °C with 500 µl of 30 nM [^{3}H]RSV and 70 nM unlabeled RSV for 0.5, 2, and 5 minutes (linear phase) in Ca^{2+}-containing HBSS with or without 200 µM BSP (to assess OATP-mediated uptake) or Na^+ (to assess NTCP-mediated uptake). Uptake was terminated by washing the SCHH with ice-cold Ca^{2+}-containing HBSS. Immediately afterwards, 1 ml of 2% SDS was added to each well to lyse the cells (uptake phase) and processed as described above.

5.3.5 *Quantification of Total or Plasma Membrane Transporter Abundance in Transporter-Expressing Cell Lines, Human Liver Tissues, Suspended, Plated, and Sandwich-Cultured Human Hepatocytes*

Data on total or PMA of OATP1B1/2B1/1B3 or NTCP transporter abundance in the transporter-expressing cells, human liver tissues (n = 39) and hepatocyte homogenates were obtained from our previous publications (Wang et al., 2016; Kumar et al., 2017; Kumar et al., 2019b).

5.3.6 *Data and Statistical Analyses*

Determination of Transporter-Mediated and Passive Diffusion CL_{int} of RSV

OATP1B1/2B1/1B3 or NTCP Transporter-Expressing Cells: The OATP or NTCP transporter-mediated intrinsic uptake CL ($CL_{int,uptake,cells,1B1,}$ $CL_{int,uptake,cells,1B3,}$ $CL_{int,uptake,cells,2B1,}$ $CL_{int,uptake,cells,NTCP,}$ hereafter referred to as $CL_{int,uptake,cells}$) of [^{3}H]RSV was determined the first by taking the difference in [^{3}H]RSV uptake into the cells in the presence and absence of BSP or Na^+, respectively. Then, the OATP- or NTCP-mediated uptake CL_{int} of [^{3}H]RSV into these cells was calculated as the ratio of the rate of transporter-mediated uptake of [^{3}H]RSV and [^{3}H]RSV concentration in the medium (30 nM). The passive diffusion Cl_{int} ($CL_{int,passive,cells}$) of [^{3}H]RSV into the cells was calculated as above except that the rate of uptake of [^{3}H]RSV uptake into the cells in the presence of 200 µM BSP or in the absence of sodium was used. The $CL_{int,passive,cells}$ used was the average of passive diffusion CL obtained in CHO, MDCKII, and HEK293 cells.

SH, PH and SCHH: The total transporter-mediated CL_{int} of [^{3}H]RSV in hepatocyte models ($CL_{int,uptake,hep}$) was calculated in the presence of 200 µM BSP (an OAPT and NTCP inhibitor) as above. Of this, the OATP-mediated CL_{int} of [^{3}H]RSV was calculated as above, but the passive diffusion CL_{int} ($CL_{int,passive,hep}$) was determined by using only the data on uptake of [^{3}H]RSV in Na^+-free HBSS buffer and in the presence of BSP. NTCP-mediated CL_{int} of [^{3}H]RSV was calculated as above but by using only the data on uptake of [^{3}H]RSV in Ca^{2+}-containing and Na^+-free HBSS buffer.

$$CL_{int,uptake,hep} = CL_{int,OATP,hep} + CL_{int,NTCP,hep} + CL_{int,passive,hep} \quad \textit{Eq. 1}$$

Where, $CL_{int,OATP,hep}$, $CL_{int,NTCP,hep}$, and $CL_{int,passive,hep}$ are OATP-mediated, NTCP-mediated and passive diffusion CL_{int} of RSV in the hepatocyte models respectively.

IVIVE of Intrinsic Hepatic Uptake CL of RSV from Transporter-Expressing Cells ($CL_{int,in\ vivo,pred,cells}$) Using REF:

The $CL_{int,in\ vivo,pred,cells}$ from the transporter-expressing cells was calculated as the sum of the contribution of uptake CL of [^{3}H]RSV by each transporter (using plasma membrane abundance, Table 5.1) and by passive diffusion as follows:

$$CL_{int,in\ vivo,pred,cells} = CL_{int,in\ vivo,pred,1B1} + CL_{int,in\ vivo,pred,1B3} + CL_{int,in\ vivo,pred,2B1} + CL_{int,in\ vivo,pred,NTCP} + CL_{int,in\ vivo,pred,passive} \quad \textit{Eq. 2}$$

Where i in $CL_{int,in\ vivo,pred,i}$ represents the contribution of the ith transporter (i.e. OATP1B1, OATP1B3, OATP2B1 or NTCP). $CL_{int,in\ vivo,pred,passive}$ was scaled as in equation 4.

The contribution of each transporter in prediction of $CL_{in\ vivo,pred,cells}$ of RSV was calculated using equation 3 as described below for OATP1B1 transporter.

$$CL_{int,in\ vivo,pred,1B1} = CL_{int,uptake,cells,1B1} \times [OATP1B1]_{avg} \quad \textit{Eq. 3}$$

Where $[OATP1B1]_{avg}$ represents average of total OATP1B1 transporter abundance in human liver samples (n=39). Since, the cell-surface biotinylation methodology to estimate PMA of transporters cannot be used with intact tissue (Kumar et al., 2019b), all the transporters quantified in liver tissue were assumed to be present in the plasma membrane.

IVIVE of Intrinsic Hepatic Uptake CL ($CL_{int,in\ vivo,pred,hep}$) of* RSV *from Hepatocyte Models:

$CL_{int,uptake,hep}$ of RSV obtained from hepatocyte models was scaled to human liver as follows:

$$CL_{int,in\ vivo,pred,hep} = CL_{int,uptake,hep}\ (\mu l/min/mg\ protein) \times liver\ weight\ (g) \times Total\ protein\ per\ unit\ liver\ weight \quad \textit{Eq. 4}$$

Where, $CL_{int,in\ vivo,pred,hep}$ is the predicted in vivo intrinsic hepatic uptake CL from data in each hepatocyte model. Liver weight is 1500 g and the total protein per unit liver weight is 88 mg/g of liver (Karlgren et al., 2012).

Prediction of In vivo Total Hepatic CL ($CL_{in\ vivo,pred}$) of RSV from Transporter-Expressing Cells ($CL_{in\ vivo,pred,cells}$) and Hepatocyte Models ($CL_{in\ vivo,pred,hep}$):

When the hepatic uptake is the rate-determining step in the in vivo hepatic CL of a drug (Yang et al., 2007; Patilea-Vrana and Unadkat, 2016), then we can predict the hepatic blood $CL_{in\ vivo,pred}$ of RSV from its hepatic intrinsic uptake CL in cells or hepatocytes as follows:

$$CL_{in\ vivo,pred} = \frac{Q_{hep} \times f_{u,b} \times CL_{int,in\ vivo,pred,cells/hep}}{Q_{hep} + f_{u.b} \times CL_{int,in\ vivo,pred,cells/hep}} \qquad Eq.\ 5$$

Where, $f_{u,b}$ is the RSV fraction unbound in blood (0.1) and was estimated using equation 6.

$$f_{u,b} = \frac{f_{u,p}}{B:P} \times (1 - H) \qquad Eq.\ 6$$

$f_{u,p}$ is the RSV fraction unbound in plasma (0.12) (Martin et al., 2003a), and B:P is the RSV blood to plasma ratio (0.69 (Martin et al., 2003a)) and H is the hematocrit value (0.4).

Prediction of $CL_{int,uptake,hep}$ of [^{3}H]RSV in Hepatocyte Models from Transporter-Expressing Cells (IVCIVH)

The $CL_{int,uptake,hep}$ of [^{3}H]RSV in each human hepatocyte model was predicted from $CL_{int,uptake,cells}$ as follow:

$$CL_{int,hep,predicted} = CL_{int,uptake,cells,OATP1B1} \times [OATP1B1]_{hep} + CL_{int,uptake,cells,OATP1B3} \times [OATP1B3]_{hep} + CL_{int,uptake,cells,OATP2B1} \times [OATP2B1]_{hep} + CL_{int,uptake,cells,NTCP} \times [NTCP]_{hep} + CL_{int,passive,cells} \qquad Eq.\ 7$$

Where, $[Transporter]_{hep}$ represents total or PMA of the transporter (picomole/mg protein) in the hepatocyte model (Kumar et al., 2019b).

Statistical analysis:

Wilcoxon matched-pair signed rank statistical test (using Prism 7, version 7.03) was used to compare the observed $CL_{int,uptake,cells}$, $CL_{int,OATP,hep}$, $CL_{int,NTCP,hep}$, and $CL_{int,passive,hep}$ of [^{3}H]RSV across the various hepatocyte models (Fig. 5.1). Tukey's multiple comparison test was used to compare $CL_{in\ vivo,pred,cells}$ with each $CL_{in\ vivo,pred,hep}$ obtained from the hepatocyte models (Fig. 5.2). The same statistical test was used to determine if the observed $CL_{int,uptake,hep}$ of [^{3}H]RSV in hepatocyte models was significantly different from that predicted by transporter-expressing cells, $CL_{int,hep,predicted}$ (IVCIVH; Fig. 5.3). Tukey's multiple comparison test was also used to determine if [^{3}H]RSV $CL_{int,passive,cells}$ was significantly different from $CL_{int,uptake,hep}$ (Fig. 5.5).

5.4 RESULTS

5.4.1 *Predicted OATP1B1, OATP1B3, OATP2B1 and NTCP-Mediated RSV $CL_{int,uptake,cells}$*

When expressed with respect to mg of cellular protein, except for OATP2B1, the transporter-mediated [^{3}H]RSV $CL_{int,uptake,cells}$ was similar across all the transporters (Table 5.1). However, when [^{3}H]RSV $CL_{int,uptake,cells}$ was expressed per pmol of total or PMA of each transporter, the picture changed. In this case, the NTCP-mediated [^{3}H]RSV was ~2-fold greater than by OATPs irrespective of whether $CL_{int,uptake,cells}$ was obtained using total or the PMA of the transporter (Table 5.1). Except for OATP2B1, the majority (>60%) of each transporter were found to be expressed in the PM. The estimated $CL_{int,passive,cells}$ of [^{3}H]RSV in CHO, MDCKII and HEK293 cells was similar across the cells (mean: 0.19±0.04 µl/min/mg cellular protein, range: 0.15 to 0.24 µl/min/mg cellular protein) and statistically not different from the corresponding passive diffusion CL in hepatocyte models ($CL_{int,passive,hep}$) (Fig. 5.5).

5.4.2 *A Comparison of [^{3}H]RSV $CL_{int,uptake,hep}$ in SH, PH and SCHH*

The total uptake of [^{3}H]RSV in all lots of hepatocytes was about the same except for JEL where it was consistently higher than the other three lots due to greater OATP-mediated uptake (Fig. 5.1). Overall, $CL_{int,uptake,hep}$, $CL_{int,OATP,hep}$, $CL_{int,NTCP,hep}$, and $CL_{int,passive,hep}$ of RSV were not significantly different between the hepatocyte models (Fig. 5.1D). In addition, the average contribution of OATPs was higher than NTCP (56% *vs.*40%) to total [^{3}H]RSV $CL_{int,uptake,hep}$ (Fig. 5.1D). Of note, the average $CL_{int,passive,hep}$ of [^{3}H]RSV in SH, PH and SCHH was only 5.6±3.2%, 2.2±1.0% and 7.4±8.0% of the total [^{3}H]RSV $CL_{int,uptake,hep}$ respectively (Fig. 5.1A-D).

5.4.3 *Prediction of RSV $CL_{in\ vivo,blood}$ from Transporter-Expressing Cells ($CL_{in\ vivo,pred,cells}$) and Hepatocyte Models ($CL_{in\ vivo,pred,hep}$) (IVIVE)*

$CL_{in\ vivo,blood}$ predicted using REF and transporter-expressing cells (OATP1B1/1B3/2B1, NTCP and passive diffusion) was within 3-fold, but, outside of our pre-defined acceptable criteria of being within 2-fold of the observed hepatic blood CL *($CL_{in\ vivo,blood}$).* The predicted RSV hepatic $CL_{in\ vivo,pred,cells}$ was 35.6% (303.2±100.6 ml/min) of the mean observed $CL_{in\ vivo,blood}$ (mean 850.5 ml/min, 95% CI 725-976 ml/min) (Martin et al., 2003a). Of the predicted total RSV $CL_{in\ vivo,blood}$ by transporter-expressing cells, ~99% was via transporters and ~1% via passive diffusion (Fig. 5.2). Of the total predicted RSV $CL_{int,in\ vivo,pred,cells}$, the contribution of OATP1B1, OATP1B3, OATP2B1, NTCP and diffusion clearance was 37.9, 15.5, 7.6, 38.3 and 0.6% respectively (Fig. 5.2). The $CL_{in\ vivo,pred,hep}$ based on SH, PH, and SCHH was about 16% (138.9±53.8 ml/min), 21% (175.2±71.2 ml/min), and 14% (121.5±31.3 ml/min) of the observed value respectively (Fig. 5.2). The $CL_{int,in\ vivo,pred,cells}$ of RSV based on transporter-expressing cells was 3934.2±1634.2 ml/min (OATP1B1: 1489.8±726.8 ml/min, OATP1B3: 610.8±306.6 ml/min, OATP2B1:

300.9±112.9 ml/min, and NTCP: 1507.6±667.5 ml/min, passive diffusion: 25.1 ml/min). The average $CL_{int,in\ vivo,pred,hep}$ of RSV based on SH, PH and SCHH (1551±672.6, 2022.6±965.6 and 1328.7±376.2 ml/min respectively) was ~50-70% lower than that based on transporter-expressing cells.

5.4.4 *Prediction of RSV $CL_{int,uptake,hep}$ from Transporter-Expressing Cells (IVCIVH)*

The total transporter-mediated $CL_{int,uptake,hep}$ in hepatocyte models predicted from cell lines (i.e. the sum of CL_{int} predicted by the individual transporter-expressing cells, OATP1B1/1B3/2B1 and NTCP) was not significantly different from the observed values, irrespective of whether the predictions were based on the total or PMA of the transporters in the cells (Fig. 5.3). The average contribution of OATP1B1, OATP1B3, OATP2B1, NTCP and passive diffusion to the [^{3}H]RSV uptake in hepatocyte models was about 42±8, 9±1, 9±1, 33±0.3, and 7±7% respectively. The [^{3}H]RSV $CL_{int,passive,hep}$ and $CL_{int,passive,cells}$ were not significantly different (Fig. 5.5).

Dr. Kazuya Ishida provided insightful suggestions to perform this experiment.

5.4.5 *Transporter Abundance-Activity Correlation in Human Hepatocyte Models*

The observed total $CL_{int,uptake,hep}$ of [^{3}H]RSV in the human hepatocyte models was well correlated with total transporter abundance of OATP1B1 (R^2 = 0.80; Fig 4A) but not with total abundance of OATP1B3, OAPT2B1, or NTCP (Fig. 5.4B-D). This conclusion did not change if the PMA of the transporters was used as the independent variable (data not shown).

5.5 DISCUSSION

We designed our study to incorporate several unique features, many of which have not been previously incorporated when conducting IVIVE of transporter-based CL. First, we studied RSV

as a model substrate as it is taken up by multiple transporters and is minimally metabolized in the liver. Thus, its hepatic clearance should reflect only hepatobiliary (and not metabolic) transport clearance of RSV. Second, because RSV is rapidly taken up by human hepatic transporters (Kitamura et al., 2008; Pan et al., 2011) and it is a relatively hydrophilic statin, we could assume with confidence that hepatic uptake clearance would be rate-determining step in it's in vivo hepatic clearance (Patilea-Vrana and Unadkat, 2018). Thus, we could determine if our proteomics-informed IVIVE approach (based on REF) could predict the in vivo hepatic CL of RSV after IV administration of the drug (Martin et al., 2003a). This is an important consideration as previous IVIVE of hepatic CL of drugs have assumed (likely erroneously) that the hepatic uptake CL of the drugs is the only rate-determining step in the clearance of the drug (Li et al., 2010). Third, we included our previously published total and PMA of transporters (OATPs) in cell lines (Kumar et al., 2018) used here to predict RSV hepatic uptake CL in vivo and in vitro in three different hepatocyte models. Thus <100 % PMA of transporters (if any) in cell lines could be taken into consideration when using REF for IVIVE of RSV hepatic uptake CL. Fourth, we studied RSV uptake into multiple hepatocyte models (isolated from the same donor) in which we previously quantified the total and PMA abundance of OATPs and NTCP (Kumar et al., 2018). Thus, we were able to test which hepatocyte model (SH, PH or SCHH) better predicted in vivo hepatic uptake CL of RSV and compared these predictions with that obtained from transporter-expressing cells. The PMA of transporters in cells and hepatocytes was determined by a cell-surface biotinylation method that was optimized and refined in our laboratory (Kumar et al., 2017). Fifth, quantifying RSV uptake CL into cells and hepatocytes allowed us to determine if there was an in vitro to in vitro (IVCIVH) agreement in the predicted transporter-based hepatic

uptake CL of RSV. This comparison is important (as described below) as both in vitro models under-estimated the in vivo hepatic uptake CL of RSV, albeit to a different extent.

The predicted $CL_{in\ vivo,pred,cells}$ by transporter-expressing cells was 303.2 ml/min. This value was about 36% of the observed mean hepatic blood clearance (850.5 ml/min; calculated from Martin et al., 2003). This value does not meet our success criteria of being within 2-fold of the observed value, a criteria widely used for wide therapeutic index drugs. The goal of proteomics-informed IVIVE of CL is not to predict CL of a drug exactly, but to provide an estimate of the eventual CL of the drug likely to be expected in a Phase 1 trial of the drug. An additional goal was to predict likely DDI liabilities of the drug in subsequent clinical trials. Our data showed that the hepatic DDI liabilities for RSV are confined to two transporters, OATP1B1 and NTCP, major contributors to the hepatic uptake of RSV. Due to greater contribution of OATP1B1 in RSV uptake vs. NTCP, the former poses greater DDI liability than the latter (Simonson et al., 2004; Lai et al., 2016). It is for this reason that the FDA has designated RSV as a probe OATP victim drug when estimating the likelihood of an OATP-based DDI when co-administered with another drug (Chu et al., 2018).

The above comparison is based on the assumption that the hepatic CL of RSV is rate-determined by its uptake by the liver. However, this assumption does not need to be made if the predicted $CL_{int,in\ vivo,pred,cells}$ is compared with the sinusoidal intrinsic uptake CL obtained in vivo. We have recently obtained an estimate of the latter through positron emission tomography (PET) imaging (unpublished data). Indeed, the predicted $CL_{int,in\ vivo,pred,cells}$ (3934.2±1634.2 ml/min) of RSV is about 33% of its observed hepatic intrinsic uptake CL (12056±3848 ml/min) in our [^{11}C]RSV PET imaging study.

Since, human hepatocytes are routinely used to predict transporter-mediated CL in vivo, we next asked whether the various human hepatocytes models (SH, PH, or SCHH) could better predict RSV $CL_{in\ vivo,blood}$ than our proteomics-informed REF approach? And, hepatocyte models did not. In fact, the predictions were poorer than that from the proteomics-informed REF approach. All the hepatocyte models studied considerably under-predicted RSV $CL_{in\ vivo,blood}$ by about 5-7 fold, with SCHH being the poorest and PH being the best (though there was no statistically significant difference between the models). Indeed, this finding is consistent with previous literature reports that hepatocytes under-predict (sometimes drastically) transporter-mediated hepatic CL of drugs (Jones et al., 2012). Based on the above discrepancy (~52%) between cells and hepatocytes in the prediction of $CL_{in\ vivo,blood}$, we investigated possible reasons for this under-prediction. To do so, we asked if the RSV $CL_{int,uptake,cells}$ by transporter-expressing cells could predict $CL_{int,uptake,hep}$ using the proteomics-informed approach (IVCIVH). Indeed, the predicted RSV $CL_{int,hep,predicted}$ was larger but not significantly different from the observed value, irrespective of whether the total or PMA of the transporters was used as REF (Fig. 5.3). In addition, the RSV $CL_{int,passive,cells}$ predicted by the transporter-expressing cells, was not significantly different than that observed in hepatocytes ($CL_{int,passive,hep}$) (Fig. 5.5). This result immediately poses the question: why was the RSV $CL_{in\ vivo,pred,cells}$ significantly greater than that predicted from the hepatocytes ($CL_{in\ vivo,pred,hep}$) (Fig. 5.2)? We believe that the reason for this is that we used PMA-based REF to predict $CL_{in\ vivo,pred,cells}$, whereas $CL_{in\ vivo,pred,hep}$ did not take into consideration PMA of transporters. Instead, it used the total protein in human liver as a scaling factor and assumed 100% PMA of the transporters in the hepatocyte models even though it was only 60-80% (OATPs and NTCP) (Kumar et al., 2019b). Indeed, when a hybrid (REF and total

protein) approach was used to scale $CL_{int,hep,predicted}$ (Table 5.1, Fig. 5.3), the $CL_{in\ vivo,pred,hep}$ was not significantly different from $CL_{in\ vivo,pred,cells}$ (data not shown).

The above IVCIVH comparison was informative to address the question as to why both approaches (cells and hepatocytes) under-estimated RSV $CL_{in\ vivo,blood}$, the hepatocytes more so than the cells. A possible explanation is that the in vitro models are not adequately capturing the *in vivo* transporter (OATP/NTCP)-mediated or the passive hepatic uptake clearance of RSV or both. This could be due to differences in the in vivo RSV affinity (K_m) or k_{cat} (catalytic turnover) of the drug by the transporters is different form that in vitro. Mechanistically, this could be due to a difference in post-translational modifications of the transporter protein(s) between in vitro and in vivo resulting in either a change in the PMA of the transporters, $k_{cat,}$ or the affinity (K_m) for the drug. Alternatively, there could be in vivo activation of the human OATP transporters by endogenous factors such plasma proteins (Patik et al., 2015; Bowman et al., 2019). While our study accounted for differences in the transporter abundance between in vitro systems and in vivo, our method assumes that the catalytic activity of the transporters (per transporter molecule) is the same in vitro and in vivo. Indeed, plasma proteins have recently been shown to increase RSV uptake (4-fold) into rat hepatocytes (Bowman et al., 2019) or human hepatocytes (2.5-fold) (Kim et al., 2019). This difference matches the magnitude by which our REF approach under-predicts $CL_{in\ vivo,blood}$. These speculative mechanistic explanations for under-estimation of in vivo RSV hepatic uptake clearance by in vitro systems must be species-dependent as it has been shown that the transporter-expressing cells successful predicted of RSV hepatic uptake clearance in rats (Ishida et al., 2018).

Although NTCP-mediated RSV $CL_{int,uptake,cells,NTCP}$ was about twice higher than that by OATP1B1 (Table 5.1), due to the greater hepatic/hepatocyte abundance of OATP1B1, the latter

was the dominant contributor (33 - 48%) to the total RSV $CL_{int,uptake,hep}$. The contribution of OATP1B1 (33 - 48%) to RSV $CL_{int,uptake,hep}$ was higher than that by OATP2B1 (8 - 10%) or OATP1B3 (8 - 9%) or NTCP (33%). Thus, it is not surprising that OATP1B1 total abundance (or PMA) showed good correlation ($R^2 \geq 0.80$) with total RSV $CL_{int,uptake,hep}$ into SH, PH and SCHH (Fig. 5.4).

Theoretically, only the transporters present in the plasma membrane of a cell are active in transporting a drug. Thus, REF based on PMA of a transporter is expected to better predict transporter-mediated clearance than REF based on total cellular transporter abundance. RSV $CL_{int,uptake,cells}$ equally well predicted RSV $CL_{int,uptake,hep}$ irrespective of whether the total or PMA REF was used (Fig. 5.3). This was because the major contributors to RSV $CL_{int,uptake,hep}$, OATP1B1 and NTCP, were found to be predominately in the plasma membrane of cells and hepatocytes (Kumar et al., 2018). The lower overall contribution of OATP2B1 to the total RSV hepatocyte uptake explains why the lower %PMA (37.1%) of OATP2B1 in MDCKII cells (Table 5.1) (Kumar et al., 2019b)) vs. that in hepatocyte models (>60%) did not affect this conclusion. But, this would not be the case if OATP2B1 (or for that matter any other transporter) was to play a greater role in the hepatic uptake of the drug (McFeely et al., 2018). Thus, as shown here, and previously for OCT2 (Kumar et al., 2018), it is important that PMA of transporters be considered in IVIVE.

One goal of IVIVE of hepatobiliary CL of drugs is to predict the hepatic concentrations of the drug when the site of toxicity or efficacy is within the liver. Obviously, predicting the in vivo hepatic CL of a drug is insufficient to predict the hepatic concentration of a drug because all in vivo hepatobiliary clearances (sinusoidal uptake CL ($CL_{s,uptake}$), metabolic CL ($CL_{metabolism}$), biliary efflux CL ($CL_{b,efflux}$), sinusoidal efflux CL($CL_{s,efflux}$)) need to be estimated or predicted in

vitro. While the SCHH have been suggested as a tool to estimate these clearances, the data presented here on lack of adequate prediction of in vivo hepatic $CL_{s,uptake}$ by SCHH suggest alternative methods are needed to estimate all these hepatobiliary clearances. One alternative method is to use proteomics-based REF for IVIVE of $CL_{s,efflux}$ and $CL_{b,efflux}$. $CL_{metabolism}$ can readily be obtained by using human liver microsomes/cytosol or S9 fraction. As to whether this proteomics-informed REF approach can successfully predict transporter-based clearance and tissue concentration of drugs in humans is yet to be determined. However, initial success in IVIVE of hepatic ^{11}C-RSV concentrations in our rat study demonstrates the potential of this approach (Ishida et al., 2018).

In summary, we have compared the ability of two in vitro systems, transporter-expressing cells and human hepatocyte models, to predict in vivo RSV hepatic uptake CL in humans. We clearly show that the REF using transporter-expressing cells resulted in a better prediction of the in vivo RSV hepatic uptake CL than when hepatocyte models are used. This finding, if replicated with other drugs, together with previous success in using REF to predict the in vivo hepatic clearance of RSV in rats (Ishida et al., 2018) and renal secretory CL of metformin in humans (Kumar et al., 2018), we recommend that this approach, rather than hepatocytes, be considered for future REF-based IVIVE of hepatobiliary drug clearance. To utilize this approach to predict hepatic drug concentrations, further studies will need to be conducted with transporter-expressing cells. Of course, such predictions in humans need to be verified with PET or any other imaging technique as we have done in the rat (Ishida et al., 2018).

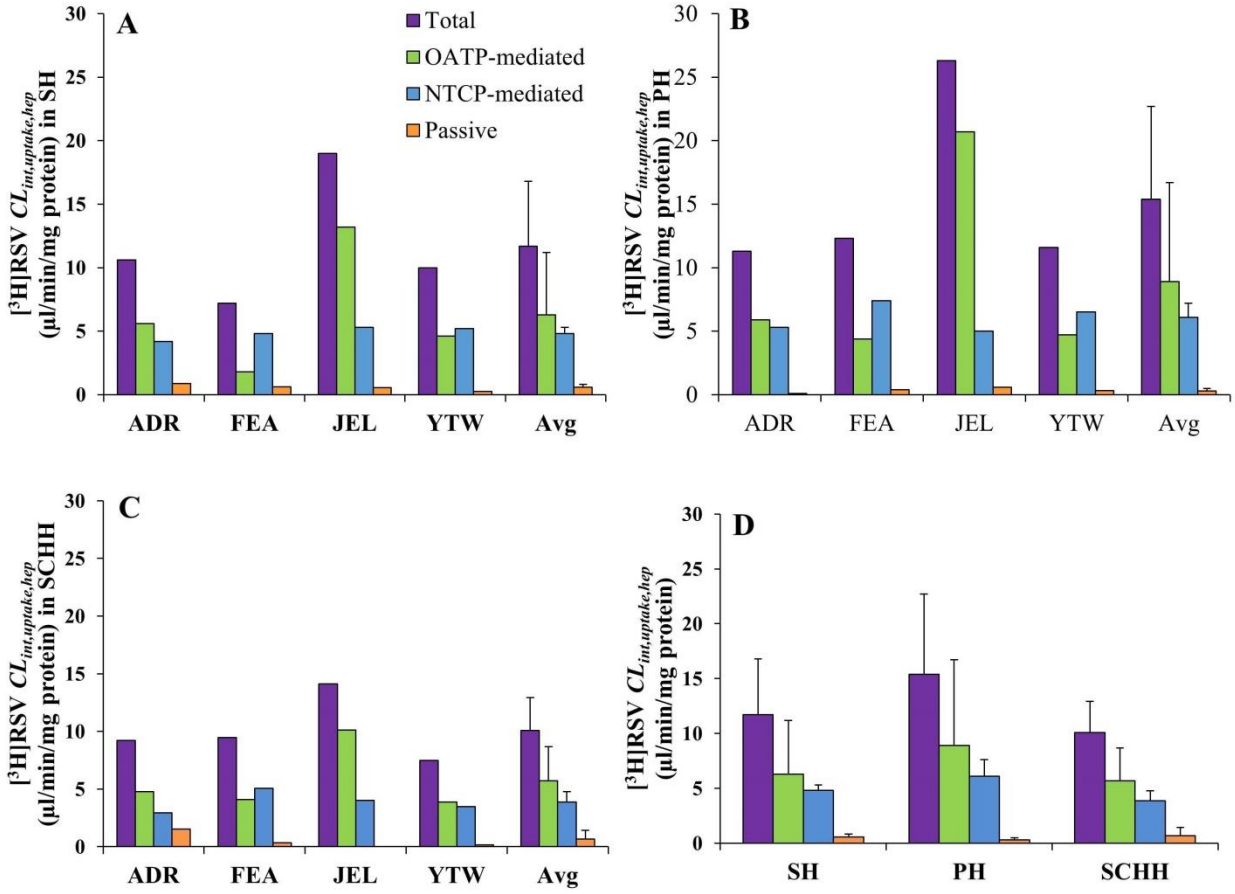

Fig. 5.1. [^{3}H]RSV $CL_{int,uptake,hep}$ in SH, PH and SCHH. [^{3}H]RSV $CL_{int,uptake,hep}$ was determined in 4 lots of SH (A), PH (B) or SCHH (C). The average contribution to [^{3}H]RSV $CL_{int,uptake,hep}$ followed the order OATPs> NTCP > passive diffusion (D). [^{3}H]RSV $CL_{int,uptake,hep}$, $CL_{int,OATP,hep}$, $CL_{int,NTCP,hep}$, *and* $CL_{int,passive,hep}$ were not significantly different between the hepatocyte models (Wilcoxon matched-pair signed rank test). The average data from panel A, B and C are shown in panel D and they are mean±SD of 4 lots of hepatocytes, each conducted in triplicate.

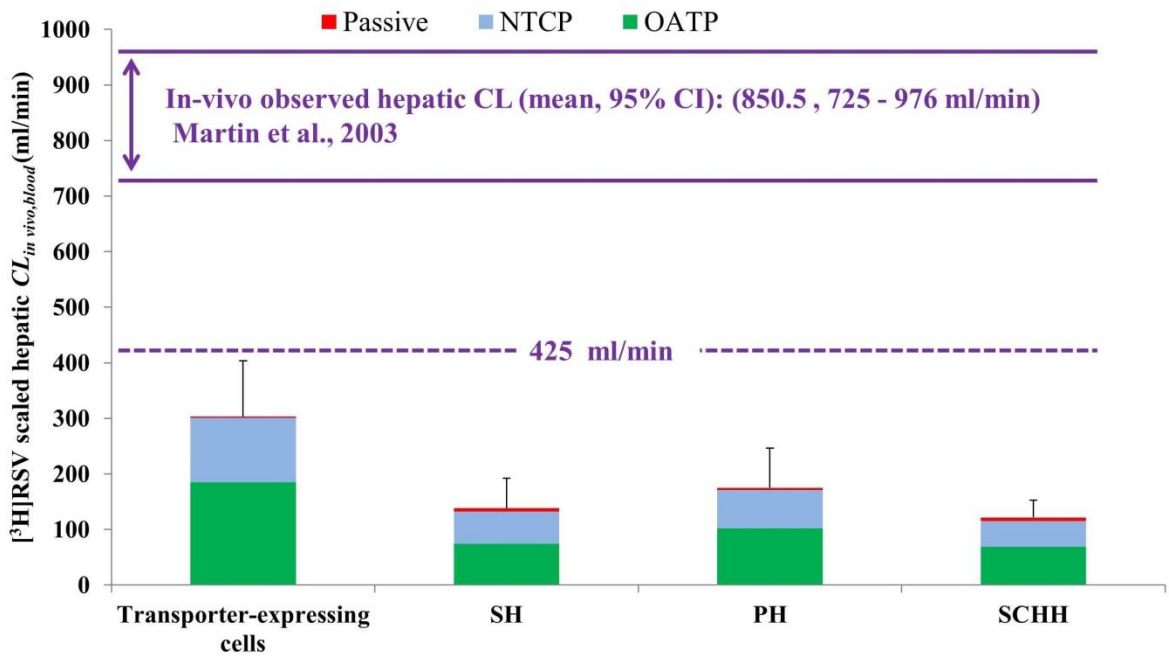

Fig. 5.2. IVIVE of RSV hepatic $CL_{in\ vivo,blood}$ based on transporter-expressing cells or the hepatocyte models, SH, PH or SCHH. The transporter-expressing cells predicted the hepatic $CL_{in\ vivo,blood}$ within 3-fold of the observed value . In contrast, the hepatocyte models underpredicted RSV $CL_{in\ vivo,blood}$ by 5- to7-fold. OATPs were the major contributors to the total RSV $CL_{int,in\ vivo,pred,cells}$ and $CL_{int,in\ vivo,pred,hep}$ followed by NTCP with smallest contributor being passive diffusion CL. The solid and dashed lines show the 95% CI of the observed hepatic $CL_{in\ vivo,blood}$ and 2-fold lower limit of the mean observed hepatic $CL_{in\ vivo,blood}$. RSV $CL_{int,in\ vivo,pred,cells}$ was significantly higher (Tukey's multiple comparison test) than $CL_{int,in\ vivo,pred,hep}$ obtained from any of the hepatocyte model. Data shown are mean±SD of 4 lots of hepatocytes, each conducted in triplicate.

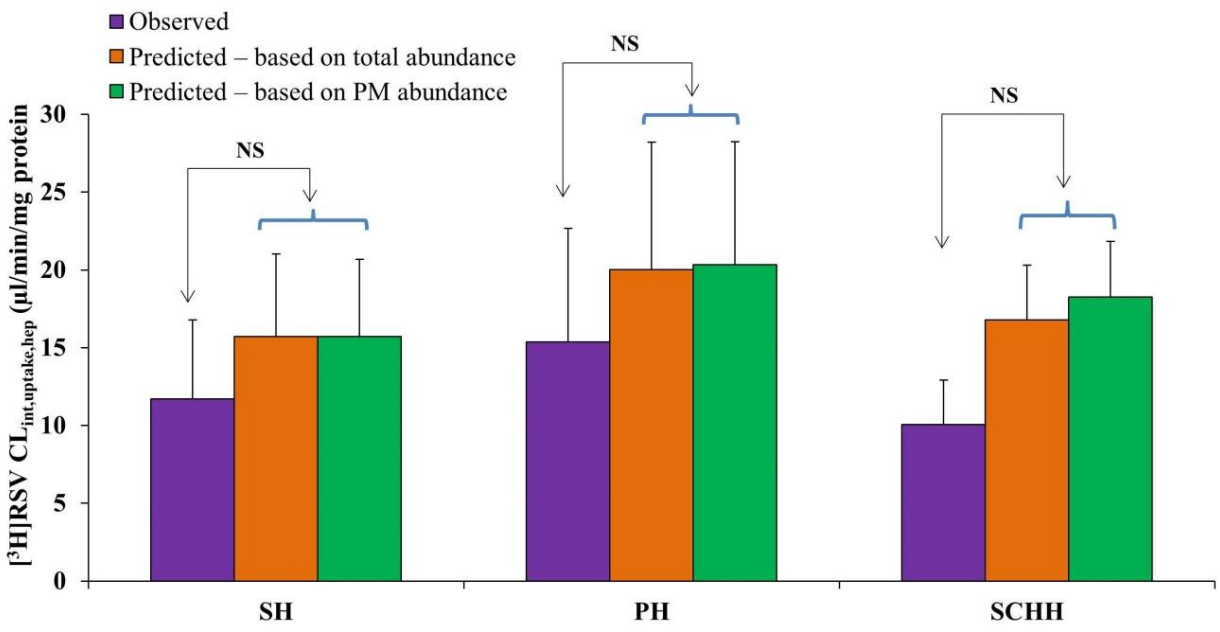

Fig. 5.3. IVCIVH of [^{3}H]RSV *$CL_{int,uptake,hep}$*. The predicted [^{3}H]RSV *$CL_{int,uptake,hep}$* from transporter-expressing cells was not significantly different from the observed [^{3}H]RSV *$CL_{int,uptake,hep}$*, irrespective of whether the predictions were made based on the total or PMA of the uptake transporters. NS: Not significantly different based on Wilcoxon matched-pair signed rank statistical test, data shown are mean ±SD of 4 lots of hepatocytes, each conducted in triplicate.

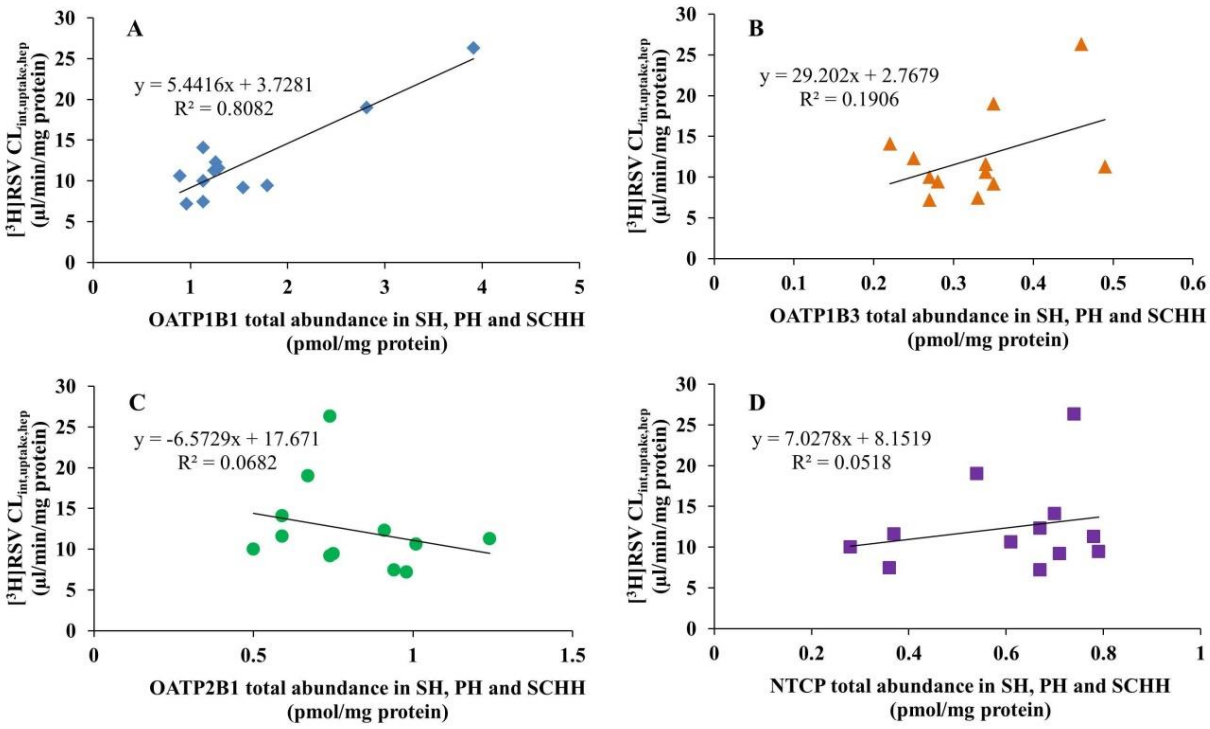

Fig. 5.4. Correlation of [^{3}H]RSV $CL_{int,uptake,hep}$ and total transporter protein abundance in hepatocyte models. The [^{3}H]RSV $CL_{int,uptake,hep}$ was highly correlated with the total abundance of OATP1B1. However, the correlation with OATP1B3, OATP2B1 and NTCP transporter abundance was poor. Similar results were obtained if the x-axis was PMA of the respective transporter. Data shown are mean of triplicates in 4 lots of hepatocytes models.

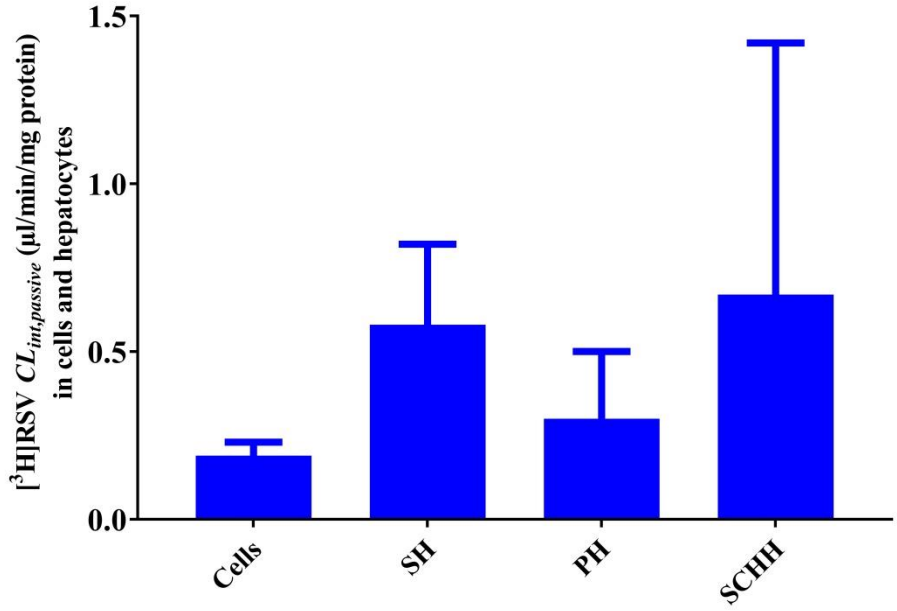

Fig. 5.5. Comparison of passive diffusion CL: [^{3}H]RSV $CL_{int,passive}$ in transporter-expressing cells and hepatocyte models was not significantly different (Tukey's multiple comparisons test). Data for hepatocyte models (SH, Ph and SCHH) are mean±SD (n=4), each conducted in triplicate. Data for the transporter-expressing cells are mean±SD of data obtained in CHO, MDCKII and HEK293 cells, each conducted in triplicate.

Table 5.1. OATP1B1/2B1/1B3- and NTCP-mediated $CL_{int,uptake,cells}$ of [^{3}H]RSV based on their total or PMA in the transporter-expressing cells

Transporter (cells)	Transporter-mediated $CL_{int,uptake,cells}$ of RSV (µL/min/mg cellular protein)[*]	Total transporter abundance (pmol/mg cellular protein) in cells[#]	Transporter-mediated RSV $CL_{int,uptake,cells}$ (µL/min/pmol total transporter protein)	PMA of transporter (% total)[$]	Transporter-mediated RSV $CL_{int,uptake,cells}$ (µL/min/pmol PM transporter protein)
OATP1B1 (CHO cells)	40.1	7.53	5.32	79.7±4.7[a]	6.68
OATP1B3 (HEK293 cells)	28.6	6.23	4.60	63.2±1.6[a]	7.27
OATP2B1 (MDCKII cells)	1.2	0.95	1.22	37.1±15.7[a]	3.29
NTCP (HEK293 cells)	34.8	3.29	10.58	77.4	13.65

[a]from Kumar et al., (Kumar et al., 2017). [$] Data shown are mean of triplicates or mean±SD of three independent experiments (except NTCP, which is mean of 2 independent determinations). [#] Data are mean of duplicate determinations from a single experiment. [*] Data from a single experiment, mean of triplicate determinations (except NTCP, average of duplicate determinations). The $CL_{int,uptake,OATP1B1}$ of RSV obtained in OATP1B1-expressing CHO cells was confirmed with $CL_{int,uptake,OATP1B1}$ of RSV in OATP1B1-expressing HEK293 cells.

Chapter 6. SUMMARY AND GENERAL CONCLUSIONS

The wealth of literature available on prediction of transporter-mediated clearance (CL) is increasing with time. Unfortunately, most of the existing methodologies (including hepatocytes) are unable to bridge the gap between the predicted and observed in vivo transporter-mediated CL of a drug. It is also important to remember that similar tissue-derived in vitro cell-based system such as hepatocytes, are not readily available for other organs (kidneys, intestine, brain), where drug transporters play an important role in drug disposition. Thus, we proposed an alternative method to predict transporter-mediated CL. We hypothesized that transporter-expressing cells can predict in vivo transporter-mediated CL of a drug using transporter abundance-based scaling factor between cells and tissues (REF). To test the above hypothesis, we also took into consideration that the transporters quantified may not all be present in the plasma membrane. With an aim to use only plasma membrane transporter abundance in cells for IVIVE, we developed and optimized a quantitative LC-MS/MS-based cell-surface biotinylation methodology (Kumar et al., 2017). This optimized methodology was successfully used to measure the plasma membrane transporter abundance in transporter-expressing cells (Kumar et al., 2017) and hepatocyte models (Kumar et al., 2019a).

To test our hypothesis, we predicted the *in vivo* transporter-mediated renal secretory CL ($CL_{r,sec}$) and hepatic uptake CL of metformin and rosuvastatin (RSV), respectively. By using the plasma membrane OCT2 transporter abundance and intrinsic uptake CL ($CL_{int,uptake}$) of metformin in the OCT2-expressing cells (HEK293 and MDCKII), and the plasma membrane potential difference between transporter-expressing cells and renal proximal tubule, we successfully predicted metformin $CL_{r,sec}$ within 2-fold of the observed in vivo $CL_{r,sec}$ (Kumar et al., 2018).

The uptake of RSV in human liver is facilitated by sinusoidal uptake transporters OATP1B1, OATP1B3, OATP2B1 and NTCP. We used transporter abundance and $CL_{int,uptake}$ of RSV in the OATP1B1-,OATP1B3-, OATP2B1-, and NTCP- expressing CHO, HEK293, MDCKII and HEK293 cells, respectively and their abundance in human liver to predict RSV in vivo hepatic uptake CL of RSV. RSV in vivo hepatic uptake CL was underpredicted (by 3-fold) by the transporter-expressing cells. The traditional approach of using hepatocyte models underpredicted RSV in vivo hepatic CL to a greater extent (by 5-to7-fold). The uptake transporter abundance in hepatocyte models and human liver was statistically not different (Kumar et al., 2019a). Therefore, the lower transporter abundance in hepatocyte models vs. human liver tissue was not the reason for the underprediction of RSV in vivo hepatic upake CL, as was the case in rats (Kotani et al., 2011; Ishida et al., 2018). Interestingly, the transporter-expressing cells successfully predicted $CL_{int,uptake}$ observed in the hepatocyte models (IVCIVH). Collectively, these data indicate that these in vitro systems are missing some in vivo factor(s) present in vivo. Indeed, plasma proteins have recently been shown to increase RSV uptake (4-fold) into rat hepatocytes (Bowman et al., 2019) or human hepatocytes (2.5-fold) (Kim et al., 2019). This difference matches the magnitude by which our transporter abundance-based REF approach under-predicts in vivo RSV hepatic uptake CL. Therefore, additional studies are warranted to address the effect of plasma proteins on the $CL_{int,uptake}$ of drugs in in vitro systems. Nevertheless, we showed that the REF approach using transporter-expressing cells appears to be a better alternative to primary cells like hepatocytes in predicting in vivo RSV hepatic uptake CL. If replicated with other drugs, together with our previous success in using REF to predict the in vivo hepatic clearance of RSV in rats (Ishida et al., 2018) and renal secretory CL of metformin in humans (Kumar et al., 2018), suggests that the REF approach using transporter-expressing

cells be considered for future REF-based IVIVE of hepatobiliary drug clearance. Of course, such predictions in humans need to be verified with PET imaging as we have done in the rat (Ishida et al., 2018).

BIBLIOGRAPHY

Abe K, Bridges AS, Yue W, and Brouwer KL (2008) In vitro biliary clearance of angiotensin II receptor blockers and 3-hydroxy-3-methylglutaryl-coenzyme A reductase inhibitors in sandwich-cultured rat hepatocytes: comparison with in vivo biliary clearance. *J Pharmacol Exp Ther* **326:**983-990.

Bi YA, Qiu X, Rotter CJ, Kimoto E, Piotrowski M, Varma MV, Ei-Kattan AF, and Lai Y (2013) Quantitative assessment of the contribution of sodium-dependent taurocholate co-transporting polypeptide (NTCP) to the hepatic uptake of rosuvastatin, pitavastatin and fluvastatin. *Biopharm Drug Dispos* **34:**452-461.

Billington S, Ray AS, Salphati L, Xiao G, Chu X, Humphreys WG, Liao M, Lee CA, Mathias A, Hop C, Rowbottom C, Evers R, Lai Y, Kelly EJ, Prasad B, and Unadkat JD (2018) Transporter Expression in Noncancerous and Cancerous Liver Tissue from Donors with Hepatocellular Carcinoma and Chronic Hepatitis C Infection Quantified by LC-MS/MS Proteomics. *Drug Metab Dispos* **46:**189-196.

Bosgra S, van de Steeg E, Vlaming ML, Verhoeckx KC, Huisman MT, Verwei M, and Wortelboer HM (2014) Predicting carrier-mediated hepatic disposition of rosuvastatin in man by scaling from individual transfected cell-lines in vitro using absolute transporter protein quantification and PBPK modeling. *Eur J Pharm Sci* **65:**156-166.

Bouchet LG, Bolch WE, Blanco HP, Wessels BW, Siegel JA, Rajon DA, Clairand I, and Sgouros G (2003) MIRD Pamphlet No 19: absorbed fractions and radionuclide S values for six age-dependent multiregion models of the kidney. *J Nucl Med* **44:**1113-1147.

Bow DA, Perry JL, Miller DS, Pritchard JB, and Brouwer KL (2008) Localization of P-gp (Abcb1) and Mrp2 (Abcc2) in freshly isolated rat hepatocytes. *Drug Metab Dispos* **36:**198-202.

Bowman CM, Okochi H, and Benet LZ (2019) The Presence of a Transporter-Induced Protein Binding Shift: A new Explanation for Protein-Facilitated Uptake and Improvement for In Vitro-In Vivo Extrapolation. *Drug Metab Dispos*.

Burt HJ, Neuhoff S, Almond L, Gaohua L, Harwood MD, Jamei M, Rostami-Hodjegan A, Tucker GT, and Rowland-Yeo K (2016) Metformin and cimetidine: Physiologically based pharmacokinetic modelling to investigate transporter mediated drug-drug interactions. *Eur J Pharm Sci* **88:**70-82.

Chen Y, Li S, Brown C, Cheatham S, Castro RA, Leabman MK, Urban TJ, Chen L, Yee SW, Choi JH, Huang Y, Brett CM, Burchard EG, and Giacomini KM (2009) Effect of genetic variation in the organic cation transporter 2 on the renal elimination of metformin. *Pharmacogenet Genomics* **19:**497-504.

Chiba M, Ishii Y, and Sugiyama Y (2009) Prediction of hepatic clearance in human from in vitro data for successful drug development. *AAPS J* **11:**262-276.

Chu X, Bleasby K, and Evers R (2013) Species differences in drug transporters and implications for translating preclinical findings to humans. *Expert Opin Drug Metab Toxicol* **9:**237-252.

Chu X, Liao M, Shen H, Yoshida K, Zur AA, Arya V, Galetin A, Giacomini KM, Hanna I, Kusuhara H, Lai Y, Rodrigues D, Sugiyama Y, Zamek-Gliszczynski MJ, Zhang L, and International Transporter C (2018) Clinical Probes and Endogenous Biomarkers as Substrates for Transporter Drug-Drug Interaction Evaluation: Perspectives From the International Transporter Consortium. *Clin Pharmacol Ther* **104:**836-864.

Cole SR, Ashman LK, and Ey PL (1987) Biotinylation: an alternative to radioiodination for the identification of cell surface antigens in immunoprecipitates. *Mol Immunol* **24:**699-705.

Condreay JP, Ames RS, Hassan NJ, Kost TA, Merrihew RV, Mossakowska DE, Pountney DJ, and Romanos MA (2006) Baculoviruses and mammalian cell-based assays for drug screening. *Adv Virus Res* **68:**255-286.

Dave RA and Morris ME (2015) Quantitative structure-pharmacokinetic relationships for the prediction of renal clearance in humans. *Drug Metab Dispos* **43:**73-81.

De Bruyn T, Chatterjee S, Fattah S, Keemink J, Nicolai J, Augustijns P, and Annaert P (2013) Sandwich-cultured hepatocytes: utility for in vitro exploration of hepatobiliary drug disposition and drug-induced hepatotoxicity. *Expert Opin Drug Metab Toxicol* **9:**589-616.

DeGorter MK and Kim RB (2009) Hepatic drug transporters, old and new: pharmacogenomics, drug response, and clinical relevance. *Hepatology* **50:**1014-1016.

Devineni D, Manitpisitkul P, Murphy J, Skee D, Wajs E, Mamidi RN, Tian H, Vandebosch A, Wang SS, Verhaeghe T, Stieltjes H, and Usiskin K (2015) Effect of canagliflozin on the pharmacokinetics of glyburide, metformin, and simvastatin in healthy participants. *Clin Pharmacol Drug Dev* **4:**226-236.

Endres CJ, Hsiao P, Chung FS, and Unadkat JD (2006) The role of transporters in drug interactions. *Eur J Pharm Sci* **27:**501-517.

Fan J, Chen S, Chow EC, and Pang KS (2010) PBPK modeling of intestinal and liver enzymes and transporters in drug absorption and sequential metabolism. *Curr Drug Metab* **11:**743-761.

Fisel P, Schaeffeler E, and Schwab M (2016) DNA Methylation of ADME Genes. *Clin Pharmacol Ther* **99:**512-527.

Gandhi YA and Morris ME (2012) Reevaluation of a quantitative structure pharmacokinetic model for biliary excretion in rats. *Drug Metab Dispos* **40:**1259-1262.

Ghibellini G, Vasist LS, Leslie EM, Heizer WD, Kowalsky RJ, Calvo BF, and Brouwer KL (2007) In vitro-in vivo correlation of hepatobiliary drug clearance in humans. *Clin Pharmacol Ther* **81:**406-413.

Giacomini KM, Huang SM, Tweedie DJ, Benet LZ, Brouwer KL, Chu X, Dahlin A, Evers R, Fischer V, Hillgren KM, Hoffmaster KA, Ishikawa T, Keppler D, Kim RB, Lee CA, Niemi M, Polli JW, Sugiyama Y, Swaan PW, Ware JA, Wright SH, Yee SW, Zamek-Gliszczynski MJ, and Zhang L (2010) Membrane transporters in drug development. *Nat Rev Drug Discov* **9:**215-236.

Grime K and Paine SW (2013) Species differences in biliary clearance and possible relevance of hepatic uptake and efflux transporters involvement. *Drug Metab Dispos* **41:**372-378.

Hibma JE, Zur AA, Castro RA, Wittwer MB, Keizer RJ, Yee SW, Goswami S, Stocker SL, Zhang X, Huang Y, Brett CM, Savic RM, and Giacomini KM (2016) The Effect of Famotidine, a MATE1-Selective Inhibitor, on the Pharmacokinetics and Pharmacodynamics of Metformin. *Clin Pharmacokinet* **55:**711-721.

Hirano M, Maeda K, Shitara Y, and Sugiyama Y (2004) Contribution of OATP2 (OATP1B1) and OATP8 (OATP1B3) to the hepatic uptake of pitavastatin in humans. *J Pharmacol Exp Ther* **311:**139-146.

Ho RH, Leake BF, Roberts RL, Lee W, and Kim RB (2004) Ethnicity-dependent polymorphism in Na+-taurocholate cotransporting polypeptide (SLC10A1) reveals a domain critical for bile acid substrate recognition. *J Biol Chem* **279:**7213-7222.

Hoffmaster KA, Turncliff RZ, LeCluyse EL, Kim RB, Meier PJ, and Brouwer KL (2004) P-glycoprotein expression, localization, and function in sandwich-cultured primary rat and human hepatocytes: relevance to the hepatobiliary disposition of a model opioid peptide. *Pharm Res* **21:**1294-1302.

Hsu K, Han J, Shinlapawittayatorn K, Deschenes I, and Marban E (2010) Membrane potential depolarization as a triggering mechanism for Vpu-mediated HIV-1 release. *Biophys J* **99:**1718-1725.

Hua WJ, Hua WX, and Fang HJ (2012) The role of OATP1B1 and BCRP in pharmacokinetics and DDI of novel statins. *Cardiovasc Ther* **30:**e234-241.

Huang F, Marzin K, Koenen R, Kammerer KP, Strelkowa N, Elgadi M, Quinson AM, and Haertter S (2017) Effect of Steady-State Faldaprevir on Pharmacokinetics of Atorvastatin or Rosuvastatin in Healthy Volunteers: A Prospective Open-Label, Fixed-Sequence Crossover Study. *J Clin Pharmacol* **57:**1305-1314.

Ishida K, Ullah M, Toth B, Juhasz V, and Unadkat JD (2018) Successful Prediction of In Vivo Hepatobiliary Clearances and Hepatic Concentrations of Rosuvastatin Using Sandwich-Cultured Rat Hepatocytes, Transporter-Expressing Cell Lines, and Quantitative Proteomics. *Drug Metab Dispos* **46:**66-74.

Izumi S, Nozaki Y, Komori T, Takenaka O, Maeda K, Kusuhara H, and Sugiyama Y (2017) Comparison of the Predictability of Human Hepatic Clearance for Organic Anion Transporting Polypeptide Substrate Drugs Between Different In Vitro-In Vivo Extrapolation Approaches. *J Pharm Sci* **106:**2678-2687.

Johansson S, Read J, Oliver S, Steinberg M, Li Y, Lisbon E, Mathews D, Leese PT, and Martin P (2014) Pharmacokinetic evaluations of the co-administrations of vandetanib and

metformin, digoxin, midazolam, omeprazole or ranitidine. *Clin Pharmacokinet* **53:**837-847.

Jones HM, Barton HA, Lai Y, Bi YA, Kimoto E, Kempshall S, Tate SC, El-Kattan A, Houston JB, Galetin A, and Fenner KS (2012) Mechanistic pharmacokinetic modeling for the prediction of transporter-mediated disposition in humans from sandwich culture human hepatocyte data. *Drug Metab Dispos* **40:**1007-1017.

Karlgren M, Vildhede A, Norinder U, Wisniewski JR, Kimoto E, Lai Y, Haglund U, and Artursson P (2012) Classification of inhibitors of hepatic organic anion transporting polypeptides (OATPs): influence of protein expression on drug-drug interactions. *J Med Chem* **55:**4740-4763.

Kim SJ, Lee KR, Miyauchi S, and Sugiyama Y (2019) Extrapolation of In Vivo Hepatic Clearance from In Vitro Uptake Clearance by Suspended Human Hepatocytes for Anionic Drugs with High Binding to Human Albumin: Improvement of In Vitro-to-In Vivo Extrapolation by Considering the "Albumin-Mediated" Hepatic Uptake Mechanism on the Basis of the "Facilitated-Dissociation Model". *Drug Metab Dispos* **47:**94-103.

Kimoto E, Yoshida K, Balogh LM, Bi YA, Maeda K, El-Kattan A, Sugiyama Y, and Lai Y (2012) Characterization of organic anion transporting polypeptide (OATP) expression and its functional contribution to the uptake of substrates in human hepatocytes. *Mol Pharm* **9:**3535-3542.

Kitamura S, Maeda K, Wang Y, and Sugiyama Y (2008) Involvement of multiple transporters in the hepatobiliary transport of rosuvastatin. *Drug Metab Dispos* **36:**2014-2023.

Klamerus KJ, Alvey C, Li L, Feng B, Wang R, Kaplan I, Shi H, Dowty ME, and Krishnaswami S (2014) Evaluation of the potential interaction between tofacitinib and drugs that

undergo renal tubular secretion using metformin, an in vivo marker of renal organic cation transporter 2. *Clin Pharmacol Drug Dev* **3:**499-507.

Kock K and Brouwer KL (2012) A perspective on efflux transport proteins in the liver. *Clin Pharmacol Ther* **92:**599-612.

Koepsell H and Keller T (2016) Functional Properties of Organic Cation Transporter OCT1, Binding of Substrates and Inhibitors, and Presumed Transport Mechanism, in: *Organic Cation Transporters: Integration of Physiology, Pathology, and Pharmacology* (Ciarimboli G, Gautron S, and Schlatter E eds), pp 49-72, Springer International Publishing, Cham.

Kopplow K, Letschert K, Konig J, Walter B, and Keppler D (2005) Human hepatobiliary transport of organic anions analyzed by quadruple-transfected cells. *Mol Pharmacol* **68:**1031-1038.

Kotani N, Maeda K, Watanabe T, Hiramatsu M, Gong LK, Bi YA, Takezawa T, Kusuhara H, and Sugiyama Y (2011) Culture period-dependent changes in the uptake of transporter substrates in sandwich-cultured rat and human hepatocytes. *Drug Metab Dispos* **39:**1503-1510.

Kumar V, Nguyen TB, Toth B, Juhasz V, and Unadkat JD (2017) Optimization and Application of a Biotinylation Method for Quantification of Plasma Membrane Expression of Transporters in Cells. *AAPS J* **19:**1377-1386.

Kumar V, Prasad B, Patilea G, Gupta A, Salphati L, Evers R, Hop CE, and Unadkat JD (2015) Quantitative transporter proteomics by liquid chromatography with tandem mass spectrometry: addressing methodologic issues of plasma membrane isolation and expression-activity relationship. *Drug Metab Dispos* **43:**284-288.

Kumar V, Salphati L, Hop C, Xiao G, Lai Y, Mathias A, Chu X, Humphreys WG, Liao M, Heyward S, and Unadkat JD (2019a) A Comparison of Total and Plasma Membrane Abundance of Transporters in Suspended, Plated, Sandwich-Cultured Human Hepatocytes Versus Human Liver Tissue Using Quantitative Targeted Proteomics and Cell Surface Biotinylation. *Drug Metab Dispos* **47:**350-357.

Kumar V, Salphati L, Hop C, Xiao G, Lai Y, Mathias A, Chu X, Humphreys WG, Liao M, Heyward S, and Unadkat JD (2019b) A Comparison of Total and Plasma Membrane Abundance of Transporters in Suspended, Plated, Sandwich-Cultured Human Hepatocytes vs. Human Liver Tissue Using Quantitative Targeted Proteomics and Cell-Surface Biotinylation. *Drug Metab Dispos*.

Kumar V, Yin J, Billington S, Prasad B, Brown CDA, Wang J, and Unadkat JD (2018) The Importance of Incorporating OCT2 Plasma Membrane Expression and Membrane Potential in IVIVE of Metformin Renal Secretory Clearance. *Drug Metab Dispos* **46:**1441-1445.

Kusuhara H, Ito S, Kumagai Y, Jiang M, Shiroshita T, Moriyama Y, Inoue K, Yuasa H, and Sugiyama Y (2011) Effects of a MATE protein inhibitor, pyrimethamine, on the renal elimination of metformin at oral microdose and at therapeutic dose in healthy subjects. *Clin Pharmacol Ther* **89:**837-844.

Lai Y, Mandlekar S, Shen H, Holenarsipur VK, Langish R, Rajanna P, Murugesan S, Gaud N, Selvam S, Date O, Cheng Y, Shipkova P, Dai J, Humphreys WG, and Marathe P (2016) Coproporphyrins in Plasma and Urine Can Be Appropriate Clinical Biomarkers to Recapitulate Drug-Drug Interactions Mediated by Organic Anion Transporting Polypeptide Inhibition. *J Pharmacol Exp Ther* **358:**397-404.

Lam JL and Benet LZ (2004) Hepatic microsome studies are insufficient to characterize in vivo hepatic metabolic clearance and metabolic drug-drug interactions: studies of digoxin metabolism in primary rat hepatocytes versus microsomes. *Drug Metab Dispos* **32:**1311-1316.

Lam JL, Okochi H, Huang Y, and Benet LZ (2006) In vitro and in vivo correlation of hepatic transporter effects on erythromycin metabolism: characterizing the importance of transporter-enzyme interplay. *Drug Metab Dispos* **34:**1336-1344.

Lang F and Paulmichl M (1995) Properties and regulation of ion channels in MDCK cells. *Kidney Int* **48:**1200-1205.

Lee W, Glaeser H, Smith LH, Roberts RL, Moeckel GW, Gervasini G, Leake BF, and Kim RB (2005) Polymorphisms in human organic anion-transporting polypeptide 1A2 (OATP1A2): implications for altered drug disposition and central nervous system drug entry. *J Biol Chem* **280:**9610-9617.

Li N, Bi YA, Duignan DB, and Lai Y (2009a) Quantitative expression profile of hepatobiliary transporters in sandwich cultured rat and human hepatocytes. *Mol Pharm* **6:**1180-1189.

Li N, Singh P, Mandrell KM, and Lai Y (2010) Improved extrapolation of hepatobiliary clearance from in vitro sandwich cultured rat hepatocytes through absolute quantification of hepatobiliary transporters. *Mol Pharm* **7:**630-641.

Li N, Zhang Y, Hua F, and Lai Y (2009b) Absolute difference of hepatobiliary transporter multidrug resistance-associated protein (MRP2/Mrp2) in liver tissues and isolated hepatocytes from rat, dog, monkey, and human. *Drug Metab Dispos* **37:**66-73.

Li Q, Yang H, Guo D, Zhang T, Polli JE, Zhou H, and Shu Y (2016) Effect of Ondansetron on Metformin Pharmacokinetics and Response in Healthy Subjects. *Drug Metab Dispos* **44:**489-494.

Li R and Barton HA (2018) Explaining Ethnic Variability of Transporter Substrate Pharmacokinetics in Healthy Asian and Caucasian Subjects with Allele Frequencies of OATP1B1 and BCRP: A Mechanistic Modeling Analysis. *Clin Pharmacokinet* **57:**491-503.

Liao M, Zhu Q, Zhu A, Gemski C, Ma B, Guan E, Li AP, Xiao G, and Xia CQ (2018) Comparison of Uptake Transporter Functions in Hepatocytes in Different Species to Determine the Optimal Model for Evaluating Drug Transporter Activities in Humans. *Xenobiotica***:**1-32.

Liu X, LeCluyse EL, Brouwer KR, Lightfoot RM, Lee JI, and Brouwer KL (1999) Use of Ca2+ modulation to evaluate biliary excretion in sandwich-cultured rat hepatocytes. *J Pharmacol Exp Ther* **289:**1592-1599.

Loder MK and Melikian HE (2003) The dopamine transporter constitutively internalizes and recycles in a protein kinase C-regulated manner in stably transfected PC12 cell lines. *J Biol Chem* **278:**22168-22174.

Lundquist P, Englund G, Skogastierna C, Loof J, Johansson J, Hoogstraate J, Afzelius L, and Andersson TB (2014) Functional ATP-binding cassette drug efflux transporters in isolated human and rat hepatocytes significantly affect assessment of drug disposition. *Drug Metab Dispos* **42:**448-458.

Mao J, Doshi U, Wright M, Hop C, Li AP, and Chen Y (2018) Prediction of the Pharmacokinetics of Pravastatin as an OATP Substrate Using Plateable Human

Hepatocytes With Human Plasma Data and PBPK Modeling. *CPT Pharmacometrics Syst Pharmacol* **7:**251-258.

Martin PD, Warwick MJ, Dane AL, Brindley C, and Short T (2003a) Absolute oral bioavailability of rosuvastatin in healthy white adult male volunteers. *Clin Ther* **25:**2553-2563.

Martin PD, Warwick MJ, Dane AL, Hill SJ, Giles PB, Phillips PJ, and Lenz E (2003b) Metabolism, excretion, and pharmacokinetics of rosuvastatin in healthy adult male volunteers. *Clin Ther* **25:**2822-2835.

Mathialagan S, Piotrowski MA, Tess DA, Feng B, Litchfield J, and Varma MV (2017) Quantitative Prediction of Human Renal Clearance and Drug-Drug Interactions of Organic Anion Transporter Substrates Using In Vitro Transport Data: A Relative Activity Factor Approach. *Drug Metab Dispos* **45:**409-417.

McFeely SJ, Wu L, Ritchie TK, and Unadkat J (2018) Organic anion transporting polypeptide 2B1 - More than a glass-full of drug interactions. *Pharmacol Ther*.

Menochet K, Kenworthy KE, Houston JB, and Galetin A (2012) Use of mechanistic modeling to assess interindividual variability and interspecies differences in active uptake in human and rat hepatocytes. *Drug Metab Dispos* **40:**1744-1756.

Murray M and Zhou F (2017) Trafficking and other regulatory mechanisms for organic anion transporting polypeptides and organic anion transporters that modulate cellular drug and xenobiotic influx and that are dysregulated in disease. *Br J Pharmacol* **174:**1908-1924.

Naritomi Y, Terashita S, Kagayama A, and Sugiyama Y (2003) Utility of hepatocytes in predicting drug metabolism: comparison of hepatic intrinsic clearance in rats and humans in vivo and in vitro. *Drug Metab Dispos* **31:**580-588.

Oefelein MG, Tong W, Kerr S, Bhasi K, Patel RK, and Yu D (2013) Effect of concomitant administration of trospium chloride extended release on the steady-state pharmacokinetics of metformin in healthy adults. *Clin Drug Investig* **33:**123-131.

Paine SW, Menochet K, Denton R, McGinnity DF, and Riley RJ (2011) Prediction of human renal clearance from preclinical species for a diverse set of drugs that exhibit both active secretion and net reabsorption. *Drug Metab Dispos* **39:**1008-1013.

Pan W, Song IS, Shin HJ, Kim MH, Choi YL, Lim SJ, Kim WY, Lee SS, and Shin JG (2011) Genetic polymorphisms in Na+-taurocholate co-transporting polypeptide (NTCP) and ileal apical sodium-dependent bile acid transporter (ASBT) and ethnic comparisons of functional variants of NTCP among Asian populations. *Xenobiotica* **41:**501-510.

Patik I, Kovacsics D, Nemet O, Gera M, Varady G, Stieger B, Hagenbuch B, Szakacs G, and Ozvegy-Laczka C (2015) Functional expression of the 11 human Organic Anion Transporting Polypeptides in insect cells reveals that sodium fluorescein is a general OATP substrate. *Biochem Pharmacol* **98:**649-658.

Patilea-Vrana G and Unadkat JD (2016) Transport vs. Metabolism: What Determines the Pharmacokinetics and Pharmacodynamics of Drugs? Insights From the Extended Clearance Model. *Clin Pharmacol Ther* **100:**413-418.

Patilea-Vrana GI and Unadkat JD (2018) When Does the Rate-Determining Step in the Hepatic Clearance of a Drug Switch from Sinusoidal Uptake to All Hepatobiliary Clearances? Implications for Predicting Drug-Drug Interactions. *Drug Metab Dispos* **46:**1487-1496.

Pentikainen PJ, Neuvonen PJ, and Penttila A (1979) Pharmacokinetics of metformin after intravenous and oral administration to man. *Eur J Clin Pharmacol* **16:**195-202.

Pfeifer ND, Yang K, and Brouwer KL (2013) Hepatic basolateral efflux contributes significantly to rosuvastatin disposition I: characterization of basolateral versus biliary clearance using a novel protocol in sandwich-cultured hepatocytes. *J Pharmacol Exp Ther* **347:**727-736.

Powell J, Farasyn T, Kock K, Meng X, Pahwa S, Brouwer KL, and Yue W (2014) Novel mechanism of impaired function of organic anion-transporting polypeptide 1B3 in human hepatocytes: post-translational regulation of OATP1B3 by protein kinase C activation. *Drug Metab Dispos* **42:**1964-1970.

Prasad B, Evers R, Gupta A, Hop CE, Salphati L, Shukla S, Ambudkar SV, and Unadkat JD (2014) Interindividual variability in hepatic organic anion-transporting polypeptides and P-glycoprotein (ABCB1) protein expression: quantification by liquid chromatography tandem mass spectroscopy and influence of genotype, age, and sex. *Drug Metab Dispos* **42:**78-88.

Prasad B, Johnson K, Billington S, Lee C, Chung GW, Brown CD, Kelly EJ, Himmelfarb J, and Unadkat JD (2016) Abundance of Drug Transporters in the Human Kidney Cortex as Quantified by Quantitative Targeted Proteomics. *Drug Metab Dispos* **44:**1920-1924.

Prasad B, Lai Y, Lin Y, and Unadkat JD (2013) Interindividual variability in the hepatic expression of the human breast cancer resistance protein (BCRP/ABCG2): effect of age, sex, and genotype. *J Pharm Sci* **102:**787-793.

Prasad B and Unadkat JD (2014a) Comparison of Heavy Labeled (SIL) Peptide versus SILAC Protein Internal Standards for LC-MS/MS Quantification of Hepatic Drug Transporters. *Int J Proteomics* **2014:**451510.

Prasad B and Unadkat JD (2014b) Optimized approaches for quantification of drug transporters in tissues and cells by MRM proteomics. *AAPS J* **16:**634-648.

Prueksaritanont T, Tatosian DA, Chu X, Railkar R, Evers R, Chavez-Eng C, Lutz R, Zeng W, Yabut J, Chan GH, Cai X, Latham AH, Hehman J, Stypinski D, Brejda J, Zhou C, Thornton B, Bateman KP, Fraser I, and Stoch SA (2017) Validation of a microdose probe drug cocktail for clinical drug interaction assessments for drug transporters and CYP3A. *Clin Pharmacol Ther* **101:**519-530.

Sager JE, Yu J, Ragueneau-Majlessi I, and Isoherranen N (2015) Physiologically Based Pharmacokinetic (PBPK) Modeling and Simulation Approaches: A Systematic Review of Published Models, Applications, and Model Verification. *Drug Metab Dispos* **43:**1823-1837.

Sambol NC, Chiang J, O'Conner M, Liu CY, Lin ET, Goodman AM, Benet LZ, and Karam JH (1996) Pharmacokinetics and pharmacodynamics of metformin in healthy subjects and patients with noninsulin-dependent diabetes mellitus. *J Clin Pharmacol* **36:**1012-1021.

Schaefer O, Ohtsuki S, Kawakami H, Inoue T, Liehner S, Saito A, Sakamoto A, Ishiguro N, Matsumaru T, Terasaki T, and Ebner T (2012) Absolute quantification and differential expression of drug transporters, cytochrome P450 enzymes, and UDP-glucuronosyltransferases in cultured primary human hepatocytes. *Drug Metab Dispos* **40:**93-103.

Shin D, Cho YM, Lee S, Lim KS, Kim JA, Ahn JY, Cho JY, Lee H, Jang IJ, and Yu KS (2014) Pharmacokinetic and pharmacodynamic interaction between gemigliptin and metformin in healthy subjects. *Clin Drug Investig* **34:**383-393.

Shugarts S and Benet LZ (2009) The role of transporters in the pharmacokinetics of orally administered drugs. *Pharm Res* **26:**2039-2054.

Simonson SG, Raza A, Martin PD, Mitchell PD, Jarcho JA, Brown CD, Windass AS, and Schneck DW (2004) Rosuvastatin pharmacokinetics in heart transplant recipients administered an antirejection regimen including cyclosporine. *Clin Pharmacol Ther* **76:**167-177.

Sirtori CR, Franceschini G, Galli-Kienle M, Cighetti G, Galli G, Bondioli A, and Conti F (1978) Disposition of metformin (N,N-dimethylbiguanide) in man. *Clin Pharmacol Ther* **24:**683-693.

Soars MG, McGinnity DF, Grime K, and Riley RJ (2007) The pivotal role of hepatocytes in drug discovery. *Chem Biol Interact* **168:**2-15.

Somogyi A, Stockley C, Keal J, Rolan P, and Bochner F (1987) Reduction of metformin renal tubular secretion by cimetidine in man. *Br J Clin Pharmacol* **23:**545-551.

Song IH, Zong J, Borland J, Jerva F, Wynne B, Zamek-Gliszczynski MJ, Humphreys JE, Bowers GD, and Choukour M (2016) The Effect of Dolutegravir on the Pharmacokinetics of Metformin in Healthy Subjects. *J Acquir Immune Defic Syndr* **72:**400-407.

Steck TL, Weinstein RS, Straus JH, and Wallach DF (1970) Inside-out red cell membrane vesicles: preparation and purification. *Science* **168:**255-257.

Sun T, Yu SH, Zhao P, Meng L, Moremen KW, Wells L, Steet R, and Boons GJ (2016) One-Step Selective Exoenzymatic Labeling (SEEL) Strategy for the Biotinylation and Identification of Glycoproteins of Living Cells. *J Am Chem Soc* **138:**11575-11582.

Tucker GT, Casey C, Phillips PJ, Connor H, Ward JD, and Woods HF (1981) Metformin kinetics in healthy subjects and in patients with diabetes mellitus. *Br J Clin Pharmacol* **12:**235-246.

Urquhart BL, Ware JA, Tirona RG, Ho RH, Leake BF, Schwarz UI, Zaher H, Palandra J, Gregor JC, Dresser GK, and Kim RB (2008) Breast cancer resistance protein (ABCG2) and drug disposition: intestinal expression, polymorphisms and sulfasalazine as an in vivo probe. *Pharmacogenet Genomics* **18:**439-448.

Varma MV, Lai Y, Feng B, Litchfield J, Goosen TC, and Bergman A (2012) Physiologically based modeling of pravastatin transporter-mediated hepatobiliary disposition and drug-drug interactions. *Pharm Res* **29:**2860-2873.

Vildhede A, Karlgren M, Svedberg EK, Wisniewski JR, Lai Y, Noren A, and Artursson P (2014) Hepatic uptake of atorvastatin: influence of variability in transporter expression on uptake clearance and drug-drug interactions. *Drug Metab Dispos* **42:**1210-1218.

Vildhede A, Kimoto E, Rodrigues AD, and Varma MVS (2018) Quantification of Hepatic Organic Anion Transport Proteins OAT2 and OAT7 in Human Liver Tissue and Primary Hepatocytes. *Mol Pharm* **15:**3227-3235.

Vildhede A, Mateus A, Khan EK, Lai Y, Karlgren M, Artursson P, and Kjellsson MC (2016) Mechanistic Modeling of Pitavastatin Disposition in Sandwich-Cultured Human Hepatocytes: A Proteomics-Informed Bottom-Up Approach. *Drug Metab Dispos* **44:**505-516.

Vildhede A, Wisniewski JR, Noren A, Karlgren M, and Artursson P (2015) Comparative Proteomic Analysis of Human Liver Tissue and Isolated Hepatocytes with a Focus on Proteins Determining Drug Exposure. *J Proteome Res* **14:**3305-3314.

Wang L, Collins C, Kelly EJ, Chu X, Ray AS, Salphati L, Xiao G, Lee C, Lai Y, Liao M, Mathias A, Evers R, Humphreys W, Hop CE, Kumer SC, and Unadkat JD (2016) Transporter Expression in Liver Tissue from Subjects with Alcoholic or Hepatitis C

Cirrhosis Quantified by Targeted Quantitative Proteomics. *Drug Metab Dispos* **44:**1752-1758.

Wang L, Prasad B, Salphati L, Chu X, Gupta A, Hop CE, Evers R, and Unadkat JD (2015) Interspecies variability in expression of hepatobiliary transporters across human, dog, monkey, and rat as determined by quantitative proteomics. *Drug Metab Dispos* **43:**367-374.

Watanabe T, Kusuhara H, Maeda K, Shitara Y, and Sugiyama Y (2009) Physiologically based pharmacokinetic modeling to predict transporter-mediated clearance and distribution of pravastatin in humans. *J Pharmacol Exp Ther* **328:**652-662.

Wegler C, Gaugaz FZ, Andersson TB, Wisniewski JR, Busch D, Groer C, Oswald S, Noren A, Weiss F, Hammer HS, Joos TO, Poetz O, Achour B, Rostami-Hodjegan A, van de Steeg E, Wortelboer HM, and Artursson P (2017) Variability in Mass Spectrometry-based Quantification of Clinically Relevant Drug Transporters and Drug Metabolizing Enzymes. *Mol Pharm* **14:**3142-3151.

Westphale HJ, Wojnowski L, Schwab A, and Oberleithner H (1992) Spontaneous membrane potential oscillations in Madin-Darby canine kidney cells transformed by alkaline stress. *Pflugers Arch* **421:**218-223.

Wright SH and Dantzler WH (2004) Molecular and cellular physiology of renal organic cation and anion transport. *Physiol Rev* **84:**987-1049.

Yang J, Jamei M, Yeo KR, Rostami-Hodjegan A, and Tucker GT (2007) Misuse of the well-stirred model of hepatic drug clearance. *Drug Metab Dispos* **35:**501-502.

Yin J, Duan H, Shirasaka Y, Prasad B, and Wang J (2015) Atenolol Renal Secretion Is Mediated by Human Organic Cation Transporter 2 and Multidrug and Toxin Extrusion Proteins. *Drug Metab Dispos* **43:**1872-1881.

Yin J, Duan H, and Wang J (2016) Impact of Substrate-Dependent Inhibition on Renal Organic Cation Transporters hOCT2 and hMATE1/2-K-Mediated Drug Transport and Intracellular Accumulation. *J Pharmacol Exp Ther* **359:**401-410.

Zhang P, Tian X, Chandra P, and Brouwer KL (2005) Role of glycosylation in trafficking of Mrp2 in sandwich-cultured rat hepatocytes. *Mol Pharmacol* **67:**1334-1341.

Zou P, Liu X, Wong S, Feng MR, and Liederer BM (2013) Comparison of in vitro-in vivo extrapolation of biliary clearance using an empirical scaling factor versus transport-based scaling factors in sandwich-cultured rat hepatocytes. *J Pharm Sci* **102:**2837-2850.